

Master's thesis

Supersymmetry in Proton–Proton Collisions

Cross-Sections for Electroweakino Pair Production in the Complex
Minimal Supersymmetric Standard Model

Carl Martin Fevang

60 ECTS study points

Department of Physics
Faculty of Mathematics and Natural Sciences

June 4, 2024



Carl Martin Fevang

Supersymmetry in Proton–Proton Collisions

Cross-Sections for Electroweakino Pair Production
in the Complex Minimal Supersymmetric Standard
Model

Supervisor:
Are Raklev

Abstract

To meaningfully scan the large parameter spaces beyond the Standard Model theories such as the Minimal Supersymmetric Standard Model (MSSM), accurate predictions are required for comparison to experimental data. Particularly, in particle collider experiments, fast and accurate cross-section calculations are necessary. In this thesis, I compute the leading order cross-sections for pair production of electroweakinos in proton–proton collisions at the Large Hadron Collider at CERN. Furthermore, next-to-leading order corrections are computed for higgsino-like neutralinos, and all neutralino pair production processes are implemented numerically for arbitrary complex-valued MSSM parameters. I explore physical scenarios derived from MSSM parameters, and present cross-section dependence with errors as the parameters are varied. Particular emphasis is placed on cross-sections with charge-parity invariance violating complex phases in the MSSM parameters, for which no implementation is currently available at next-to-leading order in the literature. I show that in at least one MSSM scenario, the effects of a complex phase is larger on leading order cross-sections than the addition of leading log resummation to next-to-leading order results.

Acknowledgements

As I finish my Master's thesis, there are many who deserve a mention. First of all, I would like to thank my supervisor Are Raklev, for being a tremendous guide and dedicating so much time in my supervision. You have been an excellent teacher and a great source of inspiration, academically and beyond. Next, I must thank my mother, who has always been my greatest supporter. Your faith in me has never wavered, and I am eternally grateful for the understanding and support you have shown in my dedication to this academic pursuit. I would also like to take a moment to recognise my roommates, Håkon Olav, Ida and Johan. During my time writing this thesis, you have not only shown me patience, but you have always provided a consoling and entertaining atmosphere making every day better.

Finally, I could not look back at my time here in the theory section without thinking of the people I have met along the way. From the people I only met in passing, to those I have seen every day – you have enriched every day, providing so many thoughtful, fun and interesting discussions and debates, in lunch breaks, next to the coffee machine, or in the numerous social events we have had. Being surrounded by such smart, insightful and enjoyable people every day has made this experience unforgettable. In particular, I would like to thank my dear friends whom I have worked with. Your contributions are evident in this thesis.

Contents

Introduction	3
1 Quantum Field Theory	7
1.1 Perturbative Quantum Field Theory	7
1.1.1 The Path Integral	7
1.1.2 Perturbing the Free Theory	8
1.1.3 Feynman Rules in Position Space	9
1.1.4 The S -Matrix and LSZ Reduction Formula	11
1.1.5 Feynman Rules for Fermions	12
1.2 Renormalised Quantum Field Theory	14
1.2.1 Loop Integrals and Divergences	15
1.2.2 Regularisation	16
1.2.3 Counterterm Renormalisation	17
1.2.4 On-Shell Renormalisation	18
1.2.5 Running Couplings and Renormalisation Group	20
1.2.6 IR Divergences	21
1.3 Yang-Mills Theories	21
1.4 Passarino-Veltman Loop Integrals	23
2 Supersymmetry	27
2.1 Introduction to Supersymmetry	27
2.2 The Super-Poincaré Group	29
2.2.1 The Poincaré and Super-Poincaré Algebras	29
2.2.2 Superspace	31
2.2.3 Superfields	32
2.2.4 Superlagrangian	33
2.2.5 Revisiting our Simple Supersymmetric Theory	34
2.3 Minimal Supersymmetric Standard Model	35
2.3.1 Supersymmetric Yang-Mills Theory	35
2.3.2 Field Content	36
2.3.3 Superlagrangian and Supersymmetry Breaking	37
2.4 Electroweakinos	39
2.4.1 Mass mixing	39
2.4.2 Feynman Rules for Neutralinos	41
2.5 Diagonalisation and Takagi Factorisation	44
2.5.1 Numerical Diagonalisation	44
2.5.2 Takagi Factorisation	46

Contents

3	Electroweakino Pair Production at Parton Level	49
3.1	Phase Space and Kinematics in Scattering Processes.	49
3.1.1	2-body Phase Space	50
3.1.2	3-body Phase Space	51
3.1.3	Differential Cross-Section	54
3.2	Leading Order Cross-Section	55
3.2.1	Kinematic Definitions	55
3.2.2	The Matrix Elements for Neutralino Pair Production.	55
3.2.3	Differential Cross-Section	57
3.2.4	Integrated Cross-Section	57
3.2.5	Generalising to All Electroweakinos	59
3.3	NLO Corrections	62
3.3.1	Factorisation	63
3.3.2	Virtual Exchange	66
3.3.3	Counterterms	68
3.3.4	Real Emission.	70
3.4	Gaugino Corrections	74
3.4.1	Catani-Seymour Dipole Formalism	75
4	Electroweakino Pair Production in Proton–Proton Collisions	79
4.1	The Parton Model and PDFs	79
4.1.1	Hadronic kinematics	79
4.1.2	Integration over PDFs.	80
4.1.3	Renormalised PDFs	81
4.2	Total Hadronic Cross-Section Result	84
5	Numerical Results	87
5.1	Setup and Execution	87
5.1.1	Renormalisation Scheme	87
5.1.2	Uncertainty and Errors	88
5.1.3	Spectrum Generation and Scenarios	89
5.2	Comparison.	92
5.2.1	Leading Order Comparison.	92
5.2.2	Next-to-Leading Order Comparison.	92
5.3	Scale Dependence and PDF Errors.	93
5.3.1	Scale Dependence	93
5.3.2	PDF Errors	95
5.4	Exploring CP-Violation.	96
5.4.1	cSPS1a scenario	97
5.4.2	Higgsino Scenario	97
5.5	Exploring Other Parameters.	98
5.5.1	Varying Higgsino Masses and CP-Violation.	99
5.5.2	Varying Squark and Gluino Masses	100
	Conclusion	103
A	Weyl Spinors & Grassmann Calculus	111
A.1	Weyl Spinors	111
A.2	Grassmann Calculus	113
B	Takagi Factorisation Algorithm	115
B.1	Proofs	115

List of Figures

1.1	Example of the arrow usage in this thesis. There is an incoming Dirac fermion ψ with a particle number flow indicated with the arrow on its line. Likewise, a complex scalar ϕ has an arrow on its line indicating particle number flow. A Majorana fermion χ has no such particle number flow indication. The arrow above the vertex indicates the defined fermion flow for this diagram.	15
1.2	Simple example of a loop diagram in a scalar theory.	15
1.3	Illustration of the momentum conventions for loop diagrams used in the Passarino-Veltman functions, with three-point and four-point loops as examples.	24
3.1	(a) Angular definition in the centre-of-mass frame of the initial particles with momenta $k_{i,j}$. (b) Angular definitions in the centre-of-mass frame of the outgoing particles with momenta $p_{i,j}$	54
3.2	The leading order diagrams contributing to neutralino pair production at parton-level.	55
3.3	Tree-level diagrams contributing to the production of a neutralino and chargino at parton level.	59
3.4	Tree-level diagrams contributing to the pair production of a chargino particle/anti-particle pair.	61
3.5	The two triangle diagrams contributing to NLO QCD corrections to the quark tensor.	67
3.6	The QCD quark self-energy diagrams used for extracting quark renormalisations.	68
3.7	Gluon emission diagrams	70
3.8	Quark emission diagrams	72
3.9	Box diagrams contributing to NLO QCD corrections to the gaugino part of neutralino pair production..	75
3.10	Vertex diagrams contributing to NLO QCD corrections to the gaugino part of neutralino pair production. The blobs are defined in Fig. 3.11.	75
3.11	The vertex insertions used in Fig. 3.10..	75
3.12	NLO QCD diagrams contributing to the self-energy of the squark.	76
3.13	Gluon emission diagrams with gaugino-like vertices for neutralino pair production.	76
3.14	Quark emission diagrams with gaugino-like vertices for neutralino pair production.	76

List of Figures

5.1	A plot showing the neutralino spectrum in the cSPS1a scenario. The first plot shows the neutralino masses as a function of the phase of μ , whereas the lower plot shows the amount of the interaction eigenstates in each neutralino mass eigenstate. The spectra were generated with <code>FlexibleSUSY</code>	90
5.2	Comparison of LO results from this thesis to those from <code>Resummino</code> for all possible neutralino pair processes. All cross-sections computed in the SPS1a benchmark point. The cross-sections computed with the implementation from this thesis are denoted σ_s , whereas results computed with <code>Resummino</code> are denoted σ_p	93
5.3	Comparison of results from this thesis to those from <code>Resummino</code> and the LHC SUSY Cross Section Working Group. Scale error is included in shaded regions around the lines in the upper plot, however, it is so inconsequential as to only be barely visible.	94
5.4	Scale dependence of the cross-section for the possible higgsino-like neutralino pairs. The vertical dashed lines indicate the lines for $\mu_0/2$ and $2\mu_0$ used to define the scale error.	95
5.5	Plot of the cross-section for $\tilde{\chi}_1^0 \tilde{\chi}_2^0$ production in the Higgsino scenario with PDF errors added. Denoting the mean mass of the final state pair $m_{\tilde{\chi}^0} = (m_{\tilde{\chi}_1^0} + m_{\tilde{\chi}_2^0})/2$, the scaling of the cross-section is given by the dimensionless quantity $\tilde{m}_{\tilde{\chi}^0} = m_{\tilde{\chi}^0} / \max(m_{\tilde{\chi}^0})$. The mass gap between the two neutralinos $m_{\tilde{\chi}_2^0} - m_{\tilde{\chi}_1^0}$ is never greater than 1.113 GeV.	96
5.6	The scaled cross-section for various neutralino pair production processes as the phase of μ is varied in the cSPS1a scenario. Underneath, the relative deviance of the scaled cross-sections as the phase moves away from $\phi_\mu = 0$ is shown. Given the average mass of the final state particles $m_{\tilde{\chi}^0} = (m_{\tilde{\chi}_i^0} + m_{\tilde{\chi}_j^0})/2$, the scaling is given by $\tilde{m}_{\tilde{\chi}^0} = m_{\tilde{\chi}^0}(\phi_\mu)/m_{\tilde{\chi}^0}(0)$. This ensures the cross-section for $\phi_\mu = 0$ is unscaled. Scale error is shown with the hatched bands around the lines..	97
5.7	The scaled cross-section for neutralino pair production of $\tilde{\chi}_1^0 \tilde{\chi}_2^0$ as the phase of μ is varied in the Higgsino scenario. Underneath, the relative deviance of the scaled cross-sections as the phase moves away from $\phi_\mu = 0$ is shown. Given the average mass of the final state particles $m_{\tilde{\chi}^0} = (m_{\tilde{\chi}_1^0} + m_{\tilde{\chi}_2^0})/2$, the scaling is given by $\tilde{m}_{\tilde{\chi}^0} = m_{\tilde{\chi}^0}(\phi_\mu)/m_{\tilde{\chi}^0}(0)$. This ensures the cross-section for $\phi_\mu = 0$ is unscaled. Scale error is shown with the hatched bands around the lines for the leading order cross-section, and filled bands for the NLO cross-section.	98
5.8	Scaled NLO cross-section results for pair production of the two lightest neutralinos in the Higgsino scenario as both $ \mu $ and ϕ_μ are varied. Given the average mass of the final state particles $m_{\tilde{\chi}^0} = (m_{\tilde{\chi}_1^0} + m_{\tilde{\chi}_2^0})/2$, the scaling is given by $\tilde{m}_{\tilde{\chi}^0} = m_{\tilde{\chi}^0}(\phi_\mu)/m_{\tilde{\chi}^0}(0)$. This ensures the cross-section for $\phi_\mu = 0$ is unscaled.	99
5.9	(a) Depicts the cross-section for pair production of the two lightest neutralinos to NLO in the simplified Higgsino scenario as the common squark mass and the gluino mass is varied separately. (b) Depicts the cross-section for neutralino pair production in the cSPS1a scenario as the common up-type and down-type squark masses are varied separately.	99

List of Tables

2.1	Table of superfields of the MSSM, and their component field names. Note that the fermion fields are left-handed Weyl spinors, in spite of any L or R in the boson field subscript. The conjugate superfields changes these to right-handed Weyl spinors. The indices i enumerate the three generations of leptons/quarks, k the three $SU(2)_L$ gauge fields and a the eight $SU(3)_C$ gauge fields.	38
2.2	Summary of quantum numbers for the MSSM scalar superfields. The charges of barred fields \bar{F} supplying the right-handed part of SM fermions are defined such that the charge of \bar{F}^\dagger matches that of its left-handed compliment. I note that the convention for the hypercharge differs from some sources, seeing as I use 1 as the generator of $U(1)_Y$ instead of $\frac{1}{2}$ used elsewhere. This amounts to shuffling some factors of $\frac{1}{2}$ around. The indices i enumerate the three generations of leptons/quarks.	39
2.3	A summary of the variables used in the derived Feynman rules and their definitions. Furthermore, it is extended with the Feynman rules beyond those derived explicitly in this thesis.	45
3.1	Table of the effective couplings defined for each type of electroweakino pair production process.	63
4.1	List of relations between hadronic and partonic kinematic variables.	80
5.1	Summary of MSSM parameters defining the Higgsino scenario used in this thesis. All parameters except $\tan\beta$ are given in GeV. m_0 denotes the common soft mass for all sfermions, taken to be diagonal in flavour space. A_0 is the common soft trilinear coupling, also taken to be diagonal in flavour space. A parametrisation of EWSB is chosen where M_A , the mass of the pseudoscalar Higgs boson, is kept as a free parameter.	92

List of Tables

List of Tables

List of Tables

Introduction

Since its inception, quantum field theory (QFT) has pushed the boundaries of what we know, and has fostered undoubtedly one of the greatest triumphs of modern physics – the Standard Model (SM). From a few principles, the SM has been able to make agreement between theory and experiment up to 12 significant digits, or one part in a trillion [1]. The predictions of the SM come from a set of matter-particles, the fermions, subjected to three internal gauge symmetries [2] providing three fundamental forces, and a Higgs mechanism [3] providing masses to the particles.

However, there still remains theoretical, as well as experimental, discrepancies in the SM – it does not explain gravity or cosmological observations such as dark matter or matter-antimatter imbalance, and its structure is somewhat *ad hoc*, without a unifying principle. Particularly, there is a large discrepancy between the energy scale of the electroweak sector at ~ 100 GeV, and the Planck scale around $\sim 10^{18}$ GeV, where we know gravity to become relevant. Without a mechanism for cancellation, the Higgs boson should be sensitive to any physics between these scales, including the Planck scale itself. The SM provides no solution to how the Higgs mass is of the same order as the physics we have already observed, known as the hierarchy problem [4, 5]. Furthermore, the matter-antimatter imbalance we see in the Universe today can only be explained by a violation of combined charge and parity (CP) invariance and baryon number [6], for which there is a mechanism in the SM [7, 8], insufficient [9]. In short, the Standard Model is not a complete theory, and the search for beyond the Standard Model (BSM) theories persists.

Motivated by solving many of these discrepancies, supersymmetry remains one of the most intensely studied and developed theories addressing them. Of all the extensions to the Standard Model, its minimal supersymmetric extension, the Minimal Supersymmetric Standard Model (MSSM), provides one of the most explored models for BSM physics. In this framework, every SM particle receives a *superpartner*, a particle with the same properties but opposite spin-statistics. That is, every fermion receives a bosonic counterpart and every boson receives a fermionic counterpart. These superpartners provide possible explanations for dark matter [10] and suggest a ‘grand unification’ of the gauge symmetries at some higher energy scale [11]. Particularly, the MSSM, where the lightest supersymmetric particle is absolutely stable, provides a stable, weakly interacting massive particle (WIMP), which is a good candidate for cold dark matter [12]. In many MSSM scenarios, the lightest supersymmetric particle will be the lightest *neutralino*, a partner to the Higgs boson, photon and Z -boson of the SM. More broadly, the Higgs and electroweak boson superpartners are called electroweakinos, and will be the focus of this thesis.

As supersymmetry must be broken at low energy scales, agnosticism to a breaking mechanism means that the parameter space of the MSSM becomes vast. In exploring

this parameter space, the most unambiguous mode of discovery is direct production of the superpartners, as in particle collider experiments. Seeing as the extra particles of the MSSM are predicted to be in a mass range of ~ 10 GeV to a few TeVs – 10 to 1000 times that of the proton mass – direct production will require great energies. This makes the proton–proton collisions at the Large Hadron Collider (LHC) at CERN a natural avenue for discovery. In this thesis, I will focus on the calculation of the production cross-sections for electroweakino pairs in the setting of proton–proton collisions at the LHC.

Particularly, I will focus on the derivation of the electroweakino interactions from the most general MSSM model, and computing the cross-sections with general scenarios in mind. This means keeping complex and off-diagonal parameter values that allow for CP violating interactions and effects from quark flavour violation in the electroweakino sector. With general parameter dependence, MSSM scenarios explaining multiple issues such as insufficient CP violation and providing dark matter candidates simultaneously can be explored. To increase the sensitivity when comparing the theoretical results to experiment, higher order corrections from perturbative QFT are needed, which in the context of proton collisions means we must add corrections to the electroweakino pair production from quantum chromodynamics (QCD). However, higher order corrections lead to many problems in the perturbative framework we have. Specifically, divergences appear in the theory, leading to the necessity of reassessing the parameters and fields. This leads to the procedure of renormalisation, which ultimately renders finite observable values for the cross-sections.

Another point of subtlety coming from the QCD nature of protons is also addressed. Due to the phenomena of colour confinement and asymptotic freedom [13], the fundamental particles of QCD are confined to structures such as the proton, whereas interactions with the proton is described by interaction with the fundamental particles of QCD. This leads to the formulation of the parton model for proton scattering, where the structure of the constituents of the proton is captured by *parton distribution functions*, allowing for the translation of scattering between fundamental QCD particles to the full proton scattering.

Outline

This Master’s thesis is roughly divided into three parts: The first two chapters deal with the theoretical framework used in the calculations later on. The next two chapters tackle the calculation of cross-sections for electroweakino pairs in proton–proton collisions. Finally, the last chapter deals with numerical implementation of the cross-sections, getting concrete results from different combination of parameter values of the MSSM. The general outline of the thesis follows:

Chapter 1: To start, I outline the theoretical framework used for the calculations in this thesis. Quantum field theory is introduced, and methods for computing finite observables are presented.

Chapter 2: Next, I introduce supersymmetry, including tools for building manifestly supersymmetric quantum field theories. These are then put to use building the Minimal Supersymmetric Standard Model, and the Feynman rules for electroweakinos are derived from this.

Chapter 3: In this chapter, the calculations for electroweakino pair production from quarks and gluons are computed, up to next-to-leading order.

Chapter 4: The calculations from the previous chapter are here sewn together to create finite, observable cross-sections for proton–proton collisions using the parton model. General forms for such cross-sections are presented to next-to-leading order.

Chapter 5: Finally, numerical implementation of the cross-sections of the previous chapter is presented. Deriving a selection of physical scenarios from the MSSM parameters using external packages, general parameter dependence with error estimates are derived.

List of Tables

Chapter 1

Quantum Field Theory

In this chapter, I will go through the basics of quantum field theory (QFT) as relevant to this thesis. I begin by formulating the perturbative approach to calculating correlation functions in interacting theories, and relate them to scattering cross-sections through the S -matrix. In doing so, I introduce Feynman diagrams and Feynman rules, and go into some detail on dealing with fermions. The Feynman rules will be a defining quality of the supersymmetric QFT model that I will discuss in the next chapter.

In the following section, I go through divergences in perturbative QFT, and outline the procedure of renormalisation to make the theory finite. I then go on to discuss Yang-Mills theory as a means for model building, which will be built on further in the next chapter. Lastly, I briefly introduce Passarino-Veltman reduction for writing out general loop integrals that will crop up in the calculations in Chapter 3.

1.1 Perturbative Quantum Field Theory

In this thesis, I will use the Lagrangian framework to formulate QFT. Here I will introduce the basics of how to formulate a QFT in such a way using the path integral formalism. It is not intended as a complete introduction with proofs, but rather a summary of the tools that are used, with some simple examples. This leads to a perturbative formulation of scattering and computation of correlation functions, which is the basis for the calculations that will be made later on.

1.1.1 The Path Integral

I will start by introducing some useful shorthands that will be used throughout this section. Consider an action $S[\{\Phi\}]$ as a functional of some classical fields $\{\Phi\}$. Let $\phi_i \equiv \phi(x_i)$ for some arbitrary field $\phi \in \{\Phi\}$ evaluated at some point in space-time x_i —the path integral approach to quantum field theory is built on time-ordered correlation functions through the relation [14]

$$\langle \Omega | T \{ \hat{\phi}_1(x_1) \cdots \hat{\phi}_n(x_n) \} | \Omega \rangle = \frac{\int \mathcal{D}\phi \phi_1(x_1) \cdots \phi_n(x_n) e^{iS[\{\Phi\}]}}{\int \mathcal{D}\phi e^{iS[\{\Phi\}]}} , \quad (1.1)$$

where $T \{.\}$ denotes the time-ordering operation and $\mathcal{D}\phi$ is the measure denoting integration over all possible *field configurations*. A field configuration here is understood as a given set of values for each of the fields $\{\Phi\}$, one for each point in space-time. The time-ordering operation will put the fields in chronological order according to the time at which they are evaluated, with the “first” field being farthest to the right. In other

words, the fields are ordered by the zeroth component of their argument space-time coordinate x . In the left-hand side of Eq. (1.1) the fields are understood as operators on the Hilbert space of states in our interacting theory (denoted by their hats), and $|\Omega\rangle$ is the vacuum state. In this way quantum effects are encapsulated through the weighted sum of all classical *paths* through configuration space, rather than just whichever one minimises the action. Qualitatively, these correlation functions tell us about how certain field values at positions \mathbf{x}_i at times t_i are correlated, i.e. if ϕ has a certain value $\phi(t, \mathbf{x})$ at position \mathbf{x} and time t , what does this tell us about the value of field $\phi'(t', \mathbf{x}')$ at time t' and position \mathbf{x}' .

1.1.2 Perturbing the Free Theory

In interacting theories, correlation functions can be obtained through a *perturbation series* by expanding them around a coupling constant λ , denoting the strength of the interaction. To compute time-ordered correlation functions with Eq. (1.1), we need to exponentiate the action. Assuming that the Lagrangian of the action can be written on the form $\mathcal{L} = \mathcal{L}_0 - \lambda \mathcal{L}_{\text{int}}$, this exponentiation can be written as

$$e^{i \int d^4x (\mathcal{L}_0 - \lambda \mathcal{L}_{\text{int}})} = e^{i \int d^4x \mathcal{L}_0} \left(1 - i\lambda \int d^4x_1 \mathcal{L}_{\text{int}}(x_1) \right. \quad (1.2)$$

$$\left. - \frac{\lambda^2}{2} \int d^4x_1 \int d^4x_2 \mathcal{L}_{\text{int}}(x_1) \mathcal{L}_{\text{int}}(x_2) + \dots \right). \quad (1.3)$$

For simplicity, let us consider a theory with just one, self-interacting field ϕ . Now say the interaction Lagrangian \mathcal{L}_{int} is some monomial of degree p in ϕ ,¹ then the interacting correlation functions can be written in terms of free-theory correlation functions! To see this, we consider the interacting n -point function $D_{\text{int}}^n(1, \dots, n) = \langle \Omega | T \{ \hat{\phi}_1 \cdots \hat{\phi}_n \} | \Omega \rangle$, and write the normalisation out in terms of the free and interacting Lagrangians:

$$D_{\text{int}}^n(1, \dots, n) = \frac{1}{\mathcal{N}} \int \mathcal{D}\phi \phi_1 \cdots \phi_n e^{i \int d^4x \mathcal{L}_0} \left(1 - i\lambda \int d^4y \mathcal{L}_{\text{int}} + \mathcal{O}(\lambda^2) \right), \quad (1.4)$$

where the normalisation is given by $\mathcal{N} = \int \mathcal{D}\phi e^{i \int d^4x \mathcal{L}}$. To relate this to the free-theory, let us take a moment to write this out. Given the free-field n -point correlator $D_0^n(1, \dots, n) \equiv \frac{1}{\mathcal{N}_0} \int \mathcal{D}\phi \phi_1 \cdots \phi_n e^{i \int d^4x \mathcal{L}_0}$ with normalisation $\mathcal{N}_0 = \int \mathcal{D}\phi e^{i \int d^4x \mathcal{L}_0}$, expanding the interacting normalisation gives

$$\mathcal{N} = \mathcal{N}_0 \left(1 - i\lambda \int d^4y D_0^p(y, \underbrace{\dots, y}_{p \text{ times}}) - \frac{\lambda^2}{2} \int d^4y \int d^4z D_0^{2p}(y, \underbrace{\dots, y}_{p \text{ times}}, \underbrace{z, \dots, z}_{p \text{ times}}) + \mathcal{O}(\lambda^3) \right). \quad (1.5)$$

Inserting this into Eq. (1.4) and expanding around $\lambda = 0$ we get

$$\begin{aligned} D_{\text{int}}^n(1, \dots, n) &= \frac{D_0^n(1, \dots, n) - i\lambda \int d^4y D_0^{n+p}(1, \dots, n, \overbrace{y, \dots, y}^{p \text{ times}}) + \mathcal{O}(\lambda^2)}{1 - i\lambda D_0^p(y, \underbrace{\dots, y}_{p \text{ times}}) + \mathcal{O}(\lambda^2)} \\ &= D_0^n(1, \dots, n) - i\lambda \int d^4y \left(D_0^{n+p}(1, \dots, n, \underbrace{y, \dots, y}_{p \text{ times}}) - D_0^n(1, \dots, n) D_0^p(y, \underbrace{\dots, y}_{p \text{ times}}) \right) + \mathcal{O}(\lambda^2). \end{aligned} \quad (1.6)$$

¹In the more general case where it can be expressed with some polynomial in the fields, we can look at each monomial term separately, without loss of generality.

We can see from this that perturbation from $\lambda = 0$ will give corrections to the free two-point correlator that add correlations with additional space-time points that are integrated over. These additional self-correlating points will diagrammatically form loops, as we will see an example of in the next section. I note that the role of the second term at order λ is to remove all *disconnected* diagrams that contribute to the first term. Disconnected diagrams are diagrams where the self-correlating additional space-time points are not connected to the external space-time points, and as such should not be causally related to them.

1.1.3 Feynman Rules in Position Space

Let us now investigate closer what we can get from the expansion around the free theory in Eq. (1.6). To do this, let us consider a concrete theory, given by the Lagrangian

$$\mathcal{L} = \underbrace{\frac{1}{2}(\partial^\mu\phi)(\partial_\mu\phi)}_{\mathcal{L}_0} - \underbrace{\frac{1}{2}m^2\phi^2}_{\mathcal{L}_{\text{int}}} - \lambda \underbrace{\phi^4}_{\mathcal{L}_{\text{int}}}. \quad (1.7)$$

Furthermore, I will use the Schwinger-Dyson equations [14] for the non-interacting theory, which relates different n -points correlators through

$$(\square_x + m^2)D_0^{n+1}(x, 1, \dots, n) = -i \sum_i \delta^4(x - x_i) D_0^{n-1}(1, \dots, i-1, i+1, \dots, n), \quad (1.8)$$

where $\square = \partial^\mu\partial_\mu$ is the d'Alembertian operator. It follows that

$$(\square_x + m^2)D_0^2(x, y) = -i\delta^4(x - y). \quad (1.9)$$

Consider the 2-point correlator $D_{\text{int}}^2(1, 2)$ of the interacting theory. By Eq. (1.6), this is given to first order in λ by

$$D_{\text{int}}^2(1, 2) = D_0^2(1, 2) - i\lambda \int d^4y \left(D_0^6(1, 2, y, y, y, y) - D_0^2(1, 2)D_0^4(y, y, y, y) \right). \quad (1.10)$$

We can rewrite the six-point correlator to employ Eq. (1.9) and get

$$\begin{aligned} D_0^6(1, 2, y, y, y, y) &= \int d^4x \delta^4(x - x_1) D_0^6(x, 2, y, y, y, y) \\ &= i \int d^4x (\square_x + m^2) D_0^2(x, 1) D_0^6(x, 2, y, y, y, y) \\ &= i \int d^4x D_0^2(x, 1) (\square_x + m^2) D_0^6(x, 2, y, y, y, y), \end{aligned} \quad (1.11)$$

where in the last equality I have used partial integration twice. We can then use Eq. (1.8) to get

$$\begin{aligned} D_0^6(1, 2, y, y, y, y) &= \int d^4x D_0^2(x, 1) \left\{ \delta^4(x - x_2) D_0^4(y, y, y, y) + 4\delta^4(x - y) D_0^4(2, y, y, y) \right\} \\ &= D_0^2(1, 2) D_0^4(y, y, y, y) + 4D_0^2(1, y) D_0^4(2, y, y, y), \end{aligned} \quad (1.12)$$

where I have used the property of the correlators that they are symmetric in their arguments because of the time-ordering operator. Notice that the first term here will

cancel the last term in Eq. (1.10) as promised. We can now use the same procedure to write out the four-point correlator

$$\begin{aligned} D_0^4(2, y, y, y) &= i \int d^4x (\square_x + m^2) D_0^2(x, 2) D_0^4(x, y, y, y) \\ &= \int d^4x D_0^2(x, 2) 3\delta^4(x - y) D_0^2(y, y) = 3D_0^2(y, y) D_0^2(y, 2). \end{aligned} \quad (1.13)$$

Putting it all together in Eq. (1.10), we get that the interacting two-point correlator in this theory is

$$D_{\text{int}}^2(1, 2) = D_0^2(1, 2) - 12i\lambda \int d^4y D_0^2(1, y) D_0^2(y, y) D_0^2(y, 2), \quad (1.14)$$

to first order in the coupling constant λ .

This procedure can be put together diagrammatically – associating the free two-point correlators $D_0^2(x, y)$ with edges between two points x, y , and vertices where multiple edges meet with a factor of $ik\lambda \int d^4x$, where k is the number of configurations of equal fields in \mathcal{L}_{int} . Due to this last point, it is therefore common to rescale the Lagrangian parameter $\lambda \rightarrow \frac{\lambda}{k}$, such that the insertions will not contain any numerical factors. In the case of our ϕ^4 theory, we should have $k = 4!$, however, comparing to our result in Eq. (1.14) we see that we only have a numerical factor of $12 = \frac{4!}{2}$. This is a result of the *symmetry factor* of the diagram, as the loop in y is (trivially) symmetric under exchange of its endpoints. By including the factor of $p!$ in the vertex rule, we must divide by the symmetry factor, which are the number of ways you can change the edges of a diagram and still get the same result. Another subtlety relates to the factor of $\frac{1}{n!}$ associated with the λ^n term in the perturbation expansion Eq. (1.6). This coincides with the fact that the n th order term gives equal contributions under the interchange of its internal vertices. There are $n!$ ways of interchanging these vertices, and so this factor cancels out neatly in the end.

Returning to our example, we can depict Eq. (1.14) diagrammatically by

$$D_{\text{int}}^n(1, 2) = x_1 \circ \dots \circ x_2 + x_1 \circ \underset{y}{\bullet} \circ x_2. \quad (1.15)$$

Here, I have denoted *vertices* associated with the coupling constant insertion with filled dots, and external points with empty dots for clarity. This practice will not be kept for the remainder of the thesis.

In summary, the following rules relate a Feynman diagram to the two-point correlators of the free theory:

- (I) A factor of $D_0^2(x, y)$ for every edge connecting two points x, y . This factor is referred to as the *propagator*
- (II) A factor of $-i\lambda \int d^4x$ for every internal vertex point x .
- (III) An overall numerical factor of S^{-1} , where S is the symmetry factor. This is the total number of ways internal lines can be exchanged without changing the diagram.

To get the full correlator to a given perturbative order, we must sum over all *different*, connected Feynman diagrams to that order.

1.1.4 The S-Matrix and LSZ Reduction Formula

To relate the correlation functions above to physical experiment, e.g. scattering amplitudes, we will need to more concretely define how an observable can be extracted from the theory. Let us for a moment go to the quantum mechanical picture of Hilbert space formalism to formulate a scattering experiment. Idealising the scenario, let us consider the amplitude of an *asymptotic* in-state $|\psi_i\rangle$ of free fields at $t = -\infty$ evolving into an asymptotic out-state $|\psi_f\rangle$ of some (potentially other) fields at $t = +\infty$. The interaction between is captured by the S -matrix, and the amplitude is given by the inner product

$$\langle \psi_f | S | \psi_i \rangle. \quad (1.16)$$

Squaring this amplitude gives us the probability for the given initial configuration to end up in the given final configuration. So, with adequately realisable in/out states, the experiment can be conducted many times to extract an experimental probability we can compare to. For scattering experiments, we will usually look at in/out states with a given particle number in certain momentum eigenstates, for which I will now outline a procedure for relating the correlation functions above to the S -matrix amplitude of Eq. (1.16).

This procedure is due Lehmann, Symanzik and Zimmermann [15], who derived the LSZ reduction formula relating the correlation functions to the S -matrix. Given initial fields with momenta p_1, \dots, p_k and final fields with momenta p_{k+1}, \dots, p_n in our scalar theory Eq. (1.7), it reads [14]

$$\begin{aligned} \langle p_{k+1} \cdots p_n | S | p_1 \cdots p_k \rangle &= \left(\prod_{i=1}^k i \int d^4 x_i e^{-ip_i \cdot x_i} (\square_{x_i} + m^2) \right) \\ &\times \left(\prod_{i=k+1}^n i \int d^4 x_i e^{+ip_i \cdot x_i} (\square_{x_i} + m^2) \right) \times \langle \Omega | T \{ \phi(x_1) \cdots \phi(x_n) \} | \Omega \rangle. \end{aligned} \quad (1.17)$$

Usually, we encapsulate the information of the S -matrix in *matrix elements* \mathcal{M} by writing it on the form

$$S = \mathbb{I} + i(2\pi)^4 \delta^4 \left(\sum_{i=1}^k p_i - \sum_{i=k+1}^n p_i \right) \mathcal{M}, \quad (1.18)$$

essentially dropping the trivial overlap between the in- and out-states and factoring out momentum conservation.

Let us now put this to use in our scalar toy model from Section 1.1.3, computing the transition for a field with momentum p_1 to end up with momentum p_2 using Eq. (1.16) to first order in λ :

$$\begin{aligned} \langle p_2 | S | p_1 \rangle &= \left(i \int d^4 x_1 e^{-ip_1 \cdot x_1} (\square_{x_1} + m^2) \right) \left(i \int d^4 x_2 e^{+ip_2 \cdot x_2} (\square_{x_2} + m^2) \right) \times D_{\text{int}}^2(1, 2) \\ &= - \int d^4 x_1 e^{-ip_1 \cdot x_1} (\square_{x_1} + m^2) \int d^4 x_2 e^{+ip_2 \cdot x_2} (\square_{x_2} + m^2) \\ &\times \left\{ D_0^2(1, 2) - \frac{i\lambda}{2} \int d^4 y D_0^2(1, y) D_0^2(y, y) D_0^2(y, 2) \right\} \\ &= - \int d^4 x_1 e^{-ip_1 \cdot x_1} (\square_{x_1} + m^2) \left\{ ie^{ip_2 \cdot x_1} - \frac{\lambda}{2} \int d^4 y e^{-ip_2 \cdot y} D_0^2(1, y) D_0^2(y, y) \right\} \\ &= \int d^4 x_1 \left\{ -i(p_2^2 - m^2) - \frac{i\lambda}{2} D_0^2(x_1, x_1) \right\} e^{-i(p_1 - p_2) \cdot x_1}, \end{aligned} \quad (1.19)$$

where in the second equality I inserted Eq. (1.14), and in the third and fourth equalities I used the Schwinger-Dyson equation Eq. (1.9). By the on-shell condition on p_2 , the first term vanishes. For the second term, we can use that the two-point correlator, see Eq. (1.9), is given by its Fourier transform as

$$D_0^2(x, y) = \int \frac{d^4 k}{(2\pi)^4} \tilde{D}_0^2(k) e^{ik \cdot (x-y)}, \quad (1.20)$$

to arrive at

$$\langle p_2 | S | p_1 \rangle = -i(2\pi)^4 \delta^4(p_1 - p_2) \frac{\lambda}{2} \int \frac{d^4 k}{(2\pi)^4} \tilde{D}_0^2(k). \quad (1.21)$$

We can relate this to the matrix element \mathcal{M} , by assuming that the asymptotic in/out-states do not overlap, to find through the definition Eq. (1.18) that

$$\begin{aligned} \langle p_2 | i(2\pi)^4 \delta^4(p_2 - p_1) \mathcal{M} | p_1 \rangle &= -i(2\pi)^4 \delta^4(p_1 - p_2) \frac{\lambda}{2} \int \frac{d^4 k}{(2\pi)^4} \tilde{D}_0^2(k) \\ &\Rightarrow i\mathcal{M} = -\frac{i\lambda}{2} \int \frac{d^4 k}{(2\pi)^4} \tilde{D}_0^2(k). \end{aligned} \quad (1.22)$$

This result can also be arrived at diagrammatically, leading us to define Feynman diagrams and Feynman rules in *momentum space*. The procedure for drawing diagrams is the same as before, but now every external point is associated with an external momentum, and every line carries momentum with it. Momentum flow can be indicated with arrows for clarity. The resulting Feynman rules are similar to before, but now give:

- (I) A factor of $\tilde{D}_0^2(p)$ for every *internal* line associated with a momentum p .
- (II) A factor of $-i\lambda$ for every internal vertex point.
- (III) External points are associated with a factor of 1.
- (IV) Momentum conservation should be enforced through every vertex point.
- (V) Any undetermined momentum k of internal lines must be integrated over with a factor $\int \frac{d^4 k}{(2\pi)^4}$.
- (VI) An overall numerical factor of S^{-1} , where S the symmetry factor. This is the total number of ways internal lines can be exchanged without changing the diagram.

1.1.5 Feynman Rules for Fermions

Later on, we will be considering fermion fields, which have spinor structure. I go into more detail on the properties of spinors in Appendix A. When considering correlation functions of spinor fields, it is usually most convenient to work with the correlation of Lorentz-invariant contractions of the spinor field components. This imposes some additional structure on the Feynman rules. More generally, external fermion points will be associated with spinors, whereas propagators and vertices can be operators on spinor space.²

²In fact, these arguments hold for other Lorentz structures such as four-vectors or tensors of any rank.

Let us first consider the external fermions. Consider a Dirac spinor field ψ with a conjugate field $\bar{\psi}$, and with mass m . The general, quantised solution for a free Dirac spinor field is [16]

$$\psi(x) = \int \frac{d^3 p}{(2\pi)^3} \frac{1}{\sqrt{2E_p}} \sum_s \left(a_s(\mathbf{p}) u_s(p) e^{-ip \cdot x} + b_s^\dagger(\mathbf{p}) v_s(p) e^{ip \cdot x} \right), \quad (1.23)$$

where $E_p = m^2 + \mathbf{p}^2$, $u_s(p), v_s(p)$ are particle and antiparticle spinors of spin s , and $a_s^\dagger(\mathbf{p}), b_s^\dagger(\mathbf{p})$ are creation operators creating particle and antiparticle states with momentum \mathbf{p} and spin s respectively. Normalisation is chosen such that $a_s^\dagger(\mathbf{p}) |0\rangle = \sqrt{2E_p} |\mathbf{p}, s\rangle$ and $\langle \mathbf{q}, r | \mathbf{p}, s \rangle = 2E_p (2\pi)^3 \delta^3(\mathbf{p} - \mathbf{q}) \delta_{rs}$, where $|\mathbf{p}, s\rangle$ denotes a fermionic particle state with momentum \mathbf{p} and spin s .

The derivation of the LSZ reduction formula will differ slightly going from scalar theory to the fermionic one. Particularly, one needs the inner product

$$\begin{aligned} \langle 0 | \psi(x) | \mathbf{q}, r \rangle &= \int \frac{d^3 p}{(2\pi)^3} \frac{1}{\sqrt{2E_p}} \sum_s \frac{1}{\sqrt{2E_p}} \langle \mathbf{p}, s | u_s(p) e^{-ip \cdot x} | \mathbf{q}, s \rangle \\ &= \int \frac{d^3 p}{(2\pi)^3} \frac{1}{\sqrt{2E_p}} \sum_s \frac{1}{\sqrt{2E_p}} 2E_p (2\pi)^3 \delta^3(\mathbf{p} - \mathbf{q}) \delta_{rs} u_s(p) e^{-ip \cdot x} \\ &= u_r(q) e^{-iq \cdot x}, \end{aligned} \quad (1.24)$$

where it was used that $q^2 = p^2 = m^2$ such that when $\mathbf{q} = \mathbf{p}$ we have $q^0 = p^0$. This differs from the scalar theory where $\langle 0 | \phi(x) | \mathbf{q} \rangle = e^{-iq \cdot x}$. In the end, the effect this has is that external fermion points of Feynman diagrams will be associated with the corresponding spinors, instead of the trivial factor of 1 for the scalar theory.

For a Lorentz-covariant theory, the Lagrangian will only contain Lorentz invariant contractions of the spinors, all of which can be decomposed into Dirac *bilinears* on the form

$$\bar{\psi} \Gamma^r \psi, \quad (1.25)$$

where Γ^r form a basis for operators on spinor space. One realisation of such a basis for four-component spinors is using the Dirac gamma-matrices $\Gamma^r = \{\mathbb{I}, \gamma^\mu, \gamma^{\mu\nu}, \gamma^\mu \gamma^5, \gamma^5\}$, where $\gamma^{\mu\nu} = \frac{i}{2} [\gamma^\mu, \gamma^\nu]$ and we understand $\nu < \mu$. Feynman rules for propagators and vertices will generally contain Lorentz invariant linear combinations of such operators.

With the additional spinor structure in the diagrams, it is important that the spinors and operators on spinor space are ordered correctly in the amplitudes, as to produce the intended Lorentz invariant contractions. This is usually done by defining a *fermion flow* in the diagrams, usually denoted by an arrow on the fermion lines. The procedure goes like this: Starting at the end of a fermion flow, insert spinors associated with external lines and spinor operators associated with internal lines and vertices until you get to the start of the fermion flow. Repeat this for all separated fermion flows in the diagram.

Another point of subtlety is that fermionic spinor fields are anticommuting. This causes the fermionic correlation functions to become antisymmetric under interchange of the fermions, e.g. $D_\psi^2(1, 2) = -D_\psi^2(2, 1)$. There are two important consequences of this: Firstly, closed fermion loops get an overall factor of -1 . Secondly, different diagrams get a *relative sign of interfering Feynman diagrams* (RSIF). By keeping the order of the fermionic fields in the correlation function consistent between diagrams, a different amount of (anti-)commutations might be needed for different terms in the expansion Eq. (1.2). The overall minus sign of the amplitude will be ambiguous, depending on how you choose to order fields, but relative signs between diagrams that are added together

will be absolute. The ambiguity can be resolved by looking at the order in which external spinors come in the amplitude, giving an additional minus sign to spinor orders that are an odd permutation as compared to some arbitrary reference permutation.

Summarised, the additional Feynman rules of fermions are

- (I) External spinors and vertex factors are inserted starting at the end of every fermion flow, moving backwards, ending on the start of a fermion line. Incoming (outgoing) fermion particles of momentum p and spin s are associated with a factor $u_s(p)$ ($\bar{u}_s(p)$). Incoming (outgoing) fermion anti-particles of momentum p and spin s are associated with a factor $\bar{v}_s(p)$ ($v_s(p)$).
- (II) A factor of -1 is associated with every closed fermion loop.
- (III) A RSIF is assigned to any diagram by evaluating the evenness of the order in which spinors arise as compared to some freely chosen reference order. The reference order must be kept consistent throughout all diagrams.

Lastly, I will note a point of added complexity when dealing with Majorana fermions, i.e. fermions that are their own anti-particles. Fermion flows as we have defined them can lead to ambiguities when dealing such fermions. This is because the fermion flows can be defined to go both ways, as the same operators are used to create both particle and anti-particle spinors $u_s(p)/v_s(p)$, creating ambiguity in the RSIF of specific diagrams. To alleviate this, I will follow a prescription due to Denner et al. [17]. Arrows on lines will be used to indicate *particle number flow*, used both for Dirac fermions and particle number conserving scalar fields. Fermion flows, however, will be denoted with an additional arrow along fermion lines. The direction of these flows can be defined arbitrarily, but the Feynman rules will be amended by whether the flow goes with/against the particle number flow, and into/out of vertices. By using the appropriate, amended Feynman rules proposed in [17], the fermion flows can be defined any way we would like, and the RSIF due to the parity of the spinor permutation can be inserted naively. The amended Feynman rules make sure that the RSIF will be correct, even though fermion flows are not defined consistently between the diagrams. In fermion lines with only Majorana particles, Feynman rules are the same regardless of fermion flow, however, for Dirac fermions, the following amendments are made:

- (I) Momentum space propagators $\tilde{D}_0^2(p)$ for a fermion propagator is replaced by $\tilde{D}_0^2(-p)$ if the particle number flow goes against the fermion flow. Otherwise, the ordinary propagator is used.
- (II) For vertex rules including Dirac fermions, the spinor operator Γ associated with the vertex must be replaced by $C\Gamma^TC^{-1}$ if the fermion flow is defined contrary to the particle number flow. Here C is the charge conjugation matrix, which I define in Appendix A.

I exemplify this use of arrows indicating particle number flow and fermion flow in Fig. 1.1.

1.2 Renormalised Quantum Field Theory

We have seen how correlation functions in interacting theories can be calculated as perturbations to the free, non-interacting theory. In this section, I will go more into

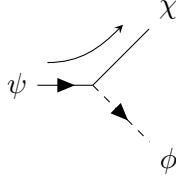


Figure 1.1: Example of the arrow usage in this thesis. There is an incoming Dirac fermion ψ with a particle number flow indicated with the arrow on its line. Likewise, a complex scalar ϕ has an arrow on its line indicating particle number flow. A Majorana fermion χ has no such particle number flow indication. The arrow above the vertex indicates the defined fermion flow for this diagram.

detail on the actual computation of the amplitudes, particularly touching on infinities that arise when computing higher order corrections naïvely. This leads to the procedure of regularisation to classify the infinities, and renormalisation to get rid of them. These methods will be necessary in the computation of higher order corrections in later chapters.

1.2.1 Loop Integrals and Divergences

Divergences appear in perturbative correlation functions in QFT, and can be categorised into *ultraviolet* (UV) divergences and *infrared* (IR) divergences. They are so named after which region of momentum space they originate from — high momentum for UV and low momentum for IR. The two types of divergences are dealt with differently, and here I will lay out how to deal with UV divergences through *renormalisation*.

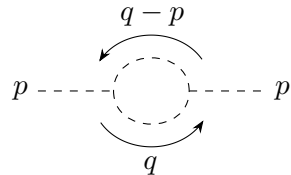


Figure 1.2: Simple example of a loop diagram in a scalar theory.

Consider a loop like the one in Fig. 1.2: The propagator of a free scalar theory is given by [14]

$$\tilde{D}(p) = \frac{i}{p^2 - m^2 + i\epsilon}, \quad (1.26)$$

where the $i\epsilon$ gives a prescription for dealing with the pole at $p^2 = m^2$ and is taken to 0 in the end. The prescription used here is called the Feynman prescription, and it ensures that the two-point correlator $D(x, y) = \int \frac{d^4 p}{(2\pi)^4} \tilde{D}(p) e^{-ip \cdot (x-y)}$ is a time-ordered correlator of x and y . If we consider a massless particle in the loop, and massless external particles $p^2 = 0$, the amplitude Fig. 1.2 will take the form³

$$\int \frac{d^4 q}{(2\pi)^4} \frac{1}{(q^2 + i\epsilon)((q-p)^2 + i\epsilon)} = \int \frac{d^4 q}{(2\pi)^4} \frac{1}{(q^2 + i\epsilon)^2}. \quad (1.27)$$

³One can see the equivalence by introducing Feynman parametrisation to rewrite

$$\frac{1}{AB} = \int_0^1 dx \frac{1}{(xA + (1-x)B)^2}$$

and shifting the integration variable.

The Lorentz signature of the momenta, giving $q^2 = q_0^2 - |\mathbf{q}|^2$ makes integration somewhat cumbersome, so we will use a trick called *Wick rotation* [14]. This entails deforming the integration contour around q_0 in the complex plane along the real and imaginary axes, making sure not to enclose the poles. By Cauchy's integral theorem, the total integral then vanishes, and the contributions going from $+\infty$ to $+i\infty$ and from $-i\infty$ to $-\infty$ vanish by Jordan's lemma. This means that the integral contribution from $+i\infty$ to $-i\infty$ must be equal but opposite of the integral along the real axis. Therefore, we can rather choose to integrate along the imaginary axis, substituting $q_0 = iq_0^E$. This will change the signature of the inner product such that

$$q_0^2 - |\mathbf{q}|^2 = q^2 = -q_E^2 = -(q_0^E)^2 - |\mathbf{q}^E|^2 \equiv -|\mathbf{q}_E|^2, \quad (1.28)$$

where I have defined $\mathbf{q}^E = \mathbf{q}$ and $\mathbf{q}_E = (q_0^E, \mathbf{q}^E)$. The result is that the loop integral Eq. (1.27) turns into

$$\int \frac{d^4 q}{(2\pi)^4} \frac{1}{(q^2 + i\epsilon)^2} = i \int \frac{d^4 \mathbf{q}_E}{(2\pi)^4} \frac{1}{|\mathbf{q}_E|^4} = \frac{i\Omega_4}{(2\pi)^4} \int_0^\infty dq_E \frac{1}{q_E}, \quad (1.29)$$

where after Wick rotation I took the limit of $\epsilon \rightarrow 0$, and I changed to four-dimensional spherical coordinates in the last equality where $\Omega_4 = 2\pi^2$ is the surface area of a unit sphere in four dimensions. For reference, the d -dimensional spherical surface is given by

$$\Omega_d = \frac{2\pi^{d/2}}{\Gamma(d/2)}, \quad (1.30)$$

where $\text{Gamma}(n)$ is the Gamma-function, analytically continuing the factorial to arbitrary real numbers, which will prove useful shortly. The factor of i comes from the change of variable from $q_0 \rightarrow q_0^E = -iq_0$. This diverges for both low and high momenta q_E . Had the particle been massive, the momentum would have a non-zero lower limit, and the IR divergence from the low-momentum limit would disappear. However, the UV divergence must be handled differently.

1.2.2 Regularisation

A first step to handle the divergences is to deform our theory in some way to make the loop integral formally finite, but recovering the divergence in the limit that the deformation disappears. An intuitive deformation would be to cap the momentum integral at some Λ , recovering our original theory in the limit $\Lambda \rightarrow \infty$. To illustrate the procedure of regularisation and subsequently renormalisation, it will be useful to have an example, for which I choose a scalar Lagrangian

$$\mathcal{L} = \frac{1}{2} (\partial_\mu \phi)^2 - \frac{1}{2} m_\phi^2 \phi^2 - \frac{\lambda}{3!} \phi^3. \quad (1.31)$$

Regularising the IR divergence in Eq. (1.27) by giving our scalar a mass m to the loop particle, and the UV divergence with a momentum cap Λ , we are left with

$$\begin{aligned} \int_{|q| < \Lambda} \frac{d^4 q}{(2\pi)^4} \frac{1}{((q^2 - m^2) + i\epsilon)^2} &= \frac{i}{(2\pi)^4} \int d\Omega_4 \int_0^\Lambda dq_E \frac{q_E^3}{(q_E^2 - m^2)^2} \\ &= \frac{i}{16\pi^2} \left\{ \ln \left(1 + \frac{\Lambda^2}{m^2} \right) - \frac{\Lambda^2}{\Lambda^2 + m^2} \right\}, \end{aligned} \quad (1.32)$$

where now evidently the divergence manifest as a logarithm.

Dimensional Regularisation

Another popular choice of regularisation, which I will use in this thesis, is *dimensional regularisation*. It entails analytically continuing the number of space-time dimension from the ordinary 4 dimensions to $d = 4 - 2\epsilon$ dimensions for some small ϵ .⁴ This removes much of the intuition for what we are doing, but turns out to be computationally very efficient. Our loop integral Eq. (1.27) will then turn into

$$\begin{aligned} \int \frac{d^d q}{(2\pi)^d} \frac{1}{(q^2 + i\epsilon)^2} &= \frac{i2\pi^{d/2}}{(2\pi)^d} \frac{1}{\Gamma(d/2)} \int_0^\infty dq_E q_E^{d-5} \\ &= \frac{i2\pi^{2-\epsilon}}{(2\pi)^{4-2\epsilon}} \frac{1}{\Gamma(2-\epsilon)} \left\{ \int_0^\mu dq \frac{1}{q_E^{1+2\epsilon}} + \int_\mu^\infty dq \frac{1}{q_E^{1+2\epsilon}} \right\} = \frac{i}{16\pi^2} \left(\frac{1}{\epsilon_{\text{IR}}} - \frac{1}{\epsilon_{\text{UV}}} \right) + O(\epsilon), \end{aligned} \quad (1.33)$$

where in the second equality, the momentum integral is split into a low-energy and high-energy part at some scale μ . Here a trick was performed, as the low-energy part requires $\epsilon < 0$ to be convergent, whereas the high-energy part requires $\epsilon > 0$. The two different divergences thus require different deformations of the theory to be finite, and should be handled separately, hence the subscripts. It is a general result that divergences coming from the low-energy parts of momentum integrals require $\epsilon_{\text{IR}} < 0$, whereas high-energy divergences require $\epsilon_{\text{UV}} > 0$, and this can be used to identify the source of divergences when using dimensional regularisation. In the end divergences when using dimensional regularisation come out as $\frac{1}{\epsilon^p}$ -terms, for some power p .

To achieve dimensional regularisation, we must analytically continue the definition of our theory in a neighbourhood around $d = 4$. The action will change accordingly to

$$S = \int d^d x \mathcal{L}, \quad (1.34)$$

and so the mass dimension of the Lagrangian in the deformed theory must therefore be $[\mathcal{L}] = \mu^d$, for some mass scale μ . From the kinetic term in our toy model Eq. (1.31), we can see we must require the field to have mass dimension $[\phi] = \mu^{(d-2)/2}$, which will imply mass dimension for the coupling $[\lambda] = \mu^{3-d/2}$. Thus, the coupling has changed from mass dimension $\mu^1 \rightarrow \mu^{3-d/2}$ – insisting on keeping the mass dimension of the coupling constant as the theory is deformed will lead to a parametrisation of the deformation by changing the coupling to

$$\lambda \rightarrow \lambda \mu^{(4-d)/2}. \quad (1.35)$$

The arbitrary mass scale μ has been incorporating into the theory, and although it vanishes in the limit $d \rightarrow 4$ in the above expression, dependence on it will not vanish completely when it is multiplied by poles in ϵ such as those in Eq. (1.33). It has been argued that the scale μ heuristically mimics the cut-off scale Λ introduced in Eq. (1.32) [18].⁵

1.2.3 Counterterm Renormalisation

To take care of UV divergences, we note that there is freedom in how we define the contents of our Lagrangian. We should be able to rescale our fields $\phi_0 = \sqrt{Z_\phi} \phi$, and rescale our couplings by $m_{\phi,0}^2 = Z_m m_\phi^2$ and $\lambda_0 = Z_\lambda \mu^{(4-d)/2} \lambda$.⁶ Although suggestively

⁴The reason for choosing 2ϵ is purely aesthetical, making some expressions neater later on.

⁵Generally, it will carry some proportionality to Λ , however, in certain *renormalisation schemes* we will discuss shortly (namely $\overline{\text{MS}}$), the proportionality is unity.

⁶The mass scale μ included in the rescaling of the coupling is there to let the renormalised coupling have the same mass dimension as the undeformed theory in $d = 4$ dimensions.

naming terms such as *mass term* with mass m_ϕ^0 implies a connection to the mass of a particle, we have yet to define what that would mean experimentally. Thus, rescaling our parameters and fields parametrises the way in which we can tune our theory, allowing us freedom in choosing the way our theory connects to experiments.

This approach of rescaling actually allows us to make a perturbative scheme for fixing our (re)normalisations of the fields and couplings to experiment. There are many choices for how to connect theory to experiment, but one common approach for field and mass renormalisation is to identify the pole in momentum space of the two-point correlation function $D_{\text{int}}^n(x, y)$ of a particle to the mass resonance associated with the on-shell production of a particle in scattering experiments. This allows us to perturbatively calculate the two-point correlator, and then fix our normalisations accordingly, such that our mass resonance condition above holds at every order in the perturbation series. We achieve this systematically with *counterterms*, which in essence are additional Feynman rules added to the theory. By expanding the renormalisation parameters as $Z = 1 + \delta$, the δ will carry the correction to the normalisation to any given order in a coupling constant so that the physical predictions are finite. To one-loop order, the self-energy of our scalar theory from Eq. (1.31) is diagrammatically given by

$$p \text{---} p + p \text{---} \textcircled{+} \text{---} p + p \text{---} \otimes \text{---} p,$$

where the crossed dot represents an insertion of the δ into the LO amplitude. Since the free theory is divergence free, the counterterms only needs to carry corrections from the first order in the coupling constant that loops arise. They are therefore understood to be of one-loop order.

This perturbative expansion can be done for any n -point correlator calculable in the theory, and the counterterm insertions can be determined from the vertices in the bare Lagrangian. Returning to our toy model in Eq. (1.31), we can expand the three-point vertex

$$\lambda_0 \phi_0^3 = Z_\lambda Z_\phi^{3/2} \lambda \phi^3 = \mu^{(4-d)/2} \lambda \phi^3 + (\delta_\lambda(\lambda) + \frac{3}{2} \delta_\phi(\lambda)) \lambda \phi^3 + \dots, \quad (1.36)$$

where the dots denote terms of higher order in λ . Using the renormalised coupling λ for the vertex Feynman rules, we must add the vertex counterterm insertions

$$\text{---} \otimes \text{---} = -i \left(\delta_\lambda + \frac{3}{2} \delta_\phi \right). \quad (1.37)$$

1.2.4 On-Shell Renormalisation

Categorising all higher order contributions that can arise to the LO self-energy of a massive particle, they come in the form of combinations of *one-particle-irreducible* (1PI) diagrams. Self-energy in this context are diagrams with the same particle coming in and out, being the quantum corrections to the free two-point correlator. 1PI diagrams are diagrams where all lines with loop momentum running through are connected. Other diagrams can be reconstructed as the sum of 1PI diagrams. Denoting the leading order correlator $\mathcal{G}_0(p)$ and the contribution from one insertion of all 1PI diagrams $i\Sigma(p)$, we

get an infinite series that can be summed⁷

$$\begin{aligned}
 i\mathcal{G}(p) &= p \text{---} p + \text{---} (1\text{PI}) \text{---} + \text{---} (1\text{PI}) \text{---} (1\text{PI}) \text{---} + \dots \\
 &= i\mathcal{G}_0(p) + i\mathcal{G}_0(p)i\Sigma(p)i\mathcal{G}_0(p) + i\mathcal{G}_0(p)i\Sigma(p)i\mathcal{G}_0(p)i\Sigma(p)i\mathcal{G}_0(p) + \dots \\
 &= i\mathcal{G}_0(p) [i\Sigma(p)i\mathcal{G}_0(p) + (i\Sigma(p)i\mathcal{G}_0(p))^2 + \dots] \\
 &= i\mathcal{G}_0(p) \frac{1}{1 + \Sigma(p)\mathcal{G}_0(p)} = \frac{i}{\mathcal{G}_0^{-1}(p) + \Sigma(p)}. \tag{1.38}
 \end{aligned}$$

So the computation of the two-point correlator to any order can be done simply by computing the sum of the 1PI diagrams to that order. These contributions will generally diverge, but then we can take into account the renormalisation parameters. Since this is a *bare* function, i.e. using the non-renormalised quantities, we can get the renormalised two-point correlator $\mathcal{G}^R(p)$ through

$$\mathcal{G}^R(p) = \frac{1}{Z_\psi} \mathcal{G}^{\text{bare}}(p) = \frac{1}{1 + \delta_\psi} \mathcal{G}^{\text{bare}}(p), \tag{1.39}$$

for any field ψ , seeing as the two-point correlator is quadratic in ψ and thereby quadratic in $\sqrt{Z_\psi}$.

On-shell mass renormalisation seeks to identify the pole of the two-point correlator with the physical mass as observed in experiment. This is a generalisation of the property of the free theory two-point function to the perturbative interacting two-point function at any order. It yields two conditions:

$$(I) \quad \left[(1 + \delta_\psi) \left(\mathcal{G}_0^{\text{bare}}(p) \right)^{-1} + \Sigma(p) \right] \Big|_{p^2=m_{\text{pole}}^2} = 0,$$

$$(II) \quad \text{Res} \left\{ \mathcal{G}^R(p), p^2 = m_{\text{pole}}^2 \right\} = 1,$$

where $\text{Res} \{f(z), z = z_0\}$ is the residue of the function f at z_0 .

For our scalar theory, where the leading order *bare* two-point correlator is $\mathcal{G}_0^{\text{bare}}(p) = \frac{1}{p^2 - m_0^2}$, this means that we get the relations

$$(I) \quad \delta_m m_\phi^2 = \Sigma(m_\phi^2),$$

$$(II) \quad \delta_\phi = - \left. \frac{d}{dp^2} \Sigma(p^2) \right|_{p^2=m_\phi^2}.$$

Later on, I will make use of *chiral* on-shell renormalisation. This happens in chiral theories where the left-handed and right-handed degrees of freedom in fermion fields are treated differently in the Lagrangian. This means that divergent corrections to the two-point correlator can be different between the fermion chiralities. Still using Dirac spinor notation, we can then rescale a fermion ψ

$$\psi^0 = \sqrt{Z_L} P_L \psi + \sqrt{Z_R} P_R \psi, \tag{1.40}$$

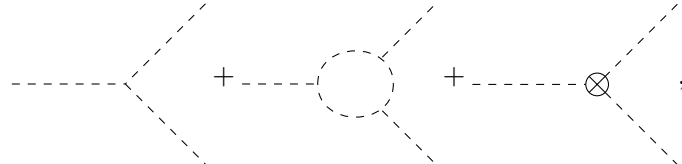
⁷A note on the argument p of these functions: The two-point-correlators in momentum space depend on the four-momentum p^μ in such a way that when it is put in between the external particle representations, i.e. 1 for scalars, spinors for fermions and polarisation vectors for vector bosons, the result will be Lorentz invariant. This means that the correlator could in principle carry Lorentz indices too, which will be suppressed here for simplicity.

where $P_{L/R} = \frac{1}{2}(1 \mp \gamma^5)$ are the chiral projection operators, and work out and renormalise the two-point correlators separately. Expanding $Z_{L/R} = 1 + \delta_{L/R}$ and writing the $\Sigma(\not{p}) = \Sigma_L(\not{p})P_L + \Sigma_R(\not{p})P_R$ we end up with three conditions analogous to the case above:

- (I) $\delta_m m_\psi = \Sigma|_{\not{p}=m_\psi},$
- (II) $\delta_L = -\left.\frac{d}{d\not{p}}\Sigma_L(\not{p})\right|_{\not{p}=m_\psi},$
- (III) $\delta_R = -\left.\frac{d}{d\not{p}}\Sigma_R(\not{p})\right|_{\not{p}=m_\psi}.$

1.2.5 Running Couplings and Renormalisation Group

So far, we have concerned ourselves with renormalisation of the fields and mass terms, but the interaction couplings of a theory also demand renormalisation. Given an interaction term in the Lagrangian with a rescaled coupling $\lambda_0 = Z_\lambda \mu^{(4-d)/2} \lambda$, the counterterm from expanding $Z_\lambda = 1 + \delta_\lambda$ is used to cancel divergences arising from higher order corrections to the LO interaction vertex. Diagrammatically to NLO in the scalar example from Eq. (1.31), we can have



$$, \quad (1.41)$$

where the loop diagram together with the counterterm is UV finite. However, as UV divergences are swallowed into the definition of the coupling, it will inherit dependence on the artificial scale μ . The bare, unrenormalised Lagrangian contains no dependence on the arbitrary mass scale, and as such, we should expect $\frac{d}{d\mu}\lambda_0 = 0$. This is the condition that leads to the *renormalisation group equations* that govern the dependence of the coupling on the *renormalisation scale* μ . In $d = 4 - 2\epsilon$ dimensions, this condition gives us

$$0 \stackrel{!}{=} \mu \frac{d}{d\mu} \lambda_0 = \mu \frac{d}{d\mu} (\mu^\epsilon Z_\lambda \lambda) = \mu^\epsilon Z_\lambda \lambda \left(\epsilon + \frac{\mu}{\lambda} \frac{d\lambda}{d\mu} + \frac{\mu}{Z_\lambda} \frac{dZ_\lambda}{d\mu} \right), \quad (1.42)$$

which can be rearranged into

$$\frac{d\lambda}{d\mu} = - \left(\frac{\epsilon}{\mu} - \frac{1}{Z_\lambda} \frac{dZ_\lambda}{d\mu} \right) \lambda. \quad (1.43)$$

The running of the coupling is therefore dependent on the conditions imposed to fix the rescaling Z_λ . In other words, the running of the coupling is dependent on the *renormalisation scheme*. In this thesis, I will employ a variation of the Minimal Subtraction (MS) scheme, known as $\overline{\text{MS}}$. As the name suggests, this entails subtracting the minimal amount necessary to make the theory UV finite. In practice, this means setting the counterterm to be the $\frac{1}{\epsilon^p}$ -poles arising from calculating loop amplitudes such as the one in Eq. (1.41). The $\overline{\text{MS}}$ scheme additionally subtracts a factor which commonly arises together with the $\frac{1}{\epsilon}$ -poles in dimensional regularisation, setting the counterterm proportional to⁸

$$\frac{1}{\bar{\epsilon}} = \frac{1}{\epsilon} - \gamma_E + \ln 4\pi, \quad (1.44)$$

⁸ At least to first order of divergence.

where γ_E is the Euler-Mascheroni constant. This fixes the counterterm, which in turn fixes the scale dependence of the renormalised coupling.

Finally, the renormalised coupling is fixed through a renormalisation condition as before. This amounts to setting a boundary condition for which to solve Eq. (1.43). A common procedure is to associate the LO vertex in Eq. (1.41) with a given experimental result. To LO the diagram only contributes $\mathcal{M} = -i\lambda$, so the squared amplitude simply becomes λ^2 . If we could concoct an experiment that measures this three-point correlator at a given energy scale, we could then fix λ to be this value, in essence encapsulating the result to all orders at this energy. A natural way would be to measure the decay of particle, where the natural energy scale would be the particle mass. Seeing as the decay $\Gamma \propto |\mathcal{M}|^2$ [14], the renormalisation condition would be

$$\lambda^2(m) = C\Gamma, \quad (1.45)$$

where C is some calculable kinematic constant. However, in our toy model with only one particle, such a decay is not kinematically possible, so the coupling would have to be fixed by looking at some other process, like the four-point correlator, where the kinematics are a bit more complicated.

1.2.6 IR Divergences

Finally, a comment on the IR divergences mentioned earlier in Section 1.2.2. These are not handled through the same renormalisation procedure as outline above, and seeing as I will keep massless particles in the loop integrals in the coming calculations, we will need some other means of dealing with them. This is done in two ways: First, by considering the process of real emission of soft massless particles together with original process. In the case where these emitted particles are *soft*, meaning their energy tends to zero, this is experimentally indistinguishable from the original process without emission. IR divergences will appear in this region of phase space to cancel IR divergences in the loop integrals. Second, by renormalising what will be *parton distribution functions* (PDFs), essentially reconsidering different processes producing the same desired final state as we are interested in with the inclusion of soft radiation of some massless particle. This will be discussed in detail in Chapter 4.

1.3 Yang-Mills Theories

Having gone through the basics of renormalised perturbative QFT, I will turn to the construction of a quantum field theory. Here I will outline imposing certain symmetries between the fields in a theory will naturally lead to an interacting theory of multiple fields. This is the basis for gauge theory, which are the foundations of modern QFTs such as the Standard Model (SM). This section does assume some background group theory.

Gauge theory in QFT is based on imposing *internal symmetries* on the Lagrangian. Internal symmetries are symmetries separate from *external symmetries* in that they are not symmetries of coordinate transformations, but rather symmetries based on transformations of the fields in themselves. Typically, the field transformations under which the Lagrangian is invariant are Lie groups, and are referred to as the *gauge group*.

A collection of fields that transform into each other under a particular representation⁹ is called a *multiplet*.

Let us consider a complex scalar field theory to illustrate. Let ϕ_i be a multiplet of complex scalar fields, and let the gauge group be a general non-Abelian Lie group, locally defined by a set of hermitian generators T^a . Locally, the group elements can then be described using the exponential map as

$$g(\boldsymbol{\alpha}) = \exp(i\alpha^a T^a), \quad (1.46)$$

for a set of real parameters $\boldsymbol{\alpha}$.¹⁰ This way of parametrising the group is convenient in that the inverse of the group elements are the hermitian conjugate, i.e. $g^{-1}(\boldsymbol{\alpha}) = g^\dagger(\boldsymbol{\alpha})$. The transformation law for $\Phi = (\phi_1, \dots)^T$ is

$$\Phi \rightarrow g(\boldsymbol{\alpha})\Phi = \exp(i\alpha^a T^a)\Phi, \quad (1.47)$$

which for an infinitesimal set of parameters ϵ^a becomes

$$\Phi \rightarrow (1 + i\epsilon^a T^a)\Phi. \quad (1.48)$$

Now, we would like to categorise the Lagrangian terms that are invariant under such transformations. The ordinary free Klein-Gordon Lagrangian

$$\mathcal{L}_{\text{KG}} = \partial^\mu \Phi^\dagger \partial_\mu \Phi - m^2 \Phi^\dagger \Phi \quad (1.49)$$

is invariant. However, if we promote our gauge symmetry to be a local symmetry, i.e. let the parameters become space-time-dependent $\boldsymbol{\alpha} \rightarrow \boldsymbol{\alpha}(x)$, this is no longer the case. Since space-time coordinates are unchanged under gauge transformations, it follows that so too is the derivative ∂_μ . However, it will be useful to rewrite this in a somewhat convoluted way, letting it “transform” according to^{11,12}

$$\partial_\mu \rightarrow \partial_\mu = g\partial_\mu g^{-1} + (\partial_\mu g)g^{-1}, \quad (1.50)$$

which in turn makes the field derivative transform to

$$\partial_\mu \Phi \rightarrow g\partial_\mu \Phi + (\partial_\mu g)\Phi, \quad (1.51)$$

which does *not* leave the kinetic term invariant. So we must rethink the kinetic term of the Lagrangian. To get the right transformation properties of the derivative term, we need a *covariant derivative* D_μ such that $D_\mu \Phi \rightarrow gD_\mu \Phi$. In order to create such a D_μ , we must require that it transforms as $D_\mu \rightarrow gD_\mu g^{-1}$. This can be done by introducing the *gauge field* $\mathcal{A}_\mu(x) \equiv A_\mu^a(x)T^a$ which transforms according to

$$\mathcal{A}_\mu \rightarrow g\mathcal{A}_\mu g^{-1} - \frac{i}{q}(\partial_\mu g)g^{-1}. \quad (1.52)$$

The last term can compensate for the extra term in the “transformation” law of ∂_μ . We can then define the covariant derivative $D_\mu = \partial_\mu - iq\mathcal{A}_\mu$ to achieve this.

⁹More on this later.

¹⁰I will use bold notation $\boldsymbol{\alpha}$ to refer to the collection of parameters α^a , of which there is one for each generator T^a .

¹¹It can be shown to be equivalent to ∂_μ when applied to any field (whether they transform under the gauge transformations or not).

¹²In the following I suppress the argument so that $g = g(\boldsymbol{\alpha}(x))$.

In summary, with a local gauge symmetry, a gauge field \mathcal{A}_μ must be introduced such that kinetic terms in the original Lagrangian can be invariant under the gauge transformation. In our case this amounts to adding the interaction term

$$\mathcal{L}_{\mathcal{A}\Phi\text{-int}} = -iq \left[(\partial^\mu \Phi^\dagger) \mathcal{A}_\mu \Phi - \Phi^\dagger \mathcal{A}^\mu (\partial_\mu \Phi) \right] + q^2 \Phi^\dagger \mathcal{A}^\mu \mathcal{A}_\mu \Phi \quad (1.53)$$

to the Klein-Gordon Lagrangian \mathcal{L}_{KG} . Note that for the Lagrangian to be real-valued, we must require \mathcal{A}_μ to be hermitian, or equivalently, the components A_μ^a must be real-valued seeing the generators T^a already are hermitian.

Now, the Lagrangian is gauge invariant, but there still remains to add dynamics to the gauge field \mathcal{A}_μ through a kinetic term. To this end, we can make a field-strength tensor $\mathcal{F}_{\mu\nu} \equiv F_{\mu\nu}^a T^a$ that transforms as $\mathcal{F}_{\mu\nu} \rightarrow g \mathcal{F}_{\mu\nu} g^{-1}$. The covariant derivative already has this property, and so we can define $\mathcal{F}_{\mu\nu} = \frac{i}{q} [D_\mu, D_\nu]$, which will include derivative terms for the \mathcal{A}_μ gauge field and let us construct a gauge invariant kinetic term $\text{Tr}\{\mathcal{F}^{\mu\nu} \mathcal{F}_{\mu\nu}\}$. Antisymmetrising $D_\mu D_\nu \rightarrow [D_\mu, D_\nu]$ serves to get rid of the $\partial_\mu \partial_\nu$ -term which would result in third derivatives of the gauge field. The kinetic term can be shown to be gauge invariant using the transformation law the field-strength tensor and the cyclic property of the trace

$$\text{Tr}\{\mathcal{F}^{\mu\nu} \mathcal{F}_{\mu\nu}\} \rightarrow \text{Tr}\{g \mathcal{F}^{\mu\nu} \mathcal{F}_{\mu\nu} g^{-1}\} = \text{Tr}\{g^{-1} g \mathcal{F}^{\mu\nu} \mathcal{F}_{\mu\nu}\} = \text{Tr}\{\mathcal{F}^{\mu\nu} \mathcal{F}_{\mu\nu}\}. \quad (1.54)$$

This results in a kinetic term for the \mathcal{A}_μ -field

$$\mathcal{L}_{\mathcal{A}\text{-kin}} = -\frac{1}{4T(R)} \text{Tr}\{\mathcal{F}^{\mu\nu} \mathcal{F}_{\mu\nu}\} = -\frac{1}{4} F^{a\mu\nu} F_{\mu\nu}^a, \quad (1.55)$$

where $T(R)$ is the Dynkin index of the representation R of the group defined by the relation $\text{Tr}\{T^a T^b\} = T(R) \delta^{ab}$ when T^a are the generators of the group in that representation.

1.4 Passarino-Veltman Loop Integrals

Lastly, I will go through a categorisation of loop integrals due to Passarino and Veltman [19], known as Passarino-Veltman reduction. This provides a useful tool for symbolically handling loop integrals, by creating basis loop integral functions with which you can write arbitrary loop integrals.

By Lorentz invariance, there are a limited set of forms that loop integrals can take. These can be categorised according to the number of propagator terms they include, which corresponds to the number of externally connected points there are in the loop. A general scalar N -point loop integral takes the form in d space-time dimensions can be written as

$$T_0^N(p_i^2, (p_i - p_j)^2; m_0^2, m_i^2) = \frac{(2\pi\mu)^{4-d}}{i\pi^2} \int d^d q \mathcal{D}_0 \prod_{i=1}^{N-1} \mathcal{D}_i, \quad (1.56)$$

where $\mathcal{D}_0 = [q^2 - m_0^2]^{-1}$ and $\mathcal{D}_i = [(q + p_i)^2 - m_i^2]^{-1}$. I note that the renormalisation scale μ coming from the coupling constant has been swallowed into the definition of these loop integrals. The conventions for the definition of the momenta and the propagator

masses are shown in Fig. 1.3. The first 4 scalar loop integrals are named accordingly

$$T_0^1 \equiv A_0(m_0^2) \quad (1.57)$$

$$T_0^2 \equiv B_0(p_1^2; m_0^2, m_1^2) \quad (1.58)$$

$$T_0^3 \equiv C_0(p_1^2, p_2^2, (p_1 - p_2)^2; m_0^2, m_1^2, m_2^2) \quad (1.59)$$

$$T_0^4 \equiv D_0(p_1^2, p_2^2, p_3^2, (p_1 - p_2)^2, (p_1 - p_3)^2, (p_2 - p_3)^2; m_0^2, m_1^2, m_2^2) \quad (1.60)$$

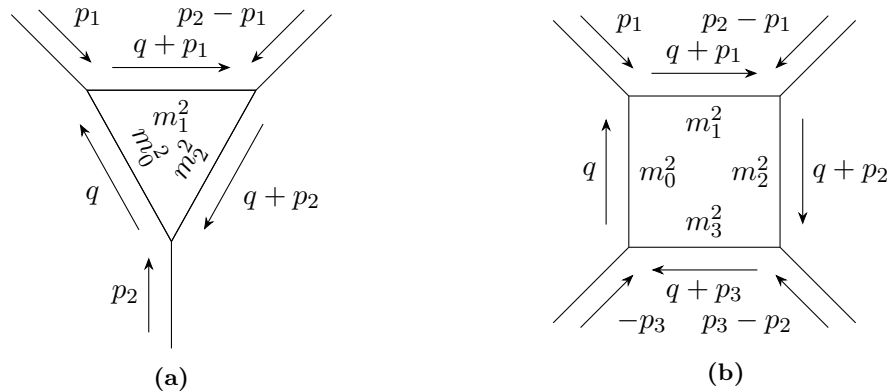


Figure 1.3: Illustration of the momentum conventions for loop diagrams used in the Passarino-Veltman functions, with three-point and four-point loops as examples.

More complicated Lorentz structure can be obtained in loop integrals, however, these can still be related to the scalar integrals by exploiting the possible tensorial structure they can have. Defining an arbitrary loop integral

$$T_{\mu_1 \dots \mu_P}^N \left(p_i^2, (p_i - p_j)^2; m_0^2, m_i^2 \right) = \frac{(2\pi\mu)^{4-d}}{i\pi^2} \int d^d q q_{\mu_1} \cdots q_{\mu_P} \mathcal{D}_0 \prod_{i=1}^{N-1} \mathcal{D}_i, \quad (1.61)$$

where the q_{μ_i} is the loop momentum with for some Lorentz indices μ_i , these tensors can only depend on the metric $g^{\mu\nu}$ and the external momenta p_i . The possible structures up

to four-point loops are as following:

$$B^\mu = p_1^\mu B_1, \quad (1.62a)$$

$$B^{\mu\nu} = g^{\mu\nu} B_{00} + p_1^\mu p_1^\nu B_{11}, \quad (1.62b)$$

$$C^\mu = \sum_{i=1}^2 p_i^\mu C_i, \quad (1.62c)$$

$$C^{\mu\nu} = g^{\mu\nu} C_{00} + \sum_{i,j=1}^2 p_i^\mu p_j^\nu C_{ij}, \quad (1.62d)$$

$$C^{\mu\nu\rho} = \sum_{i=1}^2 (g^{\mu\nu} p_i^\rho + g^{\mu\rho} p_i^\nu + g^{\nu\rho} p_i^\mu) C_{00i} + \sum_{i,j,k=1}^2 p_i^\mu p_j^\nu p_k^\rho C_{ijk}, \quad (1.62e)$$

$$D^\mu = \sum_{i=1}^3 p_i^\mu D_i, \quad (1.62f)$$

$$D^{\mu\nu} = g^{\mu\nu} D_{00} + \sum_{i,j=1}^3 p_i^\mu p_j^\nu D_{ij}, \quad (1.62g)$$

$$D^{\mu\nu\rho} = \sum_{i=1}^3 (g^{\mu\nu} p_i^\rho + g^{\mu\rho} p_i^\nu + g^{\nu\rho} p_i^\mu) D_{00i} + \sum_{i,j,k=1}^3 p_i^\mu p_j^\nu p_k^\rho D_{ijk}, \quad (1.62h)$$

$$\begin{aligned} D^{\mu\nu\rho\sigma} &= (g^{\mu\nu} g^{\rho\sigma} + g^{\mu\rho} g^{\nu\sigma} + g^{\mu\sigma} g^{\nu\rho}) D_{0000} \\ &+ \sum_{i,j=1}^3 (g_{\mu\nu} p_i^\rho p_j^\sigma + g_{\mu\nu} p_i^\sigma p_j^\rho + g_{\mu\rho} p_i^\nu p_j^\sigma + g_{\mu\rho} p_i^\sigma p_j^\nu + g_{\mu\sigma} p_i^\rho p_j^\nu + g_{\mu\nu} p_i^\rho p_j^\sigma) D_{00ij} \\ &+ \sum_{i,j,k,l=1}^3 p_i^\mu p_j^\nu p_k^\rho p_l^\sigma D_{ijkl}, \end{aligned} \quad (1.62i)$$

where all coefficients with lower case Latin indices must be completely symmetric in i, j, k, l .

Chapter 2

Supersymmetry

2.1 Introduction to Supersymmetry

In this chapter, I introduce the basic ideas behind supersymmetry, what it is, and how to construct field theories that are *supersymmetric*. I will discuss the Super-Poincaré group as an extension of the Poincaré group, and introduce superspace as a vessel for supersymmetric field theories. I go on to describe the Minimal Supersymmetric Standard Model (MSSM), the minimal (broken) supersymmetric QFT containing the Standard Model (SM) particles as a subset. The electroweakinos, the main focus of this thesis, are introduced, including general mixing of fields into mass eigenstates, and I go into some depth to derive the interaction Feynman rules of these particles from the MSSM *superlagrangian*.

This chapter makes extensive use of Weyl spinor notation and Grassmann calculus. For more details on this and the specific notation I use, I refer to Appendix A. Some background in group theory is necessary to follow certain parts of the chapter, but is not necessary to understand the broader ideas.

A Simple Supersymmetric Theory

To illustrate what supersymmetry looks like in practice, it can be helpful to look at a simple example. Take a Lagrangian for a massive complex scalar field ϕ and a massive Weyl spinor field ψ ,

$$\mathcal{L} = (\partial_\mu \phi)(\partial^\mu \phi^*) + i\psi \sigma^\mu \partial_\mu \psi^\dagger - |m_\phi|^2 \phi \phi^* - \frac{1}{2} m_\psi (\psi \psi) - \frac{1}{2} m_\psi^* (\psi \psi)^\dagger. \quad (2.1)$$

To impose some symmetry between the bosonic and fermionic degrees of freedom, we want to examine a transformation of the scalar field through the spinor field and vice versa. Imposing Lorentz invariance a general, infinitesimal, such transformation can be parametrised by

$$\delta\phi = \epsilon a(\theta\psi), \quad (2.2a)$$

$$\delta\phi^* = \epsilon a^*(\theta\psi)^\dagger, \quad (2.2b)$$

$$\delta\psi_\alpha = \epsilon \left(c(\sigma^\mu \theta^\dagger)_\alpha \partial_\mu \phi + F(\phi, \phi^*) \theta_\alpha \right), \quad (2.2c)$$

$$\delta\psi^\dagger_{\dot{\alpha}} = \epsilon \left(c^*(\theta \sigma^\mu)_{\dot{\alpha}} \partial_\mu \phi^* + F^*(\phi, \phi^*) \theta^\dagger_{\dot{\alpha}} \right), \quad (2.2d)$$

where ϵ is some infinitesimal parameter for the transformation, θ is some Grassmann-valued Weyl spinor, a, c are complex coefficients of the transformation and $F(\phi, \phi^*)$ is

some linear function of ϕ and ϕ^* . The resulting change in the scalar field part of the Lagrangian is

$$\delta\mathcal{L}_\phi/\epsilon = a(\theta\partial_\mu\psi)(\partial^\mu\phi^*) - a|m_\phi|^2(\theta\psi)\phi^* + \text{c. c.}, \quad (2.3)$$

and likewise for the spinor field part

$$\delta\mathcal{L}_\psi/\epsilon = -ic^*(\psi\sigma^\mu\bar{\sigma}^\nu\theta)\partial_\mu\partial_\nu\phi^* + i(\psi\sigma^\mu\theta^\dagger)\partial_\mu F^* + m_\psi [c(\psi\sigma^\mu\theta^\dagger)\partial_\mu\phi + (\psi\theta)F] + \text{c. c.} \quad (2.4)$$

The first term in Eq. (2.4) can be rewritten using the commutativity of partial derivatives and the identity $(\sigma^\mu\bar{\sigma}^\nu + \sigma^\nu\bar{\sigma}^\mu)_\alpha{}^\beta = -2g^{\mu\nu}\delta_\alpha^\beta$ to get $ic^*(\theta\psi)\partial_\mu\partial^\mu\phi^*$. Up to a total derivative, we can then write the change in the spinor part as

$$\delta\mathcal{L}_\psi/\epsilon = -ic^*(\theta\partial_\mu\psi)\partial^\mu\phi^* + (\psi\sigma^\mu\theta^\dagger)\partial_\mu(iF^* + m_\psi c\phi) + m_\psi(\theta\psi)F + \text{c. c..} \quad (2.5)$$

The change of the total Lagrangian (again up to a total derivative) can then be grouped as

$$\begin{aligned} \delta\mathcal{L}/\epsilon = & (a - ic^*)(\theta\partial_\mu\psi)(\partial^\mu\phi^*) + (\psi\sigma^\mu\theta^\dagger)\partial_\mu(iF^* + m_\psi c\phi) \\ & + (\theta\psi)(a|m_\phi|^2\phi^* + m_\psi F) + \text{c. c.}, \end{aligned} \quad (2.6)$$

giving us three different conditions for the action to be invariant:

$$a - ic^* = 0, \quad (2.7a)$$

$$iF^* + m_\psi c\phi = 0, \quad (2.7b)$$

$$a|m_\phi|^2\phi^* + m_\psi F = 0. \quad (2.7c)$$

This is fulfilled if

$$c = ia^*, \quad (2.8a)$$

$$F = -am_\psi^*\phi^*, \quad (2.8b)$$

$$a|m_\phi|^2 = a^*|m_\psi|^2. \quad (2.8c)$$

What is interesting is the last condition, because it requires a to be real, as both $|m_\phi|^2$ and $|m_\psi|^2$ are real, but also requires $|m_\phi|^2 = |m_\psi|^2$. For the theory to be supersymmetric in this sense, the masses of the boson and fermion must be the same! Since the phase of m_ϕ does not appear in the Lagrangian, we are free to set $m_\phi = m_\psi \equiv m$, suppressing any mass subscripts henceforth.

Revisiting F , it can be introduced as an auxiliary field to bookkeep the supersymmetry transformation. By including the non-dynamical term to the Lagrangian $\mathcal{L}_F = F^*F + mF\phi + m^*F^*\phi^*$, we make sure F takes the correct value in the transformation from its equation of motion $\frac{\partial\mathcal{L}}{\partial F} = F^* + m\phi \stackrel{!}{=} 0$. Inserting F back into the Lagrangian reproduces the mass term of the scalar field, allowing us to write the original Lagrangian as

$$\mathcal{L} = (\partial_\mu\phi)(\partial^\mu\phi^*) + i\psi\sigma^\mu\partial_\mu\psi^\dagger + F^*F + mF\phi + m^*F^*\phi^* - \frac{1}{2}m(\psi\psi) - \frac{1}{2}m^*(\psi\psi)^\dagger, \quad (2.9)$$

with the *supersymmetry transformation* rules

$$\delta\phi = \epsilon(\theta\psi), \quad \delta\phi^* = \epsilon(\theta\psi)^\dagger, \quad (2.10a)$$

$$\delta\psi_\alpha = \epsilon \left(-i(\sigma^\mu\theta^\dagger)_\alpha\partial_\mu\phi + F\theta_\alpha \right), \quad \delta\psi_\alpha^\dagger = \epsilon \left(i(\theta\sigma^\mu)_{\dot{\alpha}}\partial_\mu\phi^* + F^*\theta_{\dot{\alpha}}^\dagger \right), \quad (2.10b)$$

$$\delta F = i\epsilon \left(\partial_\mu\psi\sigma^\mu\theta^\dagger \right), \quad \delta F^* = -i\epsilon \left(\theta\sigma^\mu\partial_\mu\psi^\dagger \right), \quad (2.10c)$$

where I have set $a = 1$ without loss of generality,¹ and found the appropriate transformation law for F such that the Lagrangian is invariant up to total derivatives. The dynamics of this Lagrangian are the same as before, but the supersymmetry is now made manifest, i.e. the transformation is free of any dependence on the contents of the Lagrangian as we had in Eq. (2.8).

In fact, one can show that a general supersymmetric Lagrangian consisting of a scalar field and a fermion field can be written

$$\mathcal{L} = (\partial_\mu \phi)(\partial^\mu \phi^*) + i\psi \sigma^\mu \partial_\mu \psi^\dagger + F^* F + \left\{ mF\phi - \frac{1}{2}m(\psi\psi) - \lambda\phi(\psi\psi) + \text{c. c.} \right\} \quad (2.11)$$

up to renormalisable interactions.

2.2 The Super-Poincaré Group

To introduce more involved supersymmetric QFTs than our simple example from Section 2.1, it will be useful to first introduce a framework that will manifestly carry the supersymmetry. This will alleviate the need to figure out the correct transformation laws, and the constraints they may carry to the parameters of the theory. To this end, I will outline a common way of introducing supersymmetric theories – extending our fields from representations of the Poincaré group of coordinate transformations to the super-Poincaré group. This will hopefully give an algebraic geometrical understanding to *superfields* as the building blocks of a supersymmetric field theory.

2.2.1 The Poincaré and Super-Poincaré Algebras

As we have already seen in Section 1.3, sets of transformations for a symmetry can be described by a group. To introduce supersymmetry in this context, it will be clearer to study the *generators* of the algebra of the group, so I would like to take a moment to motivate this change of perspective, before describing the fundamental symmetries we will be using.

The group describing the basic set of *coordinate transformations* under which the theories we will consider are symmetric is called the *Poincaré group*, denoted P . Theories that are symmetric under this group will be manifestly relativistic, and will exhibit the ordinary freedom in choice of coordinate system. The Poincaré group consists of any transformation of space-time coordinates x^μ such that

$$x'^\mu = \Lambda^\mu{}_\nu x^\nu + a^\mu, \quad (2.12)$$

for a real, orthogonal 4×4 matrix Λ and real numbers a^μ . As a group it is the semi-direct product of Lorentz group $O(1, 3)$ and group of 4D space-time translations $T(1, 3)$

$$P \equiv O(1, 3) \rtimes T(1, 3). \quad (2.13)$$

For completeness, the semi-direct product is defined such that the product of two group elements $(\Lambda_1, p_1), (\Lambda_2, p_2) \in P$ where $\Lambda_1, \Lambda_2 \in O(1, 3)$ and $p_1, p_2 \in T(1, 3)$ is

$$(\Lambda_1, p_1) \circ (\Lambda_2, p_2) \equiv (\Lambda_1 \circ_O \Lambda_2, p_1 \circ_T \Lambda_1(p_2)), \quad (2.14)$$

¹It can be absorbed by a redefinition of the parameter ϵ for instance.

where we understand $\circ_{O/T}$ as the group multiplication operations of $O(1, 3)$ and $T(1, 3)$ respectively.²

For our purposes, it will suffice to work simply with the local structure of the Poincaré group, and being Lie groups, this can be reproduced with the exponential map we have used already in Eq. (1.46) $\exp : \mathfrak{g} \rightarrow G$, where \mathfrak{g} is the *Lie algebra* of the Lie group G . In this way, the algebra is said to *generate* the group, and a basis set $\{T^a\}$ of the algebra \mathfrak{g} is said to be the *generators* of the group.³ Accordingly, the local behaviour of the group can be inferred simply from the properties of the generators T^a . The generators of the Poincaré group can be structured by an antisymmetric Lorentz tensor $M^{\mu\nu}$, and a four-vector P^μ . The properties of the algebra these generators span can be inferred from their commutation relations

$$[P^\mu, P^\nu] = 0, \quad (2.15a)$$

$$[M^{\mu\nu}, P^\rho] = i(g^{\mu\sigma}P^\nu - g^{\nu\sigma}P^\mu), \quad (2.15b)$$

$$[M^{\mu\nu}, M^{\rho\sigma}] = i(g^{\mu\rho}M^{\nu\sigma} - g^{\mu\sigma}M^{\nu\rho} - g^{\nu\rho}M^{\mu\sigma} + g^{\nu\sigma}M^{\mu\rho}). \quad (2.15c)$$

To construct the super-Poincaré group, we can then just extend the algebra, and the rest of the group will follow. This is done by extending the Lie algebra to a *graded Lie superalgebra* by adding new generators. A *graded Lie superalgebra* is constructed from two vector spaces $\mathfrak{l}_0, \mathfrak{l}_1$ and is denoted $\mathfrak{l}_0 \oplus \mathfrak{l}_1$. It is itself a vector space with a bilinear operation such that for any elements $x_i \in \mathfrak{l}_i$ we have

$$x_j \circ x_j \in \mathfrak{l}_{i+j \bmod 2}, \quad (\text{grading})$$

$$x_i \circ x_j = -(-1)^{i \cdot j} x_j \circ x_i, \quad (\text{supersymmetrisation})$$

$$x_i \circ (x_j \circ x_k)(-1)^{i \cdot k} + x_j \circ (x_k \circ x_i)(-1)^{j \cdot i} + x_k \circ (x_i \circ x_j)(-1)^{k \cdot j} = 0. \quad (\text{generalised Jacobi identity})$$

I note that in this case, \mathfrak{l}_0 acts as an ordinary Lie algebra where \circ is the ordinary commutator, and \mathfrak{l}_1 gets anti-commutator relations rather than commutator relations.⁴

The *super-Poincaré algebra*, denoted \mathfrak{sp} , is the graded Lie superalgebra resulting from the Poincaré algebra \mathfrak{p} and the vector space \mathfrak{q} . Here \mathfrak{p} is the Lie algebra of the Poincaré group P and \mathfrak{q} is the vector space spanned by the generators $Q_\alpha, Q_\dot{\alpha}^\dagger$ that form two Weyl spinors. In addition to the commutation relations Eqs. (2.15a) to (2.15c), the Poincaré superalgebra is specified by the (anti-)commutator relations

$$[Q_\alpha, P^\mu] = [Q_\dot{\alpha}^\dagger, P_\mu] = 0 \quad (2.16a)$$

$$[Q_\alpha, M^{\mu\nu}] = (\sigma^{\mu\nu})_\alpha^\beta Q_\beta \quad (2.16b)$$

$$\{Q_\alpha, Q_\beta\} = \{Q_\dot{\alpha}^\dagger, Q_\dot{\beta}^\dagger\} = 0, \quad (2.16c)$$

$$\{Q_\alpha, Q_\dot{\beta}^\dagger\} = 2(\sigma^\mu)_{\alpha\dot{\beta}} P_\mu \quad (2.16d)$$

where $\sigma^{\mu\nu} = \frac{i}{4}(\sigma^\mu\bar{\sigma}^\nu - \sigma^\nu\bar{\sigma}^\mu)$, $\sigma^\mu = (\mathbb{I}, \sigma^i)$, $\bar{\sigma}^\mu = (\mathbb{I}, -\sigma^i)$ and σ^i are the Pauli matrices.

²We see also that $O(1, 3)$ must also be a map $T(1, 3) \rightarrow T(1, 3)$. We will later see that this means that the generators of translations are in a representation of the Lorentz group.

³The algebra of a Lie group can be shown to be a vector space, and as such there exists a basis set spanning the algebra.

⁴This can be seen from supersymmetrisation as for any $x_1, x'_1 \in \mathfrak{l}_1$ we have that $x_1 \circ x'_1 = x'_1 \circ x_1$.

2.2.2 Superspace

The idea behind *superspace* is to create a coordinate system for which supersymmetry transformation manifest as coordinate transformations similarly to the way Poincaré transformations work on ordinary space-time coordinates. To this end, we can start by considering a general element of the super-Poincaré group $g \in SP$; it can be parametrised through the exponential map like this.

$$g = \exp \left(ix^\mu P_\mu + i(\theta Q) + i(\theta Q)^\dagger + \frac{i}{2} \omega_{\mu\nu} M^{\mu\nu} \right), \quad (2.17)$$

where $x^\mu, \theta^\alpha, \theta_{\dot{\alpha}}^\dagger, \omega_{\mu\nu}$ parametrise the group, and $P_\mu, Q_\alpha, Q^{\dagger\dot{\alpha}}, M^{\mu\nu}$ are the generators of the group as we have already seen. Since the parameters $x^\mu, \theta^\alpha, \theta_{\dot{\alpha}}^\dagger$ live in irreducible representations of the Lorentz algebra (four-vector and Weyl spinor representations respectively) generated by $M^{\mu\nu}$, the effect of the Lorentz part of the super-Poincaré group on the parameters can be determined easily. Likewise, the parameters $\omega_{\mu\nu}$ are in a trivial representation of the algebra generated by $P_\mu, Q_\alpha, Q^{\dagger\dot{\alpha}}$, and need not then be considered. It is therefore expedient to create a space with $x^\mu, \theta^\alpha, \theta_{\dot{\alpha}}^\dagger$ as the coordinates, modding out the Lorentz algebra part.

We create superspace as a coordinate system with coordinates $z^\pi = (x^\mu, \theta^\alpha, \theta_{\dot{\alpha}}^\dagger)$, and look at how they transform under super-Poincaré group transformations. A function $F(z)$ on superspace can then be written using the generators $K_\pi = (P_\mu, Q_\alpha, Q^{\dagger\dot{\alpha}})$ as $F(z) = \exp(iz^\pi K_\pi) F(0)$. Applying a super-Poincaré group element without the Lorentz generators $\bar{g}(a, \eta) = \exp(ia^\mu P_\mu + i(\eta Q) + i(\eta Q)^\dagger)$ we have

$$F(z') = \exp(iz'^\pi K_\pi) F(0) = \exp(ia^\mu P_\mu + i(\eta Q) + i(\eta Q)^\dagger) \exp(iz^\pi K_\pi) F(0), \quad (2.18)$$

which by the Baker-Campbell-Hausdorff formula (BCH) gives to first order in the commutators

$$z'^\pi K_\pi = (x^\mu + a^\mu) P_\mu + (\theta^\alpha + \eta^\alpha) Q_\alpha + (\theta_{\dot{\alpha}}^\dagger + \eta_{\dot{\alpha}}^\dagger) Q^{\dagger\dot{\alpha}} + \frac{i}{2} [a^\mu P_\mu + (\eta Q) + (\eta Q)^\dagger, z^\pi K_\pi] + \dots \quad (2.19)$$

Now, P_μ commutes with all of K_π , and Q_α ($Q^{\dagger\dot{\alpha}}$) anti-commute with themselves, for every combination of different α ($\dot{\alpha}$), so the only relevant part of the commutator is

$$[(\eta Q), (\theta Q)^\dagger] + [(\eta Q)^\dagger, (\theta Q)] = -\eta^\alpha \{Q_\alpha, Q_{\dot{\alpha}}^\dagger\} \theta^{\dot{\alpha}} + (\eta \leftrightarrow \theta) = -2(\eta \sigma^\mu \theta^\dagger) P_\mu + (\eta \leftrightarrow \theta). \quad (2.20)$$

Since this commutator is proportional to P_μ which in turn commutes with everything, all higher order commutators of BCH vanish, and we can conclude that the transformed coordinates z'^π are given by

$$z'^\pi = (x^\mu + a^\mu + i(\theta \sigma^\mu \eta^\dagger) - i(\eta \sigma^\mu \theta^\dagger), \theta^\alpha + \eta^\alpha, \theta_{\dot{\alpha}}^\dagger + \eta_{\dot{\alpha}}^\dagger). \quad (2.21)$$

This gives us a differential representation of the K_π generators as

$$P_\mu = -i\partial_\mu, \quad (2.22a)$$

$$Q_\alpha = -(\sigma^\mu \theta^\dagger)_\alpha \partial_\mu - i\partial_\alpha, \quad (2.22b)$$

$$Q_{\dot{\alpha}}^\dagger = -(\theta \bar{\sigma}^\mu)_{\dot{\alpha}} \partial_\mu - i\partial_{\dot{\alpha}}. \quad (2.22c)$$

Now, to see what these functions of superspace look like, we can expand $F(z)$ in terms of the coordinates $\theta^\alpha, \theta_{\dot{\alpha}}^\dagger$, as these expansions are finite due to the fact that none

of these coordinates can appear more than once per term. Demanding that the function $F(z)$ be invariant under Lorentz transformations, the x^μ -dependent coefficients of the expansion must transform such that each term is a scalar (or fully contracted Lorentz structure). This limits a general such function of superspace to be written as

$$F(z) = f(x) + \theta^\alpha \phi_\alpha(x) + \theta_{\dot{\alpha}}^\dagger \chi^{\dagger\dot{\alpha}}(x) + (\theta\theta)m(x) + (\theta\theta)^\dagger n(x) \\ + (\theta\sigma^\mu\theta^\dagger)V_\mu(x) + (\theta\theta)\theta_{\dot{\alpha}}^\dagger\lambda^{\dagger\dot{\alpha}}(x) + (\theta\theta)^\dagger\theta^\alpha\psi_\alpha(x) + (\theta\theta)(\theta\theta)^\dagger d(x). \quad (2.23)$$

2.2.3 Superfields

To construct a manifestly supersymmetric theory, it will be useful to start with finding representations of the super-Poincaré group. This is exactly what we have already done; the functions on superspace find themselves in the representation space of a differential representation of the K_π generators of the super-Poincaré group, and a scalar representation of the remaining Lorentz generators (i.e. the Lorentz generators leave the superspace functions unchanged). Inside the general function on superspace Eq. (2.23), we find many component functions in different representation spaces of the Lorentz group. Furthermore, supersymmetry transformations transform these fields into one another. This seems like an ideal vessel for constructing supersymmetric fields theories.

We define the *superfield* Φ as an operator-valued function on superspace.⁵ The general superfield from Eq. (2.23) is in a reducible representation space of the super-Poincaré group, so we define three *irreducible* representations that will be useful going forward:⁶

$$\text{Left-handed scalar superfield:} \quad \bar{D}_{\dot{\alpha}}\Phi = 0, \quad (2.24)$$

$$\text{Right-handed scalar superfield:} \quad D_\alpha\Phi^\dagger = 0, \quad (2.25)$$

$$\text{Vector superfield:} \quad \Phi^\dagger = \Phi. \quad (2.26)$$

Here the dagger operation refers to complex conjugation, and the differential operators $D_\alpha, \bar{D}_{\dot{\alpha}}$ are defined as

$$D_\alpha = \partial_\alpha + i(\sigma^\mu\theta^\dagger)_\alpha\partial_\mu, \quad (2.27a)$$

$$\bar{D}_{\dot{\alpha}} = -\partial_{\dot{\alpha}} - i(\theta\sigma^\mu)_{\dot{\alpha}}\partial_\mu. \quad (2.27b)$$

These differential operators are covariant differentials in the sense that they commute with supersymmetry transformations, i.e. $D_\alpha F(z) \rightarrow D'_\alpha(\bar{g}F(z)) = \bar{g}(D_\alpha F(z))$. Collectively, the left- and right-handed scalar superfields are referred to as *chiral superfields*.

For future reference, the general forms of a left-handed scalar superfield Φ , a right-handed scalar superfield Φ^\dagger and a vector superfield V_{WZ} in the so-called Wess-Zumino

⁵For our purposes, it suffices to look at them simply as complex valued functions, but strictly speaking, they are operator-valued in a quantised field theory.

⁶I will not prove here that these in fact are irreducible representations.

gauge is [20]:

$$\begin{aligned}\Phi(x, \theta, \theta^\dagger) = & A(x) + i(\theta\sigma^\mu\theta^\dagger)\partial_\mu A(x) - \frac{1}{4}(\theta\theta)(\theta\theta)^\dagger \square A(x) \\ & + \sqrt{2}(\theta\psi(x)) - \frac{i}{\sqrt{2}}(\theta\theta)(\partial_\mu\psi(x)\sigma^\mu\theta^\dagger) + (\theta\theta)F(x),\end{aligned}\quad (2.28a)$$

$$\begin{aligned}\Phi^\dagger(x, \theta, \theta^\dagger) = & A^*(x) - i(\theta\sigma^\mu\theta^\dagger)\partial_\mu A^*(x) - \frac{1}{4}(\theta\theta)(\theta\theta)^\dagger \square A^*(x) \\ & + \sqrt{2}(\theta\psi(x))^\dagger + \frac{i}{\sqrt{2}}(\theta\theta)^\dagger(\theta\sigma^\mu\partial_\mu\psi^\dagger(x)) + (\theta\theta)^\dagger F^*(x),\end{aligned}\quad (2.28b)$$

$$V_{WZ}(x, \theta, \theta^\dagger) = (\theta\sigma^\mu\theta^\dagger)V_\mu(x) + (\theta\theta)(\theta\lambda(x))^\dagger + (\theta\theta)^\dagger(\theta\lambda(x)) + \frac{1}{2}(\theta\theta)(\theta\theta)^\dagger D(x). \quad (2.28c)$$

2.2.4 Superlagrangian

We are now ready to define the action of a supersymmetric quantum field theory on superspace. Given a set of superfields $\{\Phi_i\}$, we want to define an action through a Lagrangian density comprised of the component fields in Φ_i . A function of the superfields will still be a superfield, and will therefore take the form from Eq. (2.23). To get a supersymmetry invariant Lagrangian density, we can therefore look to extract some part of such a superspace function that at most transforms as a total derivative under a supersymmetry transformation according to Eq. (2.19). It can be shown that the $d(x)$ component field of Eq. (2.23) transforms in such a way, and likewise for the $F(x)$ component field of a chiral superfield Eqs. (2.28a) and (2.28b), so projecting out these would constitute a valid Lagrangian density for a supersymmetry invariant action. Keeping in mind that the Lagrangian density must be real, we can then get a supersymmetry invariant action through a Lagrangian density on the form⁷

$$\mathcal{L} = \text{proj}_D(V[\Phi_i]) + \text{proj}_F(W[\Phi_i]) + \text{proj}_{F^\dagger}(W^\dagger[\Phi_i]), \quad (2.29)$$

where $V[\Phi_i]$ is a vector superfield and $W[\Phi_i]$ ($W^\dagger[\Phi_i]$) is some left-handed (right-handed) scalar superfield.

The projection operators can be realised using Grassmann integration:⁸

$$\text{proj}_D V[\Phi_i] = \int d^4\theta V[\Phi_i], \quad (2.30a)$$

$$\text{proj}_F W[\Phi_i] = \int d^4\theta (\theta\theta)^\dagger W[\Phi_i], \quad (2.30b)$$

$$\text{proj}_{F^\dagger} W^\dagger[\Phi_i] = \int d^4\theta (\theta\theta) W^\dagger[\Phi_i]. \quad (2.30c)$$

Accordingly, we can write down the general supersymmetry invariant action, letting $\{\bar{\Phi}_i\}$ be the subset of chiral superfields in $\{\Phi_i\}$ using a Lagrangian density on the form

$$\mathcal{L} = \int d^4\theta \left\{ V[\Phi_i] + (\theta\theta)^\dagger W[\bar{\Phi}_i] + (\theta\theta) W[\bar{\Phi}_i^\dagger] \right\}, \quad (2.31)$$

where we restrict W to be holonomic function of its argument superfields called the *superpotential*. W being holonomic in this context simply means that $W[\bar{\Phi}_i]$ will be a

⁷To clarify potential confusion on the capitalisation of the D -projection here – for a vector superfield Eq. (2.28c) the $d(x)$ component field is the $D(x)$ auxiliary component field.

⁸As a reminder, I detail how the calculus of Grassmann coordinates is defined in Appendix A.

left-handed scalar superfield and $W[\Phi_i^\dagger]$ a right-handed scalar superfield. This leads to defining the *superlagrangian* $\tilde{\mathcal{L}}$ as a Lagrangian density analogue on superspace, where we can recognise

$$\tilde{\mathcal{L}} = V[\Phi_i] + (\theta\theta)^\dagger W[\bar{\Phi}_i] + (\theta\theta) W[\bar{\Phi}_i^\dagger], \quad (2.32)$$

and subsequently the action as

$$S[\{\Phi_i\}] = \int d^4x d^4\theta \tilde{\mathcal{L}} \left(\{\Phi_i\}, \left\{ \frac{\partial \Phi_i}{\partial z^\pi} \right\}, z \right). \quad (2.33)$$

Renormalisability puts severe restrictions on the form of the superlagrangian by imposing that any parameter of the theory cannot have a negative mass dimension. Recognising that $1 = \int d^4\theta (\theta\theta)(\theta\theta)^\dagger$, we must have that $[\int d^4\theta] = M^2$ for some mass reference scale M . Consequently, for the ordinary Lagrangian density to have mass dimension four, we must have that $[\tilde{\mathcal{L}}] = M^2$. From Eq. (2.28a) we recognise that the scalar superfield contains a scalar field term, and consequently has mass dimension $[\Phi] = M^1$. Thus, the general form of the superpotential is

$$W[\Phi_i] = \sum_i \lambda_i \Phi_i + \sum_{ij} m_{ij} \Phi_i \Phi_j + \sum_{ijk} y_{ijk} \Phi_i \Phi_j \Phi_k, \quad (2.34)$$

and the only possible form of $V[\Phi_i]$ only containing scalar superfields is

$$V[\Phi_i] = \sum_i \Phi_i \Phi_i^\dagger, \quad (2.35)$$

where the prefactor of the terms are set to 1, which can be done without loss of generality by rescaling the fields.

2.2.5 Revisiting our Simple Supersymmetric Theory

Now that we have developed a structure for creating manifestly supersymmetric theories using superfields, we can take a moment to revisit our simple theory from Eq. (2.1) to see what it would look like within the superspace framework. We can use a left-handed scalar superfield Φ as the vessel for our scalar field ϕ , fermionic field ψ and auxiliary field F :

$$\begin{aligned} \Phi(\theta, \theta^\dagger, x) = & \phi(x) + i(\theta\sigma^\mu\theta^\dagger)\partial_\mu\phi(x) - \frac{1}{4}(\theta\theta)(\theta\theta)^\dagger \square \phi(x) \\ & + \sqrt{2}(\theta\psi(x)) - \frac{i}{\sqrt{2}}(\theta\theta)(\partial_\mu\psi(x)\sigma^\mu\theta^\dagger) + (\theta\theta)F(x). \end{aligned} \quad (2.36)$$

The kinetic terms are reproduced through the first term in Eq. (2.31):

$$\begin{aligned} \mathcal{L}_{\text{kin}} = & \int d^4\theta \Phi^\dagger \Phi = \int d^4\theta \left\{ -\frac{1}{4}(\phi^* \square \phi + \phi \square \phi^*) + (\theta\sigma^\mu\theta^\dagger)(\theta\sigma^\nu\theta^\dagger)\partial_\mu\phi^*\partial_\nu\phi \right. \\ & \left. - i[(\theta\psi)^\dagger(\theta\theta)(\partial_\mu\psi\sigma^\mu\theta^\dagger) - (\theta\theta)^\dagger(\theta\sigma^\mu\partial_\mu\psi^\dagger)(\theta\psi)] + (\theta\theta)(\theta\theta)^\dagger F^*F \right\} \\ = & (\partial_\mu\phi)(\partial^\mu\phi^*) + i(\psi\sigma^\mu\partial_\mu\psi^\dagger) + F^*F. \end{aligned} \quad (2.37)$$

The remaining mass term can be recreated by the superlagrangian term $\frac{m}{2}(\theta\theta)^\dagger\Phi\Phi + \frac{m^*}{2}(\theta\theta)\Phi^\dagger\Phi^\dagger$, equivalent to a superpotential $W[\Phi] = \frac{m}{2}\Phi\Phi$, yielding

$$\begin{aligned}\mathcal{L}_{\text{mass}} &= \int d^4\theta \left\{ \frac{m}{2}(\theta\theta)^\dagger\Phi\Phi + \text{c. c.} \right\} = \int d^4\theta \left\{ \frac{m}{2}(\theta\theta)^\dagger(2\phi(\theta\theta)F + 2(\theta\psi)(\theta\psi)) + \text{c. c.} \right\} \\ &= m\phi F + m^*\phi^*F^* + \frac{m}{2}(\psi\psi) + \frac{m^*}{2}(\psi\psi)^\dagger.\end{aligned}\quad (2.38)$$

So our simple supersymmetric theory is encapsulated simply by the superlagrangian

$$\tilde{\mathcal{L}} = \Phi\Phi^\dagger + \frac{m}{2}(\theta\theta)^\dagger\Phi\Phi + \frac{m^*}{2}(\theta\theta)\Phi^\dagger\Phi^\dagger,\quad (2.39)$$

showing how superspace simplifies the model building considerably.

2.3 Minimal Supersymmetric Standard Model

Up to this point, the building blocks for the MSSM have been introduced, and I will now shift focus how these are put together to create the minimal supersymmetric extension of the SM. I will also outline the process of spontaneous symmetry breaking, and state a general parametrisation of how this is done in the MSSM.

2.3.1 Supersymmetric Yang-Mills Theory

Before getting into the MSSM content, we must introduce what Yang-Mills theory looks like at a superlagrangian level. We define a *supergauge transformation* of a left-handed scalar superfield multiplet Φ analogously to the ordinary case Eq. (1.47)

$$\Phi \rightarrow \exp(i\Lambda)\Phi,\quad (2.40)$$

where $\Lambda \equiv \Lambda^a T^a$, Λ^a are the parameters of the transformation and T^a are again the generators of the gauge group. To get a sense of what these parameters are, we can require the transformed superfield to be left-handed

$$\begin{aligned}D_{\dot{\alpha}}^\dagger \exp(i\Lambda)\Phi &= i \left(D_{\dot{\alpha}}^\dagger \Lambda^a \right) T^a \exp(i\Lambda^a T^a)\Phi + \exp(i\Lambda^a T^a) D_{\dot{\alpha}}^\dagger \Phi \\ &= i \left(D_{\dot{\alpha}}^\dagger \Lambda^a \right) T^a \exp(i\Lambda^a T^a)\Phi \stackrel{!}{=} 0,\end{aligned}$$

which means that we must require $D_{\dot{\alpha}}^\dagger \Lambda^a = 0$, meaning that the parameters are themselves left-handed scalar superfields. Examining how the kinetic term $\Phi^\dagger\Phi$ does under this transformation we can see that⁹

$$\Phi^\dagger\Phi \rightarrow \Phi^\dagger e^{-i\Lambda^\dagger} e^{i\Lambda} \Phi = \Phi^\dagger e^{i(\Lambda - \Lambda^\dagger) - \frac{1}{2}[\Lambda, \Lambda^\dagger] + \dots} \Phi,\quad (2.41)$$

which is not invariant. To remedy this, we will introduce a term to compensate for this change, like before. For this we define a *supergauge field* $\mathcal{V} \equiv V^a T^a$ which transforms according to¹⁰

$$e^{2q\mathcal{V}} \rightarrow e^{i\Lambda^\dagger} e^{2q\mathcal{V}} e^{-i\Lambda}\quad (2.42)$$

⁹Using the Baker-Campbell-Hausdorff formula (BCH) to combine the exponentials.

¹⁰The factor of 2 in the exponential here seems arbitrary at first, and is just a matter of choice. It is chosen to be 2 here such that the transformation of law for \mathcal{V} is proportional to Λ without any numerical prefactors.

or infinitesimally

$$\mathcal{V} \rightarrow \mathcal{V} - \frac{i}{2q} (\Lambda - \Lambda^\dagger) + \frac{i}{2} [\Lambda + \Lambda^\dagger, \mathcal{V}]. \quad (2.43)$$

Changing the kinetic term to $\Phi^\dagger e^{2q\mathcal{V}} \Phi$ will then yield it invariant under supergauge transformations. Since we require the superlagrangian term to be real, we must require $\mathcal{V}^\dagger = \mathcal{V}$, meaning it must be a vector superfield according to Eq. (2.26).

As before, we would also like to add dynamics to the (super)gauge field \mathcal{V} . To this end, we introduce the supersymmetric field strength $\mathcal{W}_\alpha \equiv W_\alpha^a T^a$ for which we require the transformation law

$$\mathcal{W}_\alpha \rightarrow e^{i\Lambda} \mathcal{W}_\alpha e^{-i\Lambda}. \quad (2.44)$$

It can be shown that the left-handed chiral superfield construction

$$\mathcal{W}_\alpha = -\frac{1}{4} (\bar{D}\bar{D}) (e^{-2\mathcal{V}} D_\alpha e^{2\mathcal{V}}) \quad (2.45)$$

transforms this way, and recreates field-strength tensor earlier in Section 1.3 [21]. The gauge invariant superlagrangian kinetic term for the supergauge field becomes

$$\mathcal{L}_{\mathcal{V}\text{-kin}} = \frac{1}{4T(R)} \text{Tr} \{ \mathcal{W}^\alpha \mathcal{W}_\alpha \} \quad (2.46)$$

analogously to Eq. (1.55).

2.3.2 Field Content

Here I give a very brief overview of the field content and naming scheme of the MSSM – for a more comprehensive introduction I will refer to [21]. The basic idea is to embed every SM fermion into a chiral superfield, and the vector bosons into the vector superfields arising from local gauge invariance. Since the SM fermions are Dirac fermions, they require two different Weyl spinors, which means that two superfields are required to provide each fermion.

Consider an SM Dirac fermion

$$f_D = \begin{pmatrix} f \\ \bar{f}^\dagger \end{pmatrix}, \quad (2.47)$$

where f and \bar{f}^\dagger are two *different* left-handed and right-handed Weyl spinors respectively. The left-handed Weyl spinor part f is embedded into a superfield f wherein it receives a scalar *superpartner* \tilde{f}_L .¹¹ The superfield and Weyl spinor have the exact same name, which might seem needlessly confusing. However, it does lead to less cluttered notation, and context should clarify which is meant. The right-handed Weyl spinor part \bar{f}^\dagger is likewise embedded into a right-handed scalar superfield \bar{F}^\dagger , with a scalar superfield partner \tilde{f}_R . Furthermore, the left-handed scalar superfield f is part of an $SU(2)_L$ doublet of superfields F , matching the uppercase naming of the right-handed superfield \bar{F}^\dagger . The bar on superfields and right-handed Weyl spinors signify that they are $SU(2)_L$ singlets, i.e. they do not transform under such symmetry transformations, and makes it clear that the two Weyl spinors f and \bar{f}^\dagger are separate variables belonging to the same SM fermion field. Collectively, the scalar superpartners to the SM fermions are referred to as *sfermions*.

¹¹The subscript L on the scalar fields carries no indication of any chirality, but rather alludes to the origin of the field as a superpartner to the left-handed chiral part of the fermion field f_D .

The gauge groups of the MSSM are the same as in the SM, but the gauge fields are replaced by vector superfield gauge fields as detailed in Section 2.3.1. This way, an SM vector boson V^μ is embedded in a vector superfield V where it receives a left-handed Weyl spinor superpartner \tilde{V} with its right-handed compliment \tilde{V}^\dagger .

Lastly, and perhaps the most intricate, is the extension of the Higgs sector in the MSSM. As it turns out, the MSSM requires two Higgs doublets for anomaly cancellation within the $U(1)_Y$ gauge group sector, and to construct the Yukawa terms giving mass to particles with both positive and negative weak isospin.¹² This means that there are two scalar Higgs doublets H_u, H_d before electroweak symmetry breaking (EWSB), giving mass to fermions in the upper/lower part of $SU(2)_L$ fermion doublets respectively. For the anomaly cancellation to work out, we must require hypercharge $+1/2$ for H_u and $-1/2$ for H_d . These scalar Higgs field doublets are embedded in left-handed chiral superfields $H_{u/d}$ together with fermion superpartners. The superfield doublet components are named according to $H_u = (H_u^+, H_u^0)^T$ and $H_d = (H_d^0, H_d^-)^T$, where the superscript indicates the post EWSB electric charge of the superfields. The fermion partners to both the vector bosons and the Higgs bosons are called *bosinos* collectively. For reference all the superfields in the MSSM, their symbols and their component fields are tabulated in Table 2.1.

2.3.3 Superlagrangian and Supersymmetry Breaking

Now that we have defined the field content of the MSSM, we need to define the interaction between them through the superlagrangian. As has already been noted, the gauge groups of the MSSM are the same as for the SM, and all kinetic terms are defined according to the super Yang-Mills theory of Section 2.3.1. A summary of the gauge numbers of the scalar superfields is given in Table 2.2. This results in the kinetic part of the MSSM superlagrangian being

$$\begin{aligned} \mathcal{L}_{\text{kin}}^{\text{MSSM}} = & H_u^\dagger e^{g'B+2g\mathcal{W}} H_u + H_d^\dagger e^{-g'B+2g\mathcal{W}} H_d + L_i^\dagger e^{-g'B+2g\mathcal{W}} L_i + \bar{E}_i^\dagger e^{2g'B} \bar{E}_i \\ & + Q_i^\dagger e^{\frac{1}{3}g'+2g\mathcal{W}+2g_s\mathcal{C}} Q_i + \bar{U}_i^\dagger e^{-\frac{4}{3}g'+2g_s\mathcal{C}} \bar{D}_i + e^{\frac{2}{3}g'+2g_s\mathcal{C}} \bar{D}_i \\ & \frac{1}{4} B^\alpha B_\alpha + \frac{1}{2} \text{Tr}\{\mathcal{W}^\alpha \mathcal{W}_\alpha\} + \frac{1}{2} \text{Tr}\{\mathcal{C}^\alpha \mathcal{C}_\alpha\}, \end{aligned} \quad (2.48)$$

where $B^\alpha, \mathcal{W}^\alpha, \mathcal{C}^\alpha$ are the supersymmetric field strengths of the gauge superfields B , $\mathcal{W} = W^k \frac{1}{2} \sigma^k$ and $\mathcal{C} = C^a \frac{1}{2} \lambda^a$ respectively. The matrices λ^a are the Gell-Mann matrices — the generators of $SU(3)$.

The superpotential up to gauge invariant and R -parity conserving terms is given by

$$W_{\text{MSSM}} = \mu H_u^T i\sigma_2 H_d + y_{ij}^e (L_i^T i\sigma_2 H_d) \bar{E}_j + y_{ij}^u (Q_i^T i\sigma_2 H_u) \bar{U}_j + y_{ij}^d (Q_i^T i\sigma_2 H_d) \bar{D}_j, \quad (2.49)$$

where μ is some complex, massive parameters and $y_{ij}^{e/u/d}$ are the ordinary SM Yukawa couplings. This leaves two new degrees of freedom in the MSSM superpotential beyond what is in the SM — the phase and magnitude of μ .

Seeing as we have not discovered any particles with the same mass but opposite spin-statistics to the SM particles we know, we must conclude that supersymmetry is broken at low energy. A mechanism for spontaneous symmetry breaking of supersymmetry would therefore be necessary. Constructing such a mechanism in a way as to not reintroduce the hierarchy problem leads to what we call *soft* breaking of supersymmetry [21]. Disregarding the high-energy completion of the theory, we can

¹²For a more detailed explanation, I will refer the reader to [21].

	Superfield		Boson field	Fermion field	Auxiliary field
Higgs	H_u	H_u^+	H_u^+	\tilde{H}_u^+	$F_{H_u^+}$
		H_u^0	H_u^0	\tilde{H}_u^0	$F_{H_u^0}$
	H_d	H_d^0	H_d^0	\tilde{H}_d^0	$F_{H_d^0}$
		H_d^-	H_d^-	\tilde{H}_d^-	$F_{H_d^-}$
Leptons	L_i	ν_i	$\tilde{\nu}_{iL}$	ν_i	F_{ν_i}
		l_i	\tilde{l}_{iL}	l_i	F_{l_i}
	-	\bar{E}_i	\tilde{l}_{iR}^*	\bar{e}_i	$F_{\bar{E}_i}^*$
Quarks	Q_i	u_i	\tilde{u}_{iL}	u_i	F_{u_i}
		d_i	\tilde{d}_{iL}	d_i	F_{d_i}
	-	\bar{U}_i	\tilde{u}_{iR}^*	\bar{u}_i	$F_{\bar{U}_i}^*$
	-	\bar{D}_i	\tilde{d}_{iR}^*	\bar{d}_i	$F_{\bar{D}_i}^*$
Bosons	-	B^0	B_μ^0	\tilde{B}^0	D_{B^0}
	W^k	W^0	W_μ^0	\tilde{W}^0	D_{W^0}
		W^\pm	W_μ^\pm	\tilde{W}^\pm	D_{W^\pm}
	-	C^a	C_μ^a	\tilde{g}	D_C

Table 2.1: Table of superfields of the MSSM, and their component field names. Note that the fermion fields are left-handed Weyl spinors, in spite of any L or R in the boson field subscript. The conjugate superfields changes these to right-handed Weyl spinors. The indices i enumerate the three generations of leptons/quarks, k the three $SU(2)_L$ gauge fields and a the eight $SU(3)_C$ gauge fields.

parametrise the terms that can arise in the low-energy MSSM superlagrangian up to gauge invariant and R -parity conserving terms, as

$$\begin{aligned} \mathcal{L}_{\text{soft}}^{\text{MSSM}} = & (\theta\theta)(\theta\theta)^\dagger \left\{ -\frac{1}{4}M_1 B^\alpha B_\alpha - \frac{1}{2}M_2 \text{Tr}\{\mathcal{W}^\alpha \mathcal{W}_\alpha\} - \frac{1}{2}M_3 \text{Tr}\{\mathcal{C}^\alpha \mathcal{C}_\alpha\} + \text{c. c.} \right. \\ & - \frac{1}{6}a_{ij}^e L_i^T i\sigma_2 H_d \bar{E}_j - \frac{1}{6}a_{ij}^u Q_i^T i\sigma_2 H_u \bar{U}_j - \frac{1}{6}a_{ij}^d Q_i^T i\sigma_2 H_d \bar{D}_j + \text{c. c.} \\ & - \frac{1}{2}b H_u^T i\sigma_2 H_d + \text{c. c.} \\ & - (m_{ij}^L)^2 L_i^\dagger L_j - (m_{ij}^e)^2 \bar{E}_i^\dagger \bar{E}_j - (m_{ij}^Q)^2 Q_i^\dagger Q_j - (m_{ij}^u)^2 \bar{U}_i^\dagger \bar{U}_j - (m_{ij}^d)^2 \bar{D}_i^\dagger \bar{D}_j \\ & \left. - m_{H_u}^2 H_u^\dagger H_u - m_{H_d}^2 H_d^\dagger H_d \right\}. \end{aligned} \quad (2.50)$$

All the parameters are potentially complex numbers, although all the mass terms m_{ij}^2 must be hermitian in the that $m_{ij}^2 = (m_{ji}^2)^*$, which leads to m_{ii}^2 having to be real. This is the source of the great many parameters of the MSSM, as these soft-breaking parameters alone amount to 109 degrees of freedom!¹³ For this reason, most searches of the MSSM

¹³ A few of these can be eliminated through field redefinitions, however.

focus on various simplified models [22, 23]. These can be based on simplifications like assuming all parameters to be real or assuming no flavour-violation as in the phenomenological MSSM (pMSSM) [24], or by making theoretical assumptions on the specific mechanism for symmetry breaking, as in minimal supergravity (mSUGRA) [25], or any combinations of these. In this thesis, I will not make any such assumptions and work with the general form of the MSSM, unless otherwise stated. The full MSSM superlagrangian is then

$$\mathcal{L}_{\text{MSSM}} = \mathcal{L}_{\text{kin}}^{\text{MSSM}} + (\theta\theta)^\dagger W_{\text{MSSM}} + (\theta\theta) W_{\text{MSSM}}^\dagger + \mathcal{L}_{\text{soft}}^{\text{MSSM}}. \quad (2.51)$$

	Superfield		Hypercharge Y	Isospin I^3	Electric Charge Q_e	Colour
Higgs	H_u	H_u^+	+ 1/2	+ 1/2	+1	-
		H_u^0	+ 1/2	- 1/2	0	-
	H_d	H_d^0	- 1/2	+ 1/2	0	-
		H_d^-	- 1/2	- 1/2	-1	-
Leptons	L_i	ν_i	- 1/2	+ 1/2	0	-
		l_i	- 1/2	- 1/2	-1	-
	-	\bar{E}_i	+1	-	+1	-
Quarks	Q_i	u_i	+ 1/6	+ 1/2	+ 2/3	yes
		d_i	+ 1/6	- 1/2	- 1/3	yes
	-	\bar{U}_i	- 2/3	-	- 2/3	yes
	-	\bar{D}_i	+ 1/3	-	+ 1/3	yes

Table 2.2: Summary of quantum numbers for the MSSM scalar superfields. The charges of barred fields \bar{F} supplying the right-handed part of SM fermions are defined such that the charge of \bar{F}^\dagger matches that of its left-handed compliment. I note that the convention for the hypercharge differs from some sources, seeing as I use 1 as the generator of $U(1)_Y$ instead of $\frac{1}{2}$ used elsewhere. This amounts to shuffling some factors of $\frac{1}{2}$ around. The indices i enumerate the three generations of leptons/quarks.

2.4 Electroweakinos

The focus in this thesis we be on a particular set of superpartners, namely the *electroweakinos*. These are fermion superpartners to the electroweak bosons, i.e. the photon, Z and W bosons and the Higgs bosons. These are subdivided into the vector boson superpartners, the *gauginos*, and the Higgs boson partners, the *higgsinos*. Before EWSB, the gauge fields naturally occurring in the Lagrangian are the B - and W^k -fields, and it is customary to work with the fermion superpartners of these fields. These are naturally called the *binos* and *winos* respectively.

2.4.1 Mass mixing

After EWSB, we get two oppositely charged winos, and two mixed bino/wino states, mirroring the electroweak gauge bosons. However, the higgsinos come in an oppositely

charged pair and two neutral ones, so the gauginos and higgsinos can further mix. So the general electroweak fermionic sector in the MSSM includes two particle-antiparticle pairs of charged Dirac fermions, and four neutral Majorana fermions, respectively referred to as *charginos* and *neutralinos*. The two chargino fields are denoted with the Weyl spinors $\tilde{\chi}_{i=1,2}^\pm$, and the four neutralinos are denoted with the Weyl spinors $\tilde{\chi}_{i=1,2,3,4}^0$. The indices i are numbered according to the mass hierarchy, with 1 being the lightest chargino/neutralino and 2/4 being the heaviest.

Ignoring higher order corrections, the mass terms for the gauginos and higgsinos in the MSSM Lagrangian can be structured as

$$\mathcal{L}_{\tilde{\chi}\text{-mass}} = -\frac{1}{2}(\psi^0)^T M_{\tilde{\chi}^0} \psi^0 - \frac{1}{2}\psi^\pm{}^T M_{\tilde{\chi}^\pm} \psi^\pm + \text{c. c.}, \quad (2.52)$$

where $\psi^0 = (\tilde{B}^0, \tilde{W}^0, \tilde{H}_d^0, \tilde{H}_u^0)^T$, $\psi^\pm = (\psi^+, \psi^-)^T = (\tilde{W}^+, \tilde{H}_u^+, \tilde{W}^-, \tilde{H}_d^-)^T$ and $M_{\tilde{\chi}^0}$, $M_{\tilde{\chi}^\pm}$ are the neutralino and chargino mass matrices respectively. They are given by

$$M_{\tilde{\chi}^0} = \begin{bmatrix} M_1 & 0 & -m_Z c_\beta s_W & m_Z s_\beta s_W \\ 0 & M_2 & m_Z c_\beta c_W & -m_Z s_\beta c_W \\ -m_Z c_\beta s_W & m_Z c_\beta c_W & 0 & -\mu \\ m_Z s_\beta s_W & -m_Z s_\beta c_W & -\mu & 0 \end{bmatrix}, \quad (2.53)$$

$$M_{\tilde{\chi}^\pm} = \begin{bmatrix} 0 & 0 & M_2 & \sqrt{2}c_\beta m_W \\ 0 & 0 & \sqrt{2}s_\beta m_W & \mu \\ M_2 & \sqrt{2}s_\beta m_W & 0 & 0 \\ \sqrt{2}c_\beta m_W & \mu & 0 & 0 \end{bmatrix}, \quad (2.54)$$

where $s_\beta \equiv \sin \beta$, $c_\beta \equiv \cos \beta$ and β is defined from the relation

$$\tan \beta = \frac{v_u}{v_d}, \quad (2.55)$$

where $v_{u,d}$ are the vacuum expectation values of the $H_{u/d}$ field after electroweak symmetry breaking.

These mass matrices can be diagonalised to get the mass eigenstate *neutralinos* $\tilde{\chi}_i^0$ and *charginos* $\tilde{\chi}_i^\pm$, respectively. Both the matrices are symmetric, but we will diagonalise them slightly differently. The neutralino mass matrix can be diagonalised by a unitary matrix N such that

$$\begin{aligned} \mathcal{L}_{\tilde{\chi}^0\text{-mass}} &= -\frac{1}{2}(\psi^0)^T M_{\tilde{\chi}^0} \psi^0 + \text{c. c.} = -\frac{1}{2} \underbrace{(\psi^0)^T N^T}_{\equiv (\tilde{\chi}^0)^T} \underbrace{N^* M_{\tilde{\chi}^0} N^\dagger}_{=\text{diag}(m_{\tilde{\chi}_1^0}, \dots, m_{\tilde{\chi}_4^0})} \underbrace{N \psi^0}_{\equiv \tilde{\chi}^0} + \text{c. c.} \\ &= -\frac{1}{2}(\tilde{\chi}^0)^T \text{diag}(m_{\tilde{\chi}_1^0}, \dots, m_{\tilde{\chi}_4^0}) \tilde{\chi}^0 + \text{c. c.} \end{aligned} \quad (2.56)$$

This factorisation is guaranteed by Takagi factorisation, which I prove in Appendix B. When M_1 , M_2 and μ are real-valued, we can guarantee that the mixing matrix N is real and orthogonal – however, this will cause at least one of the neutralino masses to have a negative sign. This is the assumption for the SUSY Les Houches Accord (SLHA1) [26]. In this thesis, I will allow the mixing matrices to be complex, and enforce positive neutralino masses. Details on the realisation of the neutralino mixing matrix is given in the next section Section 2.5.

The chargino mass matrix is handled slightly differently, seeing as it has the structure $M_{\tilde{\chi}^\pm} = \begin{bmatrix} 0 & X \\ X^T & 0 \end{bmatrix}$. Using singular value decomposition, we can write $X = U^T D V$

for two unitary matrices U , V and a diagonal matrix of positive singular values $D = \text{diag}(m_{\tilde{\chi}_1^\pm}, m_{\tilde{\chi}_2^\pm})$. This results in

$$\begin{aligned}\mathcal{L}_{\tilde{\chi}^\pm\text{-mass}} &= -\frac{1}{2}\psi^{\pm T}M_{\tilde{\chi}^\pm}\psi^\pm + \text{c. c.} = -\frac{1}{2}\begin{pmatrix}\psi^+ \\ \psi^-\end{pmatrix}^T \begin{bmatrix} 0 & U^T DV \\ V^T DU & 0 \end{bmatrix} \begin{pmatrix}\psi^+ \\ \psi^-\end{pmatrix} + \text{c. c.} \\ &= -\frac{1}{2}\underbrace{(\psi^+)^T U^T D V \psi^-}_{\equiv (\tilde{\chi}^+)^T} - \frac{1}{2}\underbrace{(\psi^-)^T V^T D U \psi^+}_{\equiv (\tilde{\chi}^-)^T} + \text{c. c.} \\ &= -(\tilde{\chi}^+)^T \text{diag}(m_{\tilde{\chi}_1^\pm}, m_{\tilde{\chi}_2^\pm}) \tilde{\chi}^- + \text{c. c.}\end{aligned}\quad (2.57)$$

This tells us that there are two doubly degenerate mass eigenvalues of the chargino mass matrix, constituting two massive Dirac fermion particle-antiparticle pairs.

Proof of Takagi factorisation and an algorithm for realising it are done in Appendix B.

2.4.2 Feynman Rules for Neutralinos

To calculate the cross-section for electroweakino production later on, we will need the Feynman rules of the relevant particle interactions. I will not explicitly derive the Feynman rules for all the electroweakinos, but rather exemplify how they can be derived by deriving all the relevant neutralino interactions from the MSSM superlagrangian. The relevant Feynman rules for the remaining electroweakino processes follow in much the same manner, and are listed in the end.

Fermion Interactions in Super Yang-Mills and Yukawa Theory

I will start by deriving the interactions of fermions in the chiral superfields and vector superfields of a supersymmetric Yang-Mills superlagrangian. As a reminder, the super Yang-Mills superlagrangian kinetic term is $\Phi_i^\dagger (e^{2qV})_{ij} \Phi_j$. Extracting the interaction terms containing either the fermion field multiplets ψ (ψ^\dagger) from the left-handed (right-handed) scalar superfield multiplets Φ (Φ^\dagger), and the fermion fields $\lambda \equiv \lambda^a T^a$ from vector superfields $V \equiv V^a T^a$ from terms with the appropriate amount of θ 's to survive the projection of Eq. (2.29), we have

$$\begin{aligned}\mathcal{L} \stackrel{\psi, \psi^\dagger, \lambda}{\supset} & 2q \sum_{ij} \left\{ A_i^*(\theta\theta)^\dagger (\theta\lambda_{ij}) \sqrt{2}(\theta\psi_j) + \sqrt{2}(\theta\psi_i)^\dagger (\theta\sigma^\mu\theta^\dagger) (V_\mu)_{ij} \sqrt{2}(\theta\psi_j) \right. \\ & \left. + \sqrt{2}(\theta\psi_i)^\dagger (\theta\theta)(\theta\lambda_{ij})^\dagger A_j \right\} \\ & = q(\theta\theta)(\theta\theta)^\dagger \sum_{ij} \left\{ -\sqrt{2}A_i^*(\lambda_{ij}\psi_j) + (\psi_i\sigma^\mu (V_\mu)_{ij}\psi_j^\dagger) - \sqrt{2}(\psi_i\lambda_{ij})^\dagger A_j \right\},\end{aligned}\quad (2.58)$$

where I have used Weyl spinor relations listed in Appendix A.

There are also Yukawa terms coming from the superpotential terms of the form $y_{ij}(\theta\theta)^\dagger \Phi_i \Phi \Phi_j + \text{c. c.}$ Here Φ will later represent one of the Higgs superfields. Extracting the interaction terms of fermion field ψ from Φ , we find

$$\begin{aligned}\mathcal{L} \stackrel{\psi, \psi^\dagger}{\supset} & y_{ij}(\theta\theta)^\dagger \sqrt{2}(\theta\psi) \left\{ A_i \sqrt{2}(\theta\psi_i) + \sqrt{2}(\theta\psi_j) A_j \right\} + \text{c. c.} \\ & = -y_{ij}(\theta\theta)(\theta\theta)^\dagger \{ A_i(\psi\psi_j) + (\psi_i\psi) A_j + \text{c. c.} \}\end{aligned}\quad (2.59)$$

Wino and Bino Interactions

First, I will look at the bino and wino interactions coming from the kinetic terms. Writing out the W^a vector superfields in the basis W^\pm, W^0 , we are now only interested in the electrically neutral W^0 bit. The interactions will come from kinetic terms of scalar superfields Φ , whose relevant part can be written as

$$\mathcal{L} = \Phi^\dagger e^{2g\{Y t_W B^0 (+\frac{1}{2}\sigma_3 W^0)\}} \Phi, \quad (2.60)$$

where $t_W \equiv \tan \theta_W$ is the tangent of the Weinberg angle, Y is the hypercharge of Φ and the term in parentheses only appears for fields in $SU(2)_L$ superfield doublets. To generalise this, I will use the isospin I^3 , which is $+\frac{1}{2}$ for fields in the upper part of an $SU(2)$ doublet, $-\frac{1}{2}$ for fields in the lower part and 0 for $SU(2)$ singlet fields. Then the kinetic term can be written compactly as

$$\mathcal{L} = \Phi^\dagger e^{2g\{(Q_e - I^3)t_W B^0 + I^3 W^0\}} \Phi, \quad (2.61)$$

where Q_e is the electric charge of Φ .

Extracting the interactions of the fermion fields \tilde{B}^0, \tilde{W}^0 in B^0, W^0 using Eq. (2.58), we are left with (up to appropriate θ 's)

$$\mathcal{L} \stackrel{\tilde{B}^0, \tilde{W}^0}{\supset} -\sqrt{2}g(\theta\theta)(\theta\theta)^\dagger \{(Q_e - I^3)t_W(\tilde{B}^0\psi)A^* + I^3(\tilde{W}^0\psi)A^* + \text{c. c.}\}. \quad (2.62)$$

Consider an SM quark q , from the scalar superfield components A and ψ contained in the superfields Q and \bar{Q} , with electric charge Q_e and weak isospins I^3 and 0 respectively, we can write out the interaction as

$$\mathcal{L} = -\sqrt{2}g\{(Q_e - I^3)t_W(\tilde{B}^0 q)\tilde{q}_L^* + I^3(\tilde{W}^0 q)\tilde{q}_L^* + Q_e t_W(\tilde{B}^0 \bar{q})\tilde{q}_R^* + \text{c. c.}\}. \quad (2.63)$$

Changing to the $\tilde{\chi}^0$ -basis, we have that $\tilde{B}^0 = \sum_i N_{i1}^* \tilde{\chi}_i^0$, $\tilde{W}^0 = \sum_i N_{i2}^* \tilde{\chi}_i^0$, which together with writing out the Weyl products on Dirac spinor form yields

$$\begin{aligned} \mathcal{L}_{\tilde{q}q\tilde{\chi}^0} = -\sqrt{2}g \sum_i \tilde{\chi}_i^0 & \left\{ \underbrace{[(Q_e - I^3) t_W N_{i1}^* + I^3 N_{i2}^*]}_{\equiv (C_{\tilde{q}q\tilde{\chi}_i^0}^L)^*} \tilde{q}_L^* P_L \underbrace{- Q_f t_W N_{i1}}_{\equiv (C_{\tilde{q}q\tilde{\chi}_i^0}^R)^*} \tilde{q}_R^* P_R \right\} q + \text{c. c.}, \\ \end{aligned} \quad (2.64)$$

where we understand $\tilde{\chi}_i^0$ and q as Dirac spinors.

More generally, mixing can occur between the left- and right-handed chiral squark states. The mass terms mixing the chiral states come from Yukawa terms in the superpotential and soft-breaking potential, and as such it is most prevalent in the third generation where the Yukawa couplings are larger from the SM. SLHA1 standard [26] assumes no such mixing in the first two generations, but does allow for it in the last generation.

Without flavour-violation, we have that the squarks of flavour q mix such that we get the mass eigenstates by

$$\tilde{q}_A = R_{A1}^{\tilde{q}} \tilde{q}_L + R_{A2}^{\tilde{q}} \tilde{q}_R, \quad (2.65)$$

where $R^{\tilde{q}}$ is a 2×2 unitary matrix. As such, we can write $\tilde{q}_L = \sum_A (R_{A1}^{\tilde{q}})^* \tilde{q}_A$, $\tilde{q}_R = \sum_A (R_{A2}^{\tilde{q}})^* \tilde{q}_A$ to get

$$\mathcal{L}_{\tilde{q}q\tilde{\chi}^0} = -\sqrt{2}g \sum_i \sum_A \tilde{\chi}_i^0 \left\{ \underbrace{R_{A1}^{\tilde{q}} (C_{\tilde{q}q\tilde{\chi}_i^0}^L)^*}_{\equiv (C_{\tilde{q}Aq\tilde{\chi}_i^0}^L)^*} P_L + \underbrace{R_{A2}^{\tilde{q}} (C_{\tilde{q}q\tilde{\chi}_i^0}^R)^*}_{\equiv (C_{\tilde{q}Aq\tilde{\chi}_i^0}^R)^*} P_R \right\} \tilde{q}_A^* q + \text{c. c.} \quad (2.66)$$

Flavour-Violating Squark Sector

The previous derivation was done under the assumption that squarks do not mix between fermion generations, violating flavour number. However, this can happen if there are non-zero supersymmetry-breaking parameters coupling squarks between generations or if loop corrections are added to the squark sector. The generalisation is fairly straight forward: Instead of one unitary, 2×2 mixing matrix $R^{\tilde{q}}$ for each of the six quark flavours $q = u, d, s, c, t, b$, there is one 6×6 mixing matrix $R^{\tilde{q}}$ for each of the two quark types $q = u, d$. These mixing matrices can be defined using different conventions, but in this thesis I will follow the SLHA2 standard [27]

$$\begin{pmatrix} \tilde{q}_1 \\ \tilde{q}_2 \\ \tilde{q}_3 \\ \tilde{q}_4 \\ \tilde{q}_5 \\ \tilde{q}_6 \end{pmatrix} = R^{\tilde{q}} \begin{pmatrix} \tilde{q}_{1L} \\ \tilde{q}_{2L} \\ \tilde{q}_{3L} \\ \tilde{q}_{1R} \\ \tilde{q}_{2R} \\ \tilde{q}_{3R} \end{pmatrix} \quad (2.67)$$

This means that the chiral squarks in generation $g = 1, 2, 3$ will rather be given by

$$\tilde{q}_{gL} = \sum_A (R_{A,g}^{\tilde{q}})^* \tilde{q}_A, \quad (2.68a)$$

$$\tilde{q}_{gR} = \sum_A (R_{A,g+3}^{\tilde{q}})^* \tilde{q}_A. \quad (2.68b)$$

What this means for the interaction Lagrangian in Eq. (2.64) is that the sum over A changes to go from 1 to 6 and the definition of the coupling parameter changes slightly to

$$C_{\tilde{q}_A q_g \tilde{\chi}_i^0}^L = (R_{A,g}^{\tilde{q}})^* \left[(Q_e - I^3) t_W N_{i1} + I^3 N_{i2} \right], \quad (2.69a)$$

$$C_{\tilde{q}_A q_g \tilde{\chi}_i^0}^R = - (R_{A,g+3}^{\tilde{q}})^* Q_e t_W N_{i1}^*. \quad (2.69b)$$

Higgsino Interactions

Higgsino interaction with the squarks comes from the Yukawa terms of the superpotential. As they are the mass-giving terms of for the quarks, they are proportional to the quark masses. Accordingly, at the center-of-mass energies at the LHC, for which the calculations of this thesis are intended, only the last generation of squarks will have non-negligible couplings. However, due low parton density for the bottom quark (and non-existent for the top quark), we can safely ignore these terms in the present derivation.

The remaining relevant interaction that remains then, is that with the Z -boson. This interaction again comes from the kinetic term, but this time for the neutral Higgs superfields in the superfield multiplets $H_u = (H_u^+, H_u^0)^T$, $H_d = (H_d^0, H_d^-)^T$. The Lagrangian is of the form

$$\mathcal{L} = (H_{u/d}^0)^\dagger e^{\mp g(W^0 - t_W B^0)} H_{u/d}^0. \quad (2.70)$$

Integrating over the Grassmann variables and using equation Eq. (2.58) we get

$$\int d^4\theta \mathcal{L} \stackrel{\tilde{H}_{u/d}^0, W_\mu^0, B_\mu^0}{=} \mp \frac{g}{2} (\tilde{H}_{u/d}^0 \sigma^\mu (\tilde{H}_{u/d}^0)^\dagger) (W_\mu^0 - t_W B_\mu^0). \quad (2.71)$$

Switching to Dirac spinors, the mass eigenbasis for the neutralinos and the Z boson $Z_\mu = c_W W_\mu^0 - s_W B_\mu^0$, we end up with¹⁴

$$\begin{aligned}\mathcal{L}_{Z\tilde{\chi}_i^0\tilde{\chi}_j^0} &= \frac{g}{2c_W} Z_\mu \sum_{ij} \left(-N_{i4} N_{j4}^* + N_{i3} N_{j3}^* \right) \bar{\tilde{\chi}}_i^0 \gamma^\mu P_L \tilde{\chi}_j^0 \\ &= -\frac{g}{2} Z_\mu \sum_{ij} \bar{\tilde{\chi}}_i^0 \gamma^\mu \left[\underbrace{\frac{1}{2c_W} \left(N_{i4} N_{j4}^* - N_{i3} N_{j3}^* \right) P_L}_{\equiv O''_{ij}^L} - \underbrace{\frac{1}{2c_W} \left(N_{i4}^* N_{j4} - N_{i3}^* N_{j3} \right) P_R}_{\equiv O''_{ij}^R} \right] \tilde{\chi}_j^0\end{aligned}\quad (2.72)$$

Summary of Coupling Definitions

In summary, the Feynman rules for the interactions of neutralinos with the electroweak bosons and (s)quarks are given by the interaction Lagrangians in Eqs. (2.66) and (2.72) as

$$= -ig\gamma^\mu \left[O''_{ij}^L P_L + O''_{ij}^R P_R \right], \quad (2.73a)$$

$$= -i\sqrt{2}g \left[\left(C_{q_A q_g \tilde{\chi}_i^0}^L \right)^* P_L + \left(C_{q_A q_g \tilde{\chi}_i^0}^R \right)^* P_R \right]. \quad (2.73b)$$

In fact, the interactions of all electroweakinos with W/Z -bosons and (s)quarks take the same form, and we can generalise by replacing O''_{ij}^X or $C_{q_A q_g \tilde{\chi}_i^0}^X$ with the appropriate definitions in Table 2.3 [28].

A couple of remarks these Feynman rules: The rule Eq. (2.73a) is a factor of two greater than the corresponding Lagrangian term Eq. (2.72) due to the symmetry between i, j in Eq. (2.72). Furthermore, when the incoming and outgoing states are reverse, the conjugate term of the Lagrangians Eqs. (2.66) and (2.72) must be used, effectively conjugating the couplings in Eq. (2.73a), and conjugating the couplings *and* switching $L \leftrightarrow R$ in Eq. (2.73b).

2.5 Diagonalisation and Takagi Factorisation

In this section, I will talk briefly about the diagonalisation procedure for complex, symmetric matrices due to L. Autonne [29] and T. Takagi [30]. Furthermore, I will present an algorithm for finding the diagonalising matrix numerically for a given symmetric matrix.

2.5.1 Numerical Diagonalisation

Finding the diagonalisation matrix U for some matrix A is not always entirely straightforward when done numerically. It often entails finding solutions to sets of linear

¹⁴Here I have used some of the Weyl spinor identities from Appendix A.

Interaction	Coupling	Definition
$\tilde{q}q\tilde{\chi}^0$	$C_{\tilde{q}_A q_g \tilde{\chi}_i^0}^L$	$\left(R_{A,g}^{\tilde{q}}\right)^* \left[\left(Q_e - I_q^3\right) t_W N_{i1} + I_q^3 N_{i2} \right]$
	$C_{\tilde{q}_A q_g \tilde{\chi}_i^0}^R$	$- \left(R_{A,g+3}^{\tilde{q}}\right)^* Q_e t_W N_{i1}^*$
$W\tilde{\chi}^0\tilde{\chi}^\pm$	O_{ij}^L	$\frac{1}{\sqrt{2}} N_{i4} V_{j2}^* - N_{i2} V_{j1}^*$
	O_{ij}^R	$- \frac{1}{\sqrt{2}} N_{i3}^* U_{j2} - N_{i2}^* U_{j1}$
$Z\tilde{\chi}^\pm\tilde{\chi}^\mp$	$O_{ij}^{L'}^L$	$\frac{1}{c_W} \left(V_{i1} V_{j1}^* + \frac{1}{2} V_{i2} V_{j2}^* - \delta_{ij} s_W^2 \right)$
	$O_{ij}^{L'}^R$	$\frac{1}{c_W} \left(U_{i1} U_{j1}^* + \frac{1}{2} U_{i2} U_{j2}^* - \delta_{ij} s_W^2 \right)$
$Z\tilde{\chi}^0\tilde{\chi}^0$	$O_{ij}''^L$	$\frac{1}{2c_W} \left(N_{i4} N_{j4}^* - N_{i3} N_{j3}^* \right)$
	$O_{ij}''^R$	$- \frac{1}{2c_W} \left(N_{i4}^* N_{j4} - N_{i3}^* N_{j3} \right)$
$\tilde{q}q'\tilde{\chi}^\pm$	$C_{\tilde{d}_A u_g \tilde{\chi}_i^\pm}^L$	$\frac{1}{\sqrt{2}} U_{i1} \left(R_{A,g}^{\tilde{d}}\right)^* V_{u_g d_g}^{\text{CKM}}$
	$C_{\tilde{u}_A d_g \tilde{\chi}_i^\pm}^L$	$\frac{1}{\sqrt{2}} V_{i1} \left(R_{A,g}^{\tilde{u}}\right)^* \left(V_{u_g d_g}^{\text{CKM}}\right)^*$
	$C_{\tilde{q}_A q'_g \tilde{\chi}_i^\pm}^R$	0
qqZ	C_{qqZ}^L	$- \frac{I_q^3 - Q_e s_W^2}{c_W}$
	C_{qqZ}^R	$\frac{Q_e s_W^2}{c_W}$
$qq'W$	$C_{qq'W}^L$	$- \frac{V_{qq'}^{\text{CKM}}}{c_W}$
	$C_{qq'W}^R$	0
$\tilde{q}\tilde{q}Z$	$C_{\tilde{q}_A \tilde{q}_B Z}^L$	$- \frac{I_q^3 - Q_e s_W^2}{c_W} R_{A,g}^{\tilde{q}} \left(R_{B,g}^{\tilde{q}}\right)^* = C_{qqZ}^L R_{A,g}^{\tilde{q}} \left(R_{B,g}^{\tilde{q}}\right)^*$
	$C_{\tilde{q}_A \tilde{q}_B Z}^R$	$\frac{Q_e s_W^2}{c_W} R_{A,g+3}^{\tilde{q}} \left(R_{B,g+3}^{\tilde{q}}\right)^* = C_{qqZ}^R R_{A,g+3}^{\tilde{q}} \left(R_{B,g+3}^{\tilde{q}}\right)^*$
$\tilde{q}\tilde{q}W$	$C_{\tilde{q}_A \tilde{q}'_B W}^L$	$- \frac{V_{qq'}^{\text{CKM}}}{c_W} R_{A,g}^{\tilde{q}} \left(R_{B,g}^{\tilde{q}'}\right)^* = C_{qq'W}^L R_{A,g}^{\tilde{q}} \left(R_{B,g}^{\tilde{q}'}\right)^*$
	$C_{\tilde{q}_A \tilde{q}'_B W}^R$	0

Table 2.3: A summary of the variables used in the derived Feynman rules and their definitions. Furthermore, it is extended with the Feynman rules beyond those derived explicitly in this thesis.

equations like

$$M\mathbf{x} = \lambda\mathbf{y}, \quad (2.74)$$

for some matrix M , vectors \mathbf{x}, \mathbf{y} and number λ . For vectors

2.5.2 Takagi Factorisation

Consider a complex, symmetric $n \times n$ matrix A . Takagi factorisation [31] tells us that there exists a unitary matrix U , and a real, non-negative diagonal matrix D such that

$$A = U^T D U. \quad (2.75)$$

I remark that U is potentially complex, so $U^{-1} = U^\dagger \neq U^T$, so Eq. (2.75) should not be confused with the ordinary diagonalisation of a real matrix $R = U^{-1} D U$ where $U^{-1} = U^T$.

Factorisation Procedure

I would first like to outline a practical procedure for finding such a diagonalising matrix U , and consequently D . It will be based on finding vector $\mathbf{v} \in \mathbb{C}^n$ that satisfies

$$A\mathbf{v}^* = \sigma\mathbf{v}, \quad (2.76)$$

for some real, non-negative number σ . A vector satisfying the modified eigenvalue relation Eq. (2.76) is called a *Takagi vector* for future reference. Existence of these vectors for any matrix A , where AA^* only has real, non-negative eigenvalues is detailed in Appendix B.¹⁵

To find U then, I outline a procedure based on the proof for Takagi factorisation in [31]. Given a Takagi vector \mathbf{v} of A , and an orthonormal basis $\{\mathbf{v}_1, \mathbf{v}_2, \dots, \mathbf{v}_n\}$ of \mathbb{C}^n , I show in Appendix B that we can make a diagonalisation step on A , writing it as

$$A = V \begin{bmatrix} \sigma & \mathbf{0} \\ \mathbf{0} & A_2 \end{bmatrix} V^T, \quad (2.77)$$

where A_2 is a symmetric $(n-1) \times (n-1)$ matrix and V is a unitary matrix with the aforementioned orthonormal basis as its columns. This process can be repeated with A_2 and so on until we have

$$A = V_1 \cdots V_n \begin{bmatrix} \sigma_1 & & 0 \\ & \ddots & \\ 0 & & \sigma_n \end{bmatrix} V_n^T \cdots V_1^T, \quad (2.78)$$

where

$$V_p = \begin{bmatrix} \mathbb{I}_{(p-1) \times (p-1)} & \mathbf{0} \\ \mathbf{0} & \tilde{V}_p \end{bmatrix} \quad (2.79)$$

and \tilde{V}_p is the unitary matrix that makes a diagonalisation step on A_p . Comparing to Eq. (2.75), we find that

$$U = V_n^T \cdots V_1^T, \quad (2.80a)$$

$$D = \text{diag}(\sigma_1, \dots, \sigma_n). \quad (2.80b)$$

It is easy to show that U is unitary, as promised, as all V_p are so. Furthermore, by the properties of the Takagi vector, all the values σ_p are real and positive. Now the values

¹⁵This is always true for a symmetric matrix, as $AA^* = A^T A^\dagger = (AA^*)^\dagger$ must be hermitian.

on the diagonal of D can be permuted to any order using a permutation matrix P , such that we get

$$A = U_P^T D_P U_P, \quad (2.81)$$

where $U_P = PU$ and $D_P = PDP^T$. It is rather straight-forward to show that U_P will still be unitary, and D_P diagonal.

An algorithmic implementation of this procedure is shown in Algorithm 1.

Algorithm 1 Diagonalisation step on an $n \times n$ symmetric matrix A to find a matrix U s.t. $A = U^T \begin{bmatrix} \sigma & \mathbf{0} \\ \mathbf{0} & A' \end{bmatrix} U$, where $\sigma = \sqrt{|\lambda|}$ for some eigenvalue λ of AA^* and A' is an $(n-1) \times (n-1)$ symmetric matrix. The algorithm relies on a function `eigh(M)` to give an eigenvalue with its corresponding eigenvector of a hermitian matrix M , and `GramSchmidt(M)` to orthogonalise a complex, invertible matrix M . The algorithm also relies on some machine precision parameter ϵ .

Ensure: $\dim(A) \geq 2$

```

 $\lambda, \mathbf{x} = \text{eigh}(AA^*)$ 
if  $|(Ax^*) \cdot \mathbf{x}|^2 - |Ax^*|^2 |\mathbf{x}|^2 < \epsilon$  then
     $\mathbf{v} \leftarrow \frac{\mathbf{x}}{|\mathbf{x}|}$ 
else
     $\mathbf{v} \leftarrow Ax^* + \sqrt{|\lambda[1]|} \mathbf{x}$ 
     $\mathbf{v} \leftarrow \frac{\mathbf{v}}{|\mathbf{v}|}$ 
end if
 $\mu \leftarrow \frac{\mathbf{v} \cdot \mathbf{x}}{|\mathbf{x}|^2}$ 
 $\phi_\mu \leftarrow \text{atan2}(\text{imag}(\mu), \text{real}(\mu))$ 
 $\mathbf{v} \leftarrow \exp(i\phi_\mu/2) \mathbf{v}$ 
 $I \leftarrow \text{diag}(N) i \leftarrow 1$ 
repeat
     $V \leftarrow \text{Matrix}(\text{cols}=(\mathbf{v}, \text{deleteColumn}(I, i)))$ 
     $i \leftarrow i + 1$ 
until  $\det(V) > \epsilon$  or  $i > N$ 
 $V \leftarrow \text{GramSchmidt}(V)$ 
 $U \leftarrow V^*$ 

```

Chapter 3

Electroweakino Pair Production at Parton Level

In this chapter, I will go through the details of the calculation of the leading order (LO) contributions to the cross-section of production of pairs of electroweakinos at the level of partons, i.e. the fundamental particles of QCD. The next chapter will complete the calculations at hadron level for proton–proton collisions. The possible electroweakino pairs includes neutralino pair production $\tilde{\chi}_i^0 \tilde{\chi}_j^0$, a neutralino with a chargino $\tilde{\chi}_i^0 \tilde{\chi}_j^\pm$ or a chargino pair $\tilde{\chi}_i^\pm \tilde{\chi}_j^\mp$. Furthermore, I will compute the next-to-leading order (NLO) QCD corrections to higgsino-like part of neutralino pair production. Finally, I outline how the computation of the gaugino-like NLO contributions can proceed.

All the calculations have been done with self-produced `Mathematica` [32] scripts, with double-checks done with hand-calculations and comparison to existing results [33, 34]. The scripts can be found in this repository <https://github.com/carlwmfe/MastersThesis>.

3.1 Phase Space and Kinematics in Scattering Processes

To start off, it will be useful to introduce some procedure for going forward in the phase space of an inclusive $2 \rightarrow 2(+1)$ scattering process. The phase space of 2-body and 3-body final states are quite different as there are more degrees of freedom in the 3-body final state. In the end, these extra degrees of freedom will be need to be integrated over to compare between the 2-body and 3-body processes, however, exactly how we choose to parametrise and subsequently integrate over the extra degrees of freedom can matter quite a bit.

Furthermore, I will use the shorthand $m_{i,j}$ for the neutralino masses $p_{i,j}^2$ and m_A for squark masses $m_{\tilde{q}_A}$.

To start out, let us count the degrees of freedom of a scattering problem involving N four-momenta $p_{i=1,\dots,N}$. Assuming our end result to be Lorentz invariant, there are $N(N + 1)/2$ different scalar products that can be produced using N different four-momenta. Momentum conservation allows us to eliminate one momentum, such that we have $N(N - 1)/2$ possible scalar products. Denoting the scalar products by $m_{ij}^2 \equiv (p_i + p_j)^2$ for $j \neq i$, and $m_i^2 \equiv p_i^2$, we can find a relation between scalar products

by using momentum conservation.

$$\begin{aligned}
 m_{ij}^2 &= \left(\sum_{k \neq i,j} p_k \right)^2 = \sum_{k \neq i,j} \sum_{l \neq i,j} p_k \cdot p_l \\
 &= \sum_{k \neq i,j} \sum_{\substack{l \neq i,j \\ l > k}} \frac{m_{kl}^2 - m_k^2 - m_l^2}{2} + \sum_{k \neq i,j} m_k^2 \\
 &= \sum_{\substack{k \neq i,j \\ l \neq i,j \\ l > k}} m_{kl}^2 - \frac{1}{2} \sum_{k \neq i,j} (N-3)m_k^2 - \frac{1}{2} \sum_{l \neq i,j} (N-3)m_l^2 + \sum_{k \neq i,j} m_k^2 \\
 &= \sum_{\substack{k \neq i,j \\ l \neq i,j \\ l > k}} m_{kl}^2 - (N-4) \sum_{k \neq i,j} m_k^2.
 \end{aligned} \tag{3.1}$$

To count the degrees of freedom in an N -body final state, we need to classify how many scalar products need to be specified for every scalar product to be defined. We assign the N scalar products m_i^2 to the invariant masses of the incoming and outgoing particles, thereby not counting them as kinematic degrees of freedom, which leaves us with $N(N-3)/2$ degrees of freedom.¹ This means that in a $2 \rightarrow 2$ process, we must specify two kinematic variables, and in a $2 \rightarrow 3$ process we must specify five. For instance, in the $2 \rightarrow 2$ case, the canonical Mandelstam variables s, t, u can be used together with the restriction that $s + t + u = \sum_i m_i^2$.

For reference, I give the general formula for the Lorentz invariant differential phase space for a process of n_i particles with four-momenta k_i going to n_f particles with four-momenta p_j in d space-time dimensions [14]:

$$d\Pi_{n_i \rightarrow n_f} = (2\pi)^d \delta^d \left(\sum_{i=1}^{n_i} k_i - \sum_{j=1}^{n_f} p_j \right) \prod_{j=1}^{n_f} \frac{d^{d-1} \mathbf{p}_j}{(2\pi)^{d-1}} \frac{1}{2E_j}, \tag{3.2}$$

where the particles with four-momenta p_j are understood to be on-shell, i.e. $E_j^2 = m_j^2 + \mathbf{p}_j^2$, where m_j is the mass of the particle.

3.1.1 2-body Phase Space

Two phase spaces in particular will be useful for this thesis. First, let us go over the phase space of a 2-body final state in d dimensions. From Eq. (3.2) above, the Lorentz invariant phase space differential for a 2-body final state with four-momenta p_i, p_j is

$$d\Pi_{2 \rightarrow 2} = (2\pi)^d \delta^d (P - p_i - p_j) \frac{d^{d-1} \mathbf{p}_i}{(2\pi)^{d-1}} \frac{1}{2E_i} \frac{d^{d-1} \mathbf{p}_j}{(2\pi)^{d-1}} \frac{1}{2E_j}, \tag{3.3}$$

where P^μ is the sum of four-momenta of the incoming particles. Going to the centre-of-mass frame of the incoming particles, we have $P^\mu = (\sqrt{s}, 0, 0, 0)$, where $s \equiv P^2$. This allows us to integrate over the spatial part of Dirac delta-function to arrive at

$$d\Pi_{2 \rightarrow 2} = \frac{1}{(2\pi)^{d-2}} d^{d-1} \mathbf{p} \frac{1}{4E_i E_j} \delta(\sqrt{s} - E(p, m_i) - E(p, m_j)), \tag{3.4}$$

where the $E(p, m) = \sqrt{p^2 + m^2}$ and p is the magnitude of the centre-of-mass momentum of the outgoing particles. We can write out the differential of \mathbf{p}_i in spherical coordinates

¹I note that we will often consider the invariant mass of the incoming bodies to be fixed, which would reduce our degrees of freedom by one.

as $d^{d-1}\mathbf{p} = d\Omega_{d-1} dp p^{d-2} = d\Omega_{d-2} \sin^{d-3} \theta d\theta dp p^{d-2}$. As a $2 \rightarrow 2$ process is restricted to a plane, we can always go to a frame of reference such that any amplitude we calculate will not be dependent on the spatial angles $d\Omega_{d-2}$, allowing us to integrate over them using that $\int d\Omega_{d-2} = 2\pi^{\frac{d-2}{2}} \frac{1}{\Gamma(\frac{d-2}{2})}$ to get

$$d\Pi_{2 \rightarrow 2} = \frac{1}{(4\pi)^{\frac{d-2}{2}}} \frac{1}{\Gamma\left(\frac{d-2}{2}\right)} \frac{p^{d-3}}{2\sqrt{s}} \sin^{d-3} \theta d\theta, \quad (3.5)$$

where by integrating over the remaining delta-function the momentum is given by

$$p = \frac{\sqrt{\lambda(s, m_i^2, m_j^2)}}{2\sqrt{s}}. \quad (3.6)$$

The λ function is known as the Källén function and is defined as

$$\lambda(x, y, z) = x^2 + y^2 + z^2 - 2xy - 2xz - 2yz. \quad (3.7)$$

In $d = 4$ dimensions, it is often convenient to change to the Mandelstam variable t , which for massless initial state particles becomes $t = \frac{1}{2}(-s + m_i^2 + m_j^2 + \sqrt{\lambda(s, m_i^2, m_j^2)} \cos \theta)$. Making the change of variable, the differential phase space in four dimensions reduces to

$$d\Pi_{2 \rightarrow 2}|_{d=4} = \frac{1}{8\pi s} dt. \quad (3.8)$$

3.1.2 3-body Phase Space

A bit more complicated is the phase space of a 3-body final state. When taking into account the inclusive cross-section, as we will, where we also consider the production of additional radiation in addition to our electroweakino pair, the 3-body phase space will become relevant. We will later see that this can be factorised into two 2-body phase spaces for the parts of the calculations involving higgsinos, but to get the full NLO contributions, the 3-body phase space is necessary. Here I will outline a method for parametrising the degrees of freedom in the full 3-body case, although the phase space integration for the gauginos will be beyond the scope of this thesis.

The differential Lorentz invariant phase space for a 3-body final state with four-momenta p_i, p_j, k , where $k^2 = 0$, in d dimensions is

$$d\Pi_{2 \rightarrow 3} = (2\pi)^d \delta^d(P - p_i - p_j - k) \frac{d^{d-1}\mathbf{p}_i}{(2\pi)^{d-1}} \frac{1}{2E_i} \frac{d^{d-1}\mathbf{p}_j}{(2\pi)^{d-1}} \frac{1}{2E_j} \frac{d^{d-1}\mathbf{k}}{(2\pi)^{d-1}} \frac{1}{2\omega}. \quad (3.9)$$

First, it will be useful to write out the differential in \mathbf{k} in spherical coordinates where it reads $d^{d-1}\mathbf{k} = \omega^{d-2} d\Omega_{d-1} d\omega$. The differentials in $\mathbf{p}_{i,j}$ together with the delta-function are easier to compute in the centre-of-mass frame of the electroweakinos where we have $P - k = (Q, 0, 0, 0)$, where Q is the invariant mass of the electroweakino pair. This leaves

$$d\Pi_{2 \rightarrow 3} = \frac{1}{8} \frac{1}{(2\pi)^{2d-3}} \delta(Q - E_i - E_j) \delta^{d-1}(\mathbf{p}_i + \mathbf{p}_j) \frac{\omega^{d-3}}{E_i E_j} d^{d-1}\mathbf{p}_i d^{d-1}\mathbf{p}_j d\Omega_{d-1} d\omega. \quad (3.10)$$

Integrating trivially over \mathbf{p}_j using the delta-function, and using polar coordinates $d^{d-1}\mathbf{p}_i = d\Omega_{d-1}^* d|\mathbf{p}_i| |\mathbf{p}_i|^{d-2}$ to integrate over $\delta(Q - E_i - E_j)$, we get

$$d\Pi_{2 \rightarrow 3} = \frac{1}{(2\pi)^{2d-3}} \frac{\omega^{d-3} |\mathbf{p}_i|^{d-3}}{8Q} d\Omega_{d-1}^* d\Omega_{d-1} d\omega. \quad (3.11)$$

Here, we understand the magnitude of the three-momenta to be given by

$$|\mathbf{p}_i| = \frac{\sqrt{\lambda(Q^2, m_i^2, m_j^2)}}{2Q} \quad (3.12)$$

and $\omega = \frac{s-Q^2}{2\sqrt{s}}$ set by the delta-functions. It will also be useful to make a change of integration variable to Q^2 , leaving us finally with

$$d\Pi_{2 \rightarrow 3} = \frac{1}{(2\pi)^{2d-3}} \frac{\omega^{d-3} |\mathbf{p}_i|^{d-3}}{16Q\sqrt{s}} d\Omega_{d-1}^* d\Omega_{d-1} dQ^2. \quad (3.13)$$

I note that kinematically, Q is restricted by

$$(m_i + m_j)^2 \leq Q^2 \leq s, \quad (3.14)$$

which in turn will put a lower boundary on s .

With two initial state momenta, the amplitude will be independent of the azimuthal angle of the momentum \mathbf{k} in the centre-of-mass frame of the initial partons. This lets us integrate over it for a factor of 2π .

Parametrising the free variables in a $2 \rightarrow 3$ process can be tricky, particularly since different subprocesses have different kinematic dependencies. I will define some natural variables in two different frames of reference, and rediscover the Lorentz transformation between them to parametrise all scalar products in terms of the variables in these reference frames. First, we will consider the centre-of-mass frame of the incoming partons with momenta $\mathbf{k}_{i,j}$. We can reduce this to an ordinary $2 \rightarrow 2$ scattering by considering the outgoing electroweakinos with momenta $\mathbf{p}_{i,j}$ as a single system. Letting the partons move in the z -direction, this lets us parametrise the momenta as

$$k_i^\mu = \frac{\sqrt{s}}{2} (1, 0, 0, 1), \quad (3.15a)$$

$$k_j^\mu = \frac{\sqrt{s}}{2} (1, 0, 0, -1), \quad (3.15b)$$

$$k^\mu = \frac{\sqrt{s}}{2} (1-z) (1, \sin\theta, 0, \cos\theta), \quad (3.15c)$$

$$(p_i + p_j)^\mu = \frac{\sqrt{s}}{2} ((1+z), -(1-z)\sin\theta, 0, -(1-z)\cos\theta), \quad (3.15d)$$

where I have defined

$$z = \frac{Q^2}{s}. \quad (3.16)$$

Later on, k^μ will be associated with radiation, and then z becomes a useful parametrisation of how much of the centre-of-mass energy is radiated away.

The centre-of-mass frame of the electroweakinos is defined by $(p_i^* + p_k^*)^\mu = (\sqrt{zs}, 0, 0, 0)$.² We find the transformation to this frame then by making appropriate boosts and rotations of this four-vector. Let us start by rotating the 3-momentum to lie along the positive z -direction. As the y -component is already zero in the lab-frame,

²I will from now on always put a star on quantities pertaining to the centre-of-mass frame of the electroweakinos.

3.1. Phase Space and Kinematics in Scattering Processes

we only require a rotation around the y -axis, we can be parametrised by the following matrix

$$\text{Rot}_y(\alpha) = \begin{pmatrix} 1 & 0 & 0 & 0 \\ 0 & \cos \alpha & 0 & \sin \alpha \\ 0 & 0 & 1 & 0 \\ 0 & -\sin \alpha & 0 & \cos \alpha \end{pmatrix}. \quad (3.17)$$

Using $\alpha = -\theta - \pi$ we get that $\text{Rot}_y(-\theta - \pi)(p_i + p_j)^\mu = \frac{\sqrt{s}}{2}((1+z), 0, 0, (1-z))$. We can subsequently boost along the z -axis to eliminate the z -component. Such a boost can be parametrised by

$$\text{Boost}_z(\beta) = \begin{pmatrix} \gamma & 0 & 0 & \gamma\beta \\ 0 & 1 & 0 & 0 \\ 0 & 0 & 1 & 0 \\ \gamma\beta & 0 & 0 & \gamma \end{pmatrix}, \quad (3.18)$$

where $\gamma = (1 - \beta^2)^{-1/2}$. The z -component is eliminated using $\beta = -\frac{1-z}{1+z}$, such that we end up with

$$(p_i^* + p_j^*)^\mu \equiv \text{Boost}_z \left(-\frac{1-z}{1+z} \right) \text{Rot}_y(-\theta - \pi) (p_i + p_j)^\mu = (\sqrt{zs}, 0, 0, 0), \quad (3.19)$$

as we expected.

Now we can parametrise $p_{i,j}^{*\mu}$ in this frame using two angular variables θ^*, ϕ^* , knowing that $\mathbf{p}_i^* + \mathbf{p}_j^* = 0$,

$$p_i^{*\mu} = (E_i, p \sin \theta^* \cos \phi^*, p \sin \theta^* \sin \phi^*, p \cos \theta^*), \quad (3.20a)$$

$$p_j^{*\mu} = (E_j, -p \sin \theta^* \cos \phi^*, -p \sin \theta^* \sin \phi^*, -p \cos \theta^*). \quad (3.20b)$$

To find what $E_{i,j}$ and p need to be, we can transform k^μ and $k_{i,j}^\mu$ to this reference frame, finding

$$k^{*\mu} = \frac{\sqrt{s}}{2} \frac{1-z}{\sqrt{z}} (1, 0, 0, -1), \quad (3.21a)$$

$$(k_i^* + k_j^*)^\mu = \frac{s}{2\sqrt{z}} (1+z, 0, 0, -(1-z)), \quad (3.21b)$$

and use conservation of momentum and the fact that $p_{i,j}^{*\mu}{}^2 = m_{i,j}^2$ to get

$$E_{i,j}(z) = \frac{zs + m_{i,j}^2 - m_{j,i}^2}{2\sqrt{zs}}, \quad (3.22a)$$

$$p(z) = \frac{\sqrt{\lambda(zs, m_i^2, m_j^2)}}{2\sqrt{zs}}. \quad (3.22b)$$

Now to get all momenta in the lab frame, we can apply the reverse transformations on $p_{i,j}^{*\mu}$ using that $\text{Rot}_y^{-1}(\alpha) = \text{Rot}_y(-\alpha)$ and $\text{Boost}_z^{-1}(\beta) = \text{Boost}_z(-\beta)$:

$$p_{i,j}^\mu = \text{Rot}_y(\theta + \pi) \text{Boost}_z \left(\frac{1-z}{1+z} \right) p_{i,j}^{*\mu}. \quad (3.23)$$

The explicit expressions are a bit cumbersome, and will not illuminate the discussion further, so I will not show them here. I have visualised the definition of the angular variables in Fig. 3.1.

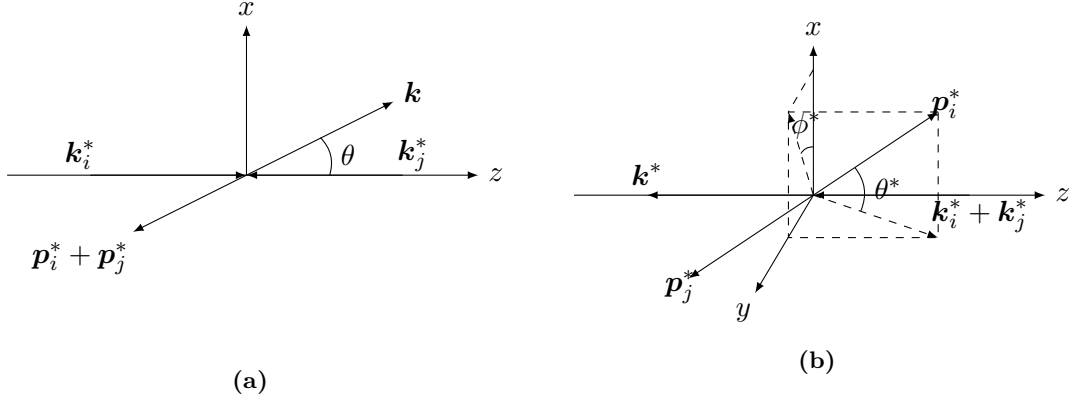


Figure 3.1:
 (a) Angular definition in the centre-of-mass frame of the initial particles with momenta $\mathbf{k}_{i,j}$.
 (b) Angular definitions in the centre-of-mass frame of the outgoing particles with momenta $\mathbf{p}_{i,j}$.

3.1.3 Differential Cross-Section

Consider a scattering process of two initial state particles $\{i\}$ going to a set of n final particles $\{f\}$. Given a transition amplitude $\mathcal{M}(\{i\} \rightarrow \{f\})$, the differential cross-section is given by [14]

$$d\sigma = \frac{1}{4|E_2\mathbf{k}_1 - E_1\mathbf{k}_2|} |\mathcal{M}(\{i\} \rightarrow \{f\})|^2 d\Pi_{2 \rightarrow n}, \quad (3.24)$$

where $k_{1/2}^\mu = (E_{1/2}, \mathbf{k}_{1/2})$ are the four-momenta of the initial particles and $d\Pi_{2 \rightarrow n}$ is the differential phase space of the final state particles as given by Eq. (3.2). In the case where the initial particles are massless, this simplifies to

$$d\sigma = \frac{1}{2s} |\mathcal{M}(\{i\} \rightarrow \{f\})|^2 d\Pi_{2 \rightarrow n}, \quad (3.25)$$

where $s = (k_1 + k_2)^2$.

For future reference, the differential cross-section in four dimensions for a $2 \rightarrow 2$ scattering process with massless initial state particles using Eq. (3.8) is

$$\frac{d\sigma}{dt} = \frac{1}{16\pi} \frac{1}{s^2} |\mathcal{M}|^2. \quad (3.26)$$

In d dimension, switching to the variable

$$y = \frac{1}{2}(1 + \cos\theta), \quad (3.27)$$

from Eq. (3.5) the differential cross-section is given by³

$$\frac{d\sigma^d}{dy} = \frac{1}{(4\pi)^{\frac{d-2}{2}}} \frac{1}{\Gamma\left(\frac{d-2}{2}\right)} \frac{p^{d-3}}{8s\sqrt{s}} |\mathcal{M}|^2 (y(1-y))^{d-4}, \quad (3.28)$$

where the momentum p is given by Eq. (3.6). The limits on the integration variables are

$$-p\sqrt{s} - \frac{1}{2} (s - m_i^2 - m_j^2) \leq t \leq p\sqrt{s} - \frac{1}{2} (s - m_i^2 - m_j^2), \quad (3.29a)$$

$$0 \leq y \leq 1. \quad (3.29b)$$

³The seemingly arbitrary change of variable is a pre-emptive change anticipating some integrals that will arise later on.

3.2 Leading Order Cross-Section

Here, I will calculate the leading order cross-section for neutralino pair production at parton level, before generalising the result to any electroweakino pair. For the leading order contributions, there are no divergences that need regulating, so we can safely set $d = 4$.

3.2.1 Kinematic Definitions

Before getting into the details of the calculation, it will be helpful to present some definitions of the variables we will need. I will make use of the shorthand notation for the spinors $w_{i,j} = w(p_{i,j}), w_{1,2} = w(k_{i,j})$ where w is either u or v . We will also need to define an appropriate set of kinematic variables. Seeing as the inclusive scattering cross-section is a $2 \rightarrow 2$ process to leading order, I will make use of the Mandelstam variables, which in this case will be defined as

$$\hat{s} \equiv (k_i + k_j)^2 = (p_i + p_j)^2, \quad (3.30a)$$

$$\hat{t} \equiv (k_i - p_i)^2 = (k_j - p_j)^2, \quad (3.30b)$$

$$\hat{u} \equiv (k_i - p_j)^2 = (k_j - p_i)^2, \quad (3.30c)$$

which by Eq. (3.1) is constrained by $\hat{s} + \hat{t} + \hat{u} = m_i^2 + m_j^2$. For clarity later on when we will be working with hadron-level kinematics in the next chapter, I will put a hat on variables that are defined at parton level which have an unhatted, hadron-level counterparts. This includes the Mandelstam variables above and the cross-sections.

3.2.2 The Matrix Elements for Neutralino Pair Production

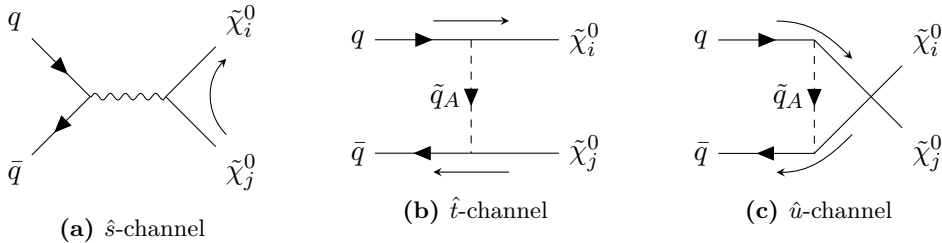


Figure 3.2: The leading order diagrams contributing to neutralino pair production at parton-level.

At leading order the contributing diagrams to the parton-level process are shown in Fig. 3.2. The resulting amplitudes, using the Feynman rules in Section 2.4.2, are then

$$\begin{aligned} \mathcal{M}_{\hat{s}} &= -g^2 D_Z(\hat{s}) \left[\bar{u}_i \gamma^\mu \left(O''_{ij}^L P_L + O''_{ij}^R P_R \right) v_j \right] \\ &\quad \times \left[\bar{v}_2 \gamma_\mu \left(C_{qqZ}^L P_L + C_{qqZ}^R P_R \right) u_1 \right], \end{aligned} \quad (3.31a)$$

$$\begin{aligned} \mathcal{M}_{\hat{t}} &= - \sum_A 2g^2 D_{\tilde{q}_A}(\hat{t}) \left[\bar{u}_i \left((C_{\tilde{q}_A q_g \tilde{\chi}_i^0}^L)^* P_L + (C_{\tilde{q}_A q_g \tilde{\chi}_i^0}^R)^* P_R \right) u_1 \right] \\ &\quad \times \left[\bar{v}_2 \left(C_{\tilde{q}_A q_g \tilde{\chi}_j^0}^R P_L + C_{\tilde{q}_A q_g \tilde{\chi}_j^0}^L P_R \right) v_j \right], \end{aligned} \quad (3.31b)$$

$$\begin{aligned} \mathcal{M}_{\hat{u}} &= + \sum_A 2g^2 D_{\tilde{q}_A}(\hat{u}) \left[\bar{u}_j \left((C_{\tilde{q}_A q_g \tilde{\chi}_j^0}^L)^* P_L + (C_{\tilde{q}_A q_g \tilde{\chi}_j^0}^R)^* P_R \right) u_1 \right] \\ &\quad \times \left[\bar{v}_2 \left(C_{\tilde{q}_A q_g \tilde{\chi}_i^0}^R P_L + C_{\tilde{q}_A q_g \tilde{\chi}_i^0}^L P_R \right) v_i \right], \end{aligned} \quad (3.31c)$$

where

$$D_p(q^2) = \frac{1}{q^2 - m_p^2 (+i\Gamma_p m_p)} \quad (3.32)$$

is the Breit-Wigner propagator [14] of a particle with mass m_p and possible decay width Γ_p and the differing sign of $\mathcal{M}_{\hat{s}}$ to $\mathcal{M}_{\hat{t}}$ comes from it being an odd permutation of the external spinors to the other two amplitudes. Among other things, the Breit-Wigner propagator regularises poles near the resonance where an intermediate particle goes on-shell, e.g. when $\hat{s} \rightarrow m_Z^2$. As it turns out, such poles will not appear in the integrated cross-section for the \hat{t} - and \hat{u} -channels, and so I will use $\Gamma_{\tilde{q}_A} = 0$ for the remainder of this thesis.

These matrix elements can be simplified using the *effective couplings* defined by

$$Z^{XY} = C_{qqZ}^X O''_{ij}^Y, \quad (3.33a)$$

$$Q_A^{XY} = C_{\tilde{q}_A q_g \tilde{\chi}_i^0}^X \left(C_{\tilde{q}_A q_g \tilde{\chi}_j^0}^Y \right)^*, \quad (3.33b)$$

and the *Dirac bilinears*

$$b_{L/R}(w_a, w_b) = \bar{w}_a P_{L/R} w_b, \quad (3.34a)$$

$$b_{L/R}^\mu(w_a, w_b) = \bar{w}_a \gamma^\mu P_{L/R} w_b, \quad (3.34b)$$

to arrive at

$$\begin{aligned} \mathcal{M}_{\hat{s}} &= -g^2 D_Z(\hat{s}) \left[Z^{LL} b_L^\mu(v_2, u_1) b_{L\mu}(u_i, v_j) + Z^{LR} b_L^\mu(v_2, u_1) b_{R\mu}(u_i, v_j) \right. \\ &\quad \left. + Z^{LR} b_R^\mu(v_2, u_1) b_{L\mu}(u_i, v_j) + Z^{RR} b_R^\mu(v_2, u_1) b_{R\mu}(u_i, v_j) \right], \end{aligned} \quad (3.35a)$$

$$\begin{aligned} \mathcal{M}_{\hat{t}} &= -\sum_A 2g^2 D_{\tilde{q}_A}(\hat{t}) \left[\left(Q_A^{LR} \right)^* b_L(u_i, u_1) b_L(v_2, v_j) + \left(Q_A^{LL} \right)^* b_L(u_i, u_1) b_R(v_2, v_j) \right. \\ &\quad \left. + \left(Q_A^{RR} \right)^* b_R(u_i, u_1) b_L(v_2, v_j) + \left(Q_A^{RL} \right)^* b_R(u_i, u_1) b_R(v_2, v_j) \right], \end{aligned} \quad (3.35b)$$

$$\begin{aligned} \mathcal{M}_{\hat{u}} &= \sum_A 2g^2 D_{\tilde{q}_A}(\hat{u}) \left[Q_A^{RL} b_L(v_2, v_i) b_L(u_j, u_1) + Q_A^{RR} b_L(v_2, v_i) b_R(u_j, u_1) \right. \\ &\quad \left. + Q_A^{LL} b_R(v_2, v_i) b_L(u_j, u_1) + Q_A^{LR} b_R(v_2, v_i) b_R(u_j, u_1) \right]. \end{aligned} \quad (3.35c)$$

To square the amplitudes we will need to use that the complex conjugates of the Dirac bilinears are

$$\left(b_{L/R}(w_a, w_b) \right)^\dagger = b_{R/L}(w_b, w_a), \quad (3.36a)$$

$$\left(b_{L/R}^\mu(w_a, w_b) \right)^\dagger = b_{L/R}^\mu(w_b, w_a). \quad (3.36b)$$

Furthermore, when summing over the spins of the various spinors in the bilinears, they have the sum identities

$$\sum_{\text{spins}} b_X(w_a, w_b) b_Y(w_b, w_a) = 2 \left[(1 - \delta_{XY})(p_a \cdot p_b) + \text{rsgn } \delta_{XY} m_a m_b \right], \quad (3.37)$$

$$\begin{aligned} \sum_{\text{spins}} b_X^\mu(w_a, w_b) b_Y^\nu(w_b, w_a) &= 2 \left[\delta_{XY} \left(p_a^\mu p_b^\nu - g^{\mu\nu} (p_a \cdot p_b) + p_a^\nu p_b^\mu \right) + (-1)^{\delta_{XL}} i \epsilon^{\mu\nu\alpha\beta} (p_a)_\alpha (p_b)_\beta \right. \\ &\quad \left. + (1 - \delta_{XY}) \text{rsgn } m_a m_b g^{\mu\nu} \right], \end{aligned} \quad (3.38)$$

where rsgn is 1 if w_a, w_b are spinors of the same type, e.g. both are u -spinors, and -1 otherwise.

3.2.3 Differential Cross-Section

Averaging the cross-section over the two spins and N_C colour charges of the initial quark, and taking account of a symmetry if the final neutralinos are identical, we get from Eq. (3.26)

$$\frac{d\hat{\sigma}}{d\hat{t}} = \left(\frac{1}{2}\right)^{\delta_{ij}} \frac{1}{64N_C^2\pi} \frac{1}{\hat{s}^2} \sum_{\substack{\text{spin} \\ \text{colour}}} |\mathcal{M}|^2. \quad (3.39)$$

Now, squaring the amplitudes and inserting them, the partonic cross-section differential in \hat{t} can be shown to be⁴

$$\begin{aligned} \frac{d\hat{\sigma}^0}{d\hat{t}} = & \frac{\pi\alpha_W^2}{N_C\hat{s}^2} \left(\frac{1}{2}\right)^{\delta_{ij}} \left\{ \sum_{X,Y} \left[|C_{\hat{t}}^{XY}|^2 (\hat{t} - m_i^2)(\hat{t} - m_j^2) + |C_{\hat{u}}^{XY}|^2 (\hat{u} - m_i^2)(\hat{u} - m_j^2) \right] \right. \\ & \left. - \sum_X \left[2 \operatorname{Re} \left\{ (C_u^{XX})^* C_t^{XX} \right\} m_i m_j \hat{s} - 2 \operatorname{Re} \left\{ (C_u^{XX'})^* C_t^{XX'} \right\} (\hat{t}\hat{u} - m_i^2 m_j^2) \right] \right\}, \end{aligned} \quad (3.40)$$

where

$$\alpha_W = \frac{g^2}{4\pi} = \frac{e^2}{4\pi s_W^2} = \frac{\alpha}{s_W^2}, \quad (3.41)$$

using the electric charge a and the fine-structure constant α . I have also defined

$$C_{\hat{t}}^{XY} = -\delta^{XY} D_Z^*(\hat{s})(Z^{XX'})^* + \sum_A \frac{Q_A^{XY}}{\hat{t} - m_A^2}, \quad (3.42a)$$

$$C_{\hat{u}}^{XY} = \delta^{XY} D_Z^*(\hat{s})(Z^{XX})^* + \sum_A \frac{(Q_A^{XY})^*}{\hat{t} - m_A^2}. \quad (3.42b)$$

$$(3.42c)$$

The sum over X, Y goes over L, R , and $L'/R' = R/L$.

The result Eq. (3.40) has been compared and verified to be equivalent to other results [33] in the literature symbolically using **Mathematica** code.

3.2.4 Integrated Cross-Section

To get the full cross-section, we will need to integrate over the \hat{t} -variable. To do this, we classify the types of integrals that will arise. After inserting $\hat{u} = m_i^2 + m_j^2 - \hat{s} - \hat{t}$, all the integrals take the form

$$T^p(\Delta_1, \Delta_2) \equiv \int_{t_-}^{t_+} dt \frac{\hat{t}^p}{(\hat{t} - \Delta_1)(\hat{t} - \Delta_2)}, \quad (3.43)$$

for some $\Delta_{1,2}$ dependent on \hat{s} , the neutralino masses and the squark masses, and where p is some non-negative integer. Here $T^p(\Delta_1, \Delta_2)$ is symmetric in its arguments.

⁴I note that the amplitudes in Eq. (3.31) have the quark colour indices suppressed, including a Kronecker-delta in the vertex rule for qqZ and in the squark propagators. In the end, summing over the colours of the squared amplitudes amounts to a sum over this Kronecker-delta, producing a factor of N_C .

Using the integral limits from Eq. (3.29) the relevant integrals evaluate to

$$T^2(0,0) = 2p\sqrt{\hat{s}}, \quad (3.44a)$$

$$T^3(0,0) = -p\sqrt{\hat{s}}(\hat{s} - m_i^2 - m_j^2), \quad (3.44b)$$

$$T^4(0,0) = p\sqrt{\hat{s}}\left(\frac{8}{3}\hat{s}p^2 + 2m_i^2m_j^2\right), \quad (3.44c)$$

$$T^1(\Delta, 0) = -L(\Delta), \quad (3.44d)$$

$$T^2(\Delta, 0) = 2p\sqrt{\hat{s}} - \Delta L(\Delta), \quad (3.44e)$$

$$T^3(\Delta, 0) = p\sqrt{\hat{s}}\left(2\Delta - (\hat{s} - m_i^2 - m_j^2)\right) - \Delta^2 L(\Delta), \quad (3.44f)$$

$$T^0(\Delta_1, \Delta_2) = \begin{cases} \frac{1}{\Delta_2 - \Delta_1} \{L(\Delta_1) - L(\Delta_2)\} & \text{if } \Delta_1 \neq \Delta_2 \\ \frac{2p\sqrt{\hat{s}}}{\Delta^2 + \Delta(\hat{s} - m_i^2 - m_j^2) + m_i^2m_j^2} & \text{if } \Delta_1 = \Delta_2 \equiv \Delta \end{cases}, \quad (3.44g)$$

$$T^1(\Delta_1, \Delta_2) = \begin{cases} \frac{1}{\Delta_2 - \Delta_1} \{\Delta_1 L(\Delta_1) - \Delta_2 L(\Delta_2)\} & \text{if } \Delta_1 \neq \Delta_2 \\ \frac{2\Delta p\sqrt{\hat{s}}}{\Delta^2 + \Delta(\hat{s} - m_i^2 - m_j^2) + m_i^2m_j^2} - L(\Delta) & \text{if } \Delta_1 = \Delta_2 \equiv \Delta \end{cases}, \quad (3.44h)$$

$$T^2(\Delta_1, \Delta_2) = \begin{cases} \frac{2p\sqrt{\hat{s}} + \frac{1}{\Delta_2 - \Delta_1} \{\Delta_1^2 L(\Delta_1) - \Delta_2^2 L(\Delta_2)\}}{\Delta^2 + \Delta(\hat{s} - m_i^2 - m_j^2) + m_i^2m_j^2} & \text{if } \Delta_1 \neq \Delta_2 \\ \frac{2(2\Delta^2 + \Delta(\hat{s} - m_i^2 - m_j^2) + m_i^2m_j^2)p\sqrt{\hat{s}}}{\Delta^2 + \Delta(\hat{s} - m_i^2 - m_j^2) + m_i^2m_j^2} - 2\Delta L(\Delta) & \text{if } \Delta_1 = \Delta_2 \equiv \Delta \end{cases} \quad (3.44i)$$

where I have defined

$$L(\Delta) = \log \frac{\Delta + \frac{1}{2}(\hat{s} - m_i^2 - m_j^2) + p\sqrt{\hat{s}}}{\Delta + \frac{1}{2}(\hat{s} - m_i^2 - m_j^2) - p\sqrt{\hat{s}}}. \quad (3.45)$$

The two non-zero arguments to these functions that will arise are $\Delta_A^{\hat{t}} = m_A^2$ and $\Delta_A^{\hat{u}} = -(\hat{s} - m_i^2 - m_j^2) - m_A^2$, and I note that $L(\Delta_A^{\hat{u}}) = -L(\Delta_A^{\hat{t}})$.

Putting it all together, this lets us write the total cross-section

$$\hat{\sigma}^0 = \frac{4\pi p\alpha_W^2}{\hat{s}^{3/2} N_C} \left(\frac{1}{2}\right)^{\delta_{ij}} \left(F''_{\tilde{q}} + F''_Z + F''_{\tilde{q}Z}\right) \equiv \hat{\sigma}_B \left(F''_{\tilde{q}} + F''_Z + F''_{\tilde{q}Z}\right), \quad (3.46)$$

with contributions from each mediator given by

$$F''_{\tilde{q}} = \sum_{A,B,X,Y} \left\{ \operatorname{Re} \left\{ Q_A^{XY} (Q_B^{XY})^* \right\} \left(1 - L_2^{AB}\right) + \delta_{XY} \operatorname{Re} \left\{ Q_A^{XX} Q_B^{XX} \right\} L_1^{AB} \right. \\ \left. + \delta_{XY} \operatorname{Re} \left\{ Q_A^{XX'} Q_B^{X'X} \right\} \left(1 - L_3^{AB}\right) \right\}, \quad (3.47)$$

$$F''_Z = \sum_{X,Y} \left\{ \frac{1}{12} \left(\hat{s}(\hat{s} - m_i^2 - m_j^2) + \hat{s}^2 - (m_i^2 - m_j^2)^2 \right) |Z^{XY}|^2 + \delta_{XY} \hat{s} m_i m_j \operatorname{Re} \left\{ Z^{XX} (Z^{XX'})^* \right\} \right\}, \quad (3.48)$$

and from the interference term

$$F''_{\tilde{q}Z} = \frac{1}{2} \sum_{A,X} \left\{ \left[\hat{s} m_i m_j \operatorname{Re} \left\{ Q_A^{XX} (Z^{XX} - (Z^{XX'})^*) \right\} \right. \right. \\ \left. \left. - (m_A^2 - m_i^2)(m_A^2 - m_j^2) \operatorname{Re} \left\{ Q_A^{XX} ((Z^{XX})^* - Z^{XX'}) \right\} \right] \frac{L(m_A^2)}{p\sqrt{\hat{s}}} \right. \\ \left. - (\hat{s} + m_i^2 + m_j^2 - 2m_A^2) \operatorname{Re} \left\{ Q_A^{XX} ((Z^{XX})^* - Z^{XX'}) \right\} \right\}, \quad (3.49)$$

where $X, Y \in L, R$, $L'/R' = R/L$ and I have defined shorthands for some functions of the kinematics

$$L_1^{AB} = \frac{\hat{s}m_i m_j}{m_A^2 + m_B^2 + \hat{s} - m_i^2 - m_j^2} \frac{L(m_A^2)}{p\sqrt{\hat{s}}}, \quad (3.50a)$$

$$L_2^{AB} = \begin{cases} \frac{(m_A^2 - m_i^2)(m_A^2 - m_j^2)}{m_A^2 - m_B^2} \frac{L(m_A^2)}{p\sqrt{\hat{s}}} & \text{if } m_A \neq m_B \\ \frac{1}{2}(2m_A^2 - m_i^2 - m_j^2) \frac{L(m_A^2)}{p\sqrt{\hat{s}}} & \text{if } m_A = m_B \end{cases}, \quad (3.50b)$$

$$L_3^{AB} = \frac{m_A^4 + m_A^2(\hat{s} - m_i^2 - m_j^2) + m_i^2 m_j^2}{m_A^2 + m_B^2 + \hat{s} + m_i^2 - m_j^2} \frac{L(m_A^2)}{p\sqrt{\hat{s}}}. \quad (3.50c)$$

I would like to take a moment to comment on the sums over the squark eigenstates here. In the SLHA1 [26] standard, the first two generations of squark do not mix, and so the chiral and mass indices coincide. This means we simply take the sum where $A = B = X = Y \in L, R$ in the above contributions, since $Q_A^{XY} \propto \delta_{AX}\delta_{AY}$. For the third generation, where mixing occurs, we sum over $A, B \in 1, 2$. Now, in the SLHA2 [27] standard, we allow for general, possibly flavour violating, mixing. This means that all the sums are $A, B \in 1, \dots, 6$.

3.2.5 Generalising to All Electroweakinos

So far, we have only calculated the cross-section for production of a pair of neutralinos. However, the amplitude structure is very similar both for pair production of charginos and production of a neutralino with a chargino. With a few modifications, we can thus generalise the result from Eq. (3.46) to any electroweakino pair. The LO diagrams for the other electroweakino processes at parton level are shown in Figs. 3.3 and 3.4.

Neutralino and Chargino Production

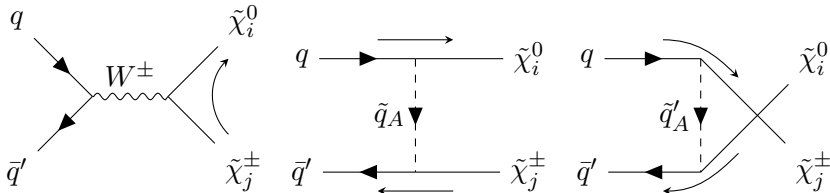


Figure 3.3: Tree-level diagrams contributing to the production of a neutralino and chargino at parton level.

Producing a chargino together with a neutralino requires the total charge of the process to differ from zero. The partonic processes that contribute are of the form $q\bar{q}' \rightarrow \tilde{\chi}_i^0 \tilde{\chi}_j^\pm$. Now the indices j will refer to chargino mass eigenstates and $m_j = m_{\tilde{\chi}_j^\pm}$. Furthermore, since both up- and down-type quarks are involved in the process, I will be explicit in the squark indices A, B whether they refer to up- or down-type squarks.

Using the Feynman rules from Section 2.4.2 we get the amplitudes

$$\mathcal{M}_{\hat{s}} = -g^2 D_W(\hat{s}) \left[\bar{u}_i \gamma^\mu \left(O_{ij}^L P_L + O_{ij}^R P_R \right) v_j \right] \left[\bar{v}_2 \gamma_\mu C_{qq'W}^L P_L u_1 \right], \quad (3.51a)$$

$$\begin{aligned} \mathcal{M}_{\hat{t}} &= - \sum_A 2g^2 D_{\tilde{q}_A}(\hat{t}) \left[\bar{u}_i \left((C_{q\tilde{q}_A\tilde{\chi}_i^0}^L)^* P_L + (C_{q\tilde{q}_A\tilde{\chi}_i^0}^R)^* P_R \right) u_1 \right] \\ &\quad \times \left[\bar{v}_2 C_{q'\tilde{q}_A\tilde{\chi}_j^\pm}^L P_R v_j \right], \end{aligned} \quad (3.51b)$$

$$\begin{aligned} \mathcal{M}_{\hat{u}} &= + \sum_A 2g^2 D_{\tilde{q}'_A}(\hat{u}) \left[\bar{u}_j (C_{q\tilde{q}'_A\tilde{\chi}_j^\pm}^L)^* P_L u_1 \right] \\ &\quad \times \left[\bar{v}_2 \left(C_{q'\tilde{q}'_A\tilde{\chi}_i^0}^R P_L + C_{q'\tilde{q}'_A\tilde{\chi}_i^0}^L P_R \right) v_i \right], \end{aligned} \quad (3.51c)$$

from the diagrams in Fig. 3.3. Redefining the effective couplings in Eq. (3.33) to

$$\begin{aligned} W^{XY} &= C_{qq'W}^X O_{ij}^Y, \\ Q_A^{XY} &= C_{q\tilde{q}_A\tilde{\chi}_i^0}^X C_{q'\tilde{q}_A\tilde{\chi}_j^\pm}^Y, \end{aligned}$$

we can rewrite the amplitudes to

$$\mathcal{M}_{\hat{s}} = -g^2 D_W(\hat{s}) \left[W^{LL} b_L^\mu(v_2, u_1) b_{L\mu}(u_i, v_j) + W^{LR} b_L^\mu(v_2, u_1) b_{R\mu}(u_i, v_j) \right], \quad (3.53a)$$

$$\mathcal{M}_{\hat{t}} = - \sum_A 2g^2 D_{\tilde{q}_A}(\hat{t}) \left[(Q_A^{LL})^* b_L(u_i, u_1) b_R(v_2, v_j) + (Q_A^{RL})^* b_R(u_i, u_1) b_R(v_2, v_j) \right] \Big|_{q=q}, \quad (3.53b)$$

$$\mathcal{M}_{\hat{u}} = \sum_A 2g^2 D_{\tilde{q}'_A}(\hat{u}) \left[Q_A^{RL} b_L(v_2, v_i) b_L(u_j, u_1) + Q_A^{LL} b_R(v_2, v_i) b_L(u_j, u_1) \right] \Big|_{q=q'}, \quad (3.53c)$$

mimicking the structure of Eq. (3.35). It is worth noting that the structure is not entirely the same as for the neutralinos, as the charges and propagator in $\mathcal{M}_{\hat{t}}$ and $\mathcal{M}_{\hat{u}}$ are not the same, owing to a different squark type being mediated. Nevertheless, we can follow the calculation for the neutralinos to arrive at a similar cross-section to the one in Eq. (3.46), but altering the individual mediator contributions slightly. We get

$$\hat{\sigma}^0(q\bar{q}' \rightarrow \tilde{\chi}_i^0 \tilde{\chi}_j^\pm) = \frac{4\pi p \alpha_W^2}{\hat{s}^{3/2} N_C} (F_{\tilde{u}} + F_{\tilde{d}} + F_W + F_{\tilde{u}W} + F_{\tilde{d}W}), \quad (3.54)$$

where I note that the identical particle factor from Eq. (3.46) is no longer necessary, and with the individual mediator contributions defined as⁵

$$F_{\tilde{u}} = \frac{1}{2} \sum_{A,B,X,Y} (1 - L_{u2}^{AB}) \text{Re} \left\{ Q_A^{XY} (Q_B^{XY})^* \right\} \Big|_{q=u} + \delta_{XY} L_{u1}^{AB} \text{Re} \left\{ Q_A^{XX} \Big|_{q=u} Q_{dB}^{XX} \Big|_{q=d} \right\}, \quad (3.55a)$$

$$F_{\tilde{d}} = \frac{1}{2} \sum_{A,B,X,Y} (1 - L_{d2}^{AB}) \text{Re} \left\{ Q_A^{XY} (Q_B^{XY})^* \right\} \Big|_{q=d} + \delta_{XY} L_{d1}^{AB} \text{Re} \left\{ Q_A^{XX} \Big|_{q=d} Q_{dB}^{XX} \Big|_{q=u} \right\}, \quad (3.55b)$$

$$F_W = \sum_{X,Y} |D_W(\hat{s})| \left\{ \frac{1}{12} \left(2\hat{s}(\hat{s} - m_i^2 - m_j^2) + m_i^4 + m_j^4 \right) |W^{XY}|^2 + \delta_{XY} \hat{s} m_i m_j \text{Re} \left\{ W^{XX} (W^{XX'})^* \right\} \right\}, \quad (3.55c)$$

⁵The observant reader will notice that there is one term missing from the definitions of $F_{\tilde{u}/\tilde{d}}$ as compared to Eq. (3.47) — this term disappears due to $Q_{qA}^{XR} = 0$ for $X = L, R$.

and interference contributions

$$F_{\tilde{u}W} = \frac{1}{2} \sum_{A,X} \left\{ \hat{s} m_i m_j \operatorname{Re} \left\{ D_W^*(\hat{s}) Q_{uA}^{XX} (W^{XX'})^* \right\} \frac{L(m_{\tilde{u}_A}^2)}{p\sqrt{\hat{s}}} \right. \\ \left. + \left[(m_{\tilde{u}_A}^2 - m_i^2)(m_{\tilde{u}_A}^2 - m_j^2) \frac{L(m_{\tilde{u}_A}^2)}{p\sqrt{\hat{s}}} + (\hat{s} + m_i^2 + m_j^2 - 2m_{\tilde{u}_A}^2) \right] \operatorname{Re} \left\{ D_W^*(\hat{s}) Q_{uA}^{XX} (W^{XX})^* \right\} \right\}, \quad (3.55d)$$

$$F_{\tilde{d}W} = -\frac{1}{2} \sum_{A,X} \left\{ \hat{s} m_i m_j \operatorname{Re} \left\{ D_W(\hat{s}) Q_{dA}^{XX} W^{XX} \right\} \right. \\ \left. + \left[(m_{\tilde{d}_A}^2 - m_i^2)(m_{\tilde{d}_A}^2 - m_j^2) \frac{L(m_{\tilde{d}_A}^2)}{p\sqrt{\hat{s}}} + (\hat{s} + m_i^2 + m_j^2 - 2m_{\tilde{d}_A}^2) \right] \operatorname{Re} \left\{ D_W(\hat{s}) Q_{dA}^{XX} W^{XX'} \right\} \right\}, \quad (3.55e)$$

and where I have defined slightly altered kinematic functions⁶

$$L_{q1}^{AB} = \frac{\hat{s} m_i m_j}{m_{\tilde{q}_A}^2 + m_{\tilde{q}'_B}^2 + \hat{s} - m_i^2 - m_j^2} \frac{L(m_{\tilde{q}_A}^2)}{p\sqrt{\hat{s}}}, \quad (3.56)$$

$$L_{q2}^{AB} = \begin{cases} \frac{(m_{\tilde{q}_A}^2 - m_i^2)(m_{\tilde{q}_A}^2 - m_j^2)}{m_{\tilde{q}_A}^2 - m_{\tilde{q}_B}^2} \frac{L(m_{\tilde{q}_A}^2)}{p\sqrt{\hat{s}}} & \text{if } m_{\tilde{q}_A} \neq m_{\tilde{q}_B} \\ \frac{1}{2}(2m_{\tilde{q}_A}^2 - m_i^2 - m_j^2) \frac{L(m_{\tilde{q}_A}^2)}{p\sqrt{\hat{s}}} & \text{if } m_{\tilde{q}_A} = m_{\tilde{q}_B} \end{cases}. \quad (3.57)$$

Chargino Pair Production

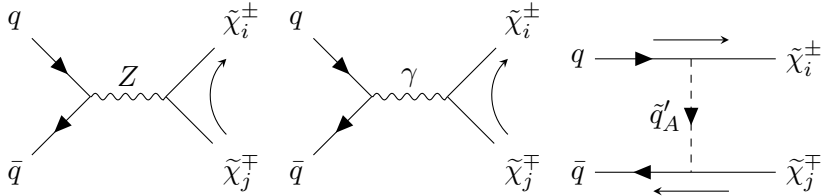


Figure 3.4: Tree-level diagrams contributing to the pair production of a chargino particle/anti-particle pair.

The above derivation can be repeated for the chargino pair production process. This time, the total charge is zero, and the partonic processes are all on the form $q\bar{q} \rightarrow \tilde{\chi}_i^\pm \tilde{\chi}_j^\mp$. Now both indices i, j will refer to the chargino eigenstates, and $m_{i,j} = m_{\tilde{\chi}_{i,j}^\pm}$. I will also note the mediating squark in the \hat{t} -channel is of opposite type to the quarks in the initial state. From the diagrams in Fig. 3.4 and the Feynman rules from Section 2.4.2 we get the amplitudes

$$\mathcal{M}_{\hat{s}} = -g^2 D_Z(\hat{s}) \left[\bar{u}_i \gamma^\mu \left(O'_{ij}^L P_L + O'_{ij}^R P_R \right) v_j \right] \left[\bar{v}_2 \gamma_\mu \left(C_{qqZ}^L P_L + C_{qqZ}^R P_R \right) u_1 \right] \\ - \frac{g^2}{\hat{s}} [\bar{u}_i \gamma^\mu \delta_{ij} s_W v_j] [\bar{v}_2 \gamma_\mu Q_e s_W u_1], \quad (3.58a)$$

$$\mathcal{M}_{\hat{t}} = - \sum_A 2g^2 D_{\tilde{q}'_A}(\hat{t}) \left[\bar{u}_i \left(C_{\tilde{q}_A q_g' \tilde{\chi}_i^\pm}^L \right)^* P_L u_1 \right] \left[\bar{v}_2 C_{\tilde{q}_A q_g' \tilde{\chi}_j^\pm}^L P_R v_j \right] \quad (3.58b)$$

⁶The only difference in these definitions is that the squark type is specified. Make note that both squark types (up and down) are used in L_{q1}^{AB} .

again mimicking the same structure as Eq. (3.31). However, this time there is no \hat{u} -channel analogue. Redefining the effective couplings from Eq. (3.33) to be

$$Z^{XY} = C_{qqZ}^X O_{ij}^{Y'}, \quad (3.59a)$$

$$A^{XY} = Q_e s_W^2 \delta_{ij}, \quad (3.59b)$$

$$Q_A^{XY} = C_{\tilde{q}_A q_g \tilde{\chi}_i^\pm}^X (C_{\tilde{q}_A q_g \tilde{\chi}_j^\pm}^Y)^*, \quad (3.59c)$$

where we have added a charge for the photon mediator A^{XY} . We can then rewrite the amplitudes to

$$\mathcal{M}_{\hat{s}} = -g^2 \sum_{XY} (D_Z(\hat{s}) Z^{XY} + \frac{1}{\hat{s}} A^{XY}) b_X^\mu(v_2, u_1) b_{Y\mu}(u_i, v_j) \quad (3.60a)$$

$$\mathcal{M}_{\hat{t}} = -2g^2 \sum_A D_{\tilde{q}'_A}(\hat{t}) (Q_A^{LL})^* b_L(u_i, u_1) b_R(v_2, v_j) \quad (3.60b)$$

Following the procedure for calculating the total cross-section again, we find that it can be written as

$$\sigma^0(q\bar{q} \rightarrow \tilde{\chi}_i^\pm \tilde{\chi}_j^\mp) = \frac{4\pi p \alpha_W^2}{\hat{s}^{3/2} N_C} (F'_{\tilde{q}'} + F'_Z + F'_{\tilde{q}'Z}), \quad (3.61)$$

where the contributions from each channel are⁷

$$F'_{\tilde{q}'} = \frac{1}{2} \sum_{A,B,X,Y} \text{Re} \left\{ Q_A^{XY} (Q_B^{XY})^* \right\} \left(1 - L_2^{AB} \right), \quad (3.62a)$$

$$F'_Z = \sum_{X,Y} \left\{ \frac{1}{12} \left(\hat{s}(\hat{s} - m_i^2 - m_j^2) + \hat{s} - (m_i^2 - m_j^2)^2 \right) |D_Z(\hat{s}) Z^{XY} + \frac{1}{\hat{s}} A^{XY}|^2 \right. \\ \left. + \delta_{XY} \hat{s} m_i m_j \text{Re} \left\{ (D_Z(\hat{s}) Z^{XX} + \frac{1}{\hat{s}} A^{XX})(D_Z(\hat{s}) Z^{XX'} + \frac{1}{\hat{s}} A^{XX'})^* \right\} \right\}, \quad (3.62b)$$

and the interference term

$$F'_{\tilde{q}'Z} = -\frac{1}{2} \sum_{A,X} \left\{ \hat{s} m_i m_j \text{Re} \left\{ Q_A^{XX} (D_Z(\hat{s}) Z^{XX} + \frac{1}{\hat{s}} A^{XX}) \right\} \frac{L(m_{\tilde{q}'_A}^2)}{p\sqrt{\hat{s}}} \right. \\ \left. + \left[(m_{\tilde{q}'_A}^2 - m_i^2)(m_{\tilde{q}'_A}^2 - m_j^2) \frac{L(m_{\tilde{q}'_A}^2)}{p\sqrt{\hat{s}}} + (\hat{s} + m_i^2 + m_j^2 - 2m_{\tilde{q}'_A}^2) \right] \right. \\ \left. \times \text{Re} \left\{ Q_A^{XX} (D_Z(\hat{s}) Z^{XX'} + \frac{1}{\hat{s}} A^{XX'}) \right\} \right\}. \quad (3.62c)$$

Lastly, I end with a summary of the effective couplings are summarised in Table 3.1.

3.3 NLO Corrections

In this section, I will investigate at the NLO QCD corrections associated with the production of a pair of neutralinos. I will perform the computation of the NLO corrections to the higgsino cross-section, as this goes through an intermediate Z -boson state, making it kinematically simpler. This corresponds at LO to the \hat{s} -channel diagram Fig. 3.2a. The corrections to the gaugino cross-section is beyond the scope of this thesis, but I will comment on a procedure for doing it.

⁷ Again, two terms are missing from $F'_{\tilde{q}'}$ as compared to Eq. (3.47), this time due to lack of any interference between \hat{t} and \hat{u} channels. I also note that the sum over X, Y in $F'_{\tilde{q}'}$ is purely to align with the earlier results, the only non-zero contribution of Q_A^{XY} is for $X = Y = L$.

	$Z^{XY}/W^{XY}/Z^{XY}, A^{XY}$	Q_A^{XY}
$\tilde{\chi}_i^0 \tilde{\chi}_j^0$	$C_{qqZ}^X O_{ij}^{\prime Y}$	$C_{q\tilde{q}_A \tilde{\chi}_i^0}^X (C_{q\tilde{q}_A \tilde{\chi}_j^0}^Y)^*$
$\tilde{\chi}_i^0 \tilde{\chi}_j^\pm$	$C_{qqW}^X O_{ij}^Y$	$C_{q\tilde{q}_A \tilde{\chi}_i^0}^X (C_{q'\tilde{q}_A \tilde{\chi}_j^\pm}^Y)^*$
$\tilde{\chi}_i^\pm \tilde{\chi}_j^\mp$	$C_{qqZ}^X O_{ij}^Y, Q_e s_W^2 \delta_{ij}$	$C_{q\tilde{q}'_A \tilde{\chi}_i^\pm}^X (C_{q\tilde{q}'_A \tilde{\chi}_j^\pm}^Y)^*$

Table 3.1: Table of the effective couplings defined for each type of electroweakino pair production process.

3.3.1 Factorisation

As we will only look at NLO contributions to the \hat{s} -channel contribution through a Z -boson, we can do a trick to simplify the process and its corrections. This trick is factorisation, which involves splitting the total cross-section into the two separate processes of the production of an off-shell Z -boson, and its subsequent decay into two neutralinos. Seeing as we are calculating the inclusive cross-section, I include the potential emission of another hard massless particle (gluon or quark) along with the Z -boson production.

Factorisation of the Phase Space

To start off, we can factorise the d -dimensional differential $2 \rightarrow 3$ phase space Eq. (3.10) into two processes by adding an intermediate momentum q with ‘mass’ squared Q^2 . Adding a factor $\frac{1}{2q^0} d^{d-1} \mathbf{q} \delta^d(k + q - P) dQ^2 \delta(q^2 - Q^2)$, which integrates to one, we can rewrite the differential $2 \rightarrow 3$ phase space as

$$\begin{aligned} \frac{d^{d-1} \mathbf{q}}{2q^0} \delta^d(k + q - P) dQ^2 \delta(q^2 - Q^2) d\Pi_{2 \rightarrow 3} &= \frac{1}{(2\pi)^{2d-3}} d^{d-1} \mathbf{p}_i d^{d-1} \mathbf{p}_j d^{d-1} \mathbf{k} d^{d-1} \mathbf{q} dQ^2 \\ &\times \frac{1}{16E_i E_j \omega q^0} \delta^d(q + k - k_i - k_j) \delta^d(p_i + p_j + k - k_i - k_j) \\ &\equiv \frac{1}{2\pi} d\Pi_H d\Pi_N dQ^2, \end{aligned} \quad (3.63)$$

where

$$d\Pi_H = \frac{d^{d-1} \mathbf{k} d^{d-1} \mathbf{q}}{(2\pi)^{d-2}} \frac{1}{4\omega q^0} \delta^d(q + k - k_i - k_j), \quad (3.64a)$$

$$d\Pi_N = \frac{d^{d-1} \mathbf{p}_i d^{d-1} \mathbf{p}_j}{(2\pi)^{d-2}} \frac{1}{4E_i E_j} \delta^d(p_i + p_j - q), \quad (3.64b)$$

which are recognisable as differential phase spaces for a $2 \rightarrow 2$ processes going from momenta $k_i + k_j \rightarrow q + k$ and a $1 \rightarrow 2$ phase space going from $q \rightarrow p_i + p_j$. The total phase space integrates over all possible off-shell masses Q^2 for the intermediate momentum q .

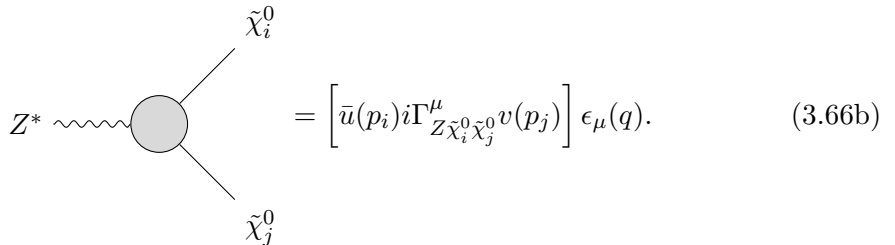
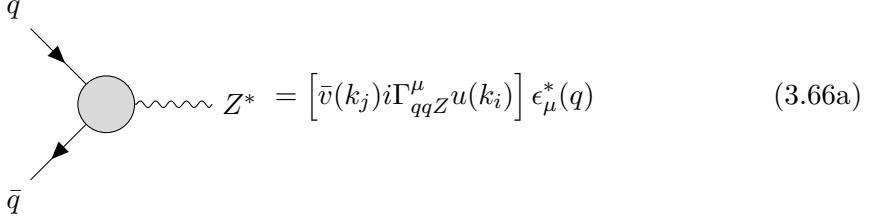
Factorisation of Cross-Section

So, we have factorised the differential phase space of the differential cross-section Eq. (3.25), but it remains to factorise the amplitude part $|\mathcal{M}|^2$ into parts only dependent

on either q, k or p_i, p_j . Looking at the tree-level amplitudes Eq. (3.31) this happens neatly with the \hat{s} -channel contribution Eq. (3.31). It has the Lorentz structure

$$\mathcal{M}_s = D_Z(\hat{s})g_{\mu\nu} \left[\bar{v}(k_j)\Gamma_{qqZ}^\mu u(k_i) \right] \left[\bar{u}(p_i)\Gamma_{Z\tilde{\chi}_i^0\tilde{\chi}_j^0}^\nu v(p_j) \right]. \quad (3.65)$$

The two terms in brackets are individually only dependent on couplings and the momenta of either the initial partons or the final neutralinos. In fact, they individually take the form of the processes



Squaring $\mathcal{M}_{\hat{s}}$, we can write the differential cross-section from Eq. (3.25) as

$$\frac{d\hat{\sigma}}{dQ^2} = \frac{1}{4\pi\hat{s}} |D_Z(\hat{s})|^2 H^{\mu\nu} N_{\mu\nu}, \quad (3.67)$$

where

$$\epsilon_\mu(q)\epsilon_\nu^*(q)H^{\mu\nu} = \int d\Pi_H |\mathcal{M}(q\bar{q} \rightarrow Z^*)|^2, \quad (3.68a)$$

$$\epsilon_\mu^*(q)\epsilon_\nu(q)N^{\mu\nu} = \int d\Pi_N |\mathcal{M}(Z^* \rightarrow \tilde{\chi}_i^0\tilde{\chi}_j^0)|^2. \quad (3.68b)$$

Writing the amplitude in this way shows that Q^2 is not a real degree of freedom in the cross-section, but rather put in by hand. However, it will become relevant when we look at the *inclusive* cross-section, where we take into account any contributions from processes resulting in the neutralino pair and something else. Seeing as at least one more vertex is necessary to produce another particle, these contributions must come in at NLO. The NLO QCD contribution for a process producing a neutralino pair and a strongly interacting particle can only come from the quark tensor $H^{\mu\nu}$, as the neutralino tensor $N^{\mu\nu}$ contains no strongly interacting particles at LO. Q^2 will then parametrise the extra kinetic degree of freedom when going from a $2 \rightarrow 1$ phase space to a $2 \rightarrow 2$ phase space in the hadronic tensor.

Since the neutralino tensor will not receive any higher order corrections to the order we will calculate, we can take a look at it right away. It describes the decay of an off-shell Z -boson, and as such it can only depend on its four-momentum and on the metric, so it can be parametrised as

$$N^{\mu\nu} = N_0(Q^2)g^{\mu\nu} + N_1(Q^2)\frac{q^\mu q^\nu}{Q^2}, \quad (3.69)$$

where N_0, N_1 are scalar functions of the off-shell Z -boson mass Q . We can write the hadronic tensor as

$$H^{\mu\nu} = \int d\Pi_H \mathcal{M}^\mu (\mathcal{M}^\nu)^*, \quad (3.70)$$

where \mathcal{M}^μ is defined such that $\epsilon_\mu^*(q)\mathcal{M}^\mu = \mathcal{M}(q\bar{q} \rightarrow Z^*(+X))$. Now, the form of the neutralino tensor Eq. (3.69) is particularly convenient, as due to the Ward identity, $q_\mu \mathcal{M}^\mu(q\bar{q} \rightarrow Z^*(+X)) = 0$. This means that only the coefficient N_0 is necessary to calculate. Using that $\sum_{\text{pol.}} \epsilon_\mu(q)\epsilon_\nu^*(q) = -g_{\mu\nu}$ we can write the cross-section on a convenient form

$$\frac{d\hat{\sigma}}{dQ^2} = -\frac{1}{4\pi\hat{s}} |D_Z(\hat{s})|^2 N_0 \int d\Pi_H \sum_{\text{pol.}} |\mathcal{M}(ij \rightarrow Z^*(+X))|^2, \quad (3.71)$$

where I have generalised the hadronic tensor further, by letting any two incoming partons i, j produce the off-shell boson and potential radiation. I note that LO, only a quark-antiquark pair contributes.

We can now calculate the coefficient $N_0(Q^2)$, and given that there are no loops or divergences that need regularisation, we can compute it in $d = 4$ dimensions. From Eq. (3.69) we find it is given by

$$N_0(Q^2) = \frac{1}{3} \left(g_{\mu\nu} - \frac{q_\mu q_\nu}{Q^2} \right) N^{\mu\nu}. \quad (3.72)$$

Furthermore,

$$N^{\mu\nu} = \int d\Pi_N \mathcal{M}^\mu (\mathcal{M}^\nu)^*, \quad (3.73)$$

where $\epsilon_\mu(q)\mathcal{M}^\mu = \mathcal{M}(Z^* \rightarrow \tilde{\chi}_i^0 \tilde{\chi}_j^0)$, and is given by

$$\mathcal{M}^\mu = g \left[(O''_{ij}^L)^* b_L^\mu(u_i, v_j) + (O''_{ij}^R)^* b_R^\mu(u_i, v_j) \right]. \quad (3.74)$$

Summing over the spins, using the relations Eqs. (3.36) and (3.38), we get

$$\begin{aligned} N^{\mu\nu} &= g^2 \int d\Pi_N \sum_{\text{spin}} \left[(O''_{ij}^L)^* b_L^\mu(u_i, v_j) + (O''_{ij}^R)^* b_R^\mu(u_i, v_j) \right] \left[O''_{ij}^L b_L^\nu(v_j, u_i) + O''_{ij}^R b_R^\nu(v_j, u_i) \right] \\ &= 2g^2 \int d\Pi_N \left\{ \left(|O''_{ij}^L|^2 + |O''_{ij}^R|^2 \right) \left(p_i^\mu p_j^\nu - (p_i \cdot p_j) g^{\mu\nu} + p_i^\nu p_j^\mu \right) \right. \\ &\quad \left. - 2 \text{Re} \left\{ O''_{ij}^L (O''_{ij}^R)^* \right\} m_i m_j g^{\mu\nu} \right\}. \end{aligned} \quad (3.75)$$

The contraction of the four-momenta are fixed by momentum conservation $q = p_i + p_j$ from the delta function in Eq. (3.64b), meaning $p_i \cdot p_j = \frac{1}{2}(Q^2 - m_i^2 - m_j^2)$, leaving

$$\begin{aligned} N_0(Q^2) &= -g^2 \int d\Pi_N \left\{ \frac{Q^2(Q^2 - m_i^2 - m_j^2) + Q^4 - (m_i^2 - m_j^2)^2}{3Q^2} \left(|O''_{ij}^L|^2 + |O''_{ij}^R|^2 \right) \right. \\ &\quad \left. + 4m_i m_j \text{Re} \left\{ O''_{ij}^L (O''_{ij}^R)^* \right\} \right\}. \end{aligned} \quad (3.76)$$

There is no longer any dependence on $p_{i,j}$ in the integrand. This lets us do the integral over the phase space in Eq. (3.64b) in isolation, leaving in the centre-of-mass frame of the Z -boson,

$$\begin{aligned} \int d\Pi_N &= \int \frac{d^3 \mathbf{p}_i d^3 \mathbf{p}_j}{(2\pi)^2} \frac{1}{4E_i E_j} \delta(E_i + E_j - Q) \delta^3(\mathbf{p}_i + \mathbf{p}_j) \\ &= \frac{1}{16\pi^2} \int d^3 \mathbf{p}_i \frac{1}{E_i E_j} \delta(E_i + E_j - Q)|_{\mathbf{p}_j = -\mathbf{p}_i} \\ &= \frac{p}{4\pi Q}, \end{aligned} \quad (3.77)$$

where in the last equality we switch to polar coordinates and use the delta-function identity

$$\int dx f(x) \delta(g(x)) = \sum_{x_0} \frac{f(x_0)}{|g'(x_0)|}, \quad (3.78)$$

where x_0 are the zero(es) of $g(x)$. The momentum is understood to be

$$p(Q^2) = \frac{\sqrt{\lambda}(Q^2, m_i, m_j)}{2Q}. \quad (3.79)$$

Finally, inserting this into the cross-section expression Eq. (3.71), averaging over the initial four quark spins and N_C^2 colours, and inserting a symmetry factor of a half in the case where the final state particles are identical, we get

$$\begin{aligned} \frac{d\hat{\sigma}}{dQ^2} &= \frac{\alpha_W p}{16N_C^2 \pi \hat{s} Q} \left(\frac{1}{2}\right)^{\delta_{ij}} |D_Z(\hat{s})|^2 \left(K_1 \left(|O''_{ij}^L|^2 + |O''_{ij}^R|^2\right) + K_2 \operatorname{Re} \left\{ O''_{ij}^L (O''_{ij}^R)^*\right\}\right) \\ &\times \int d\Pi_H \sum_{\substack{\text{spins} \\ \text{colours}}} \sum_{\text{pol.}} |\mathcal{M}(ij \rightarrow Z^*(+X))|^2, \end{aligned} \quad (3.80)$$

where I have defined

$$K_1 = \frac{Q^2(Q^2 - m_i^2 - m_j^2) + Q^4 - (m_i^2 - m_j^2)^2}{3Q^2}, \quad (3.81a)$$

$$K_2 = 4m_i m_j. \quad (3.81b)$$

Eq. (3.80) gives us an expression for the contribution to the differential cross-section $\frac{d\hat{\sigma}}{dQ^2}$ only based on calculating the squared amplitude for partonic production of an off-shell Z -boson, potentially together with emission of a strongly interacting particle. The phase space integral $\int d\Pi_H$ is given from the differential Eq. (3.64a) in the case of $Z^* + X$ as a final state, and simply

$$d\Pi_H = \frac{d^{d-1}\mathbf{q}}{(2\pi)^{d-1}} \frac{1}{2q^0} \delta^d(q - k_i - k_j) \quad (3.82)$$

in case of simple Z -boson production.

Considering the specific process $q\bar{q} \rightarrow Z^*$ as in the LO case, contributions at NLO in QCD will come from interference with the LO cross-section $\mathcal{M}_0 \equiv \mathcal{M}_{\text{LO}}(q\bar{q} \rightarrow Z^*)$. Given an NLO amplitude $\mathcal{M}_1 \equiv \mathcal{M}_{\text{NLO}}(q\bar{q} \rightarrow Z^*)$, we get the a contribution proportional to $2\operatorname{Re}\{\mathcal{M}_0^* \mathcal{M}_1\}$. When considering other processes, there can be no interference with the LO amplitude, so the contributions will come proportional to the square $|\mathcal{M}_{\text{NLO}}(ij \rightarrow Z^*(+X))|^2$.

3.3.2 Virtual Exchange

Now that we have reduced the NLO QCD contributions to the total cross-section to the NLO QCD contributions to Z -boson production, we can start with the virtual exchange diagrams in Fig. 3.5. Let us consider first the SM contribution from the exchange of a gluon between the quarks, Fig. 3.5a. Labelling the quark colours a, b and the gluon indices k , we get

$$\mathcal{M}_g = -i\delta_{ab}C_F \epsilon_\mu^*(q) \mu^{4-d} g_s^2 g \int \frac{d^d \ell}{(2\pi)^d} \frac{\bar{v}_2 \gamma^\nu (\not{\ell} - \not{k}_j) \gamma^\mu (\not{\ell} + \not{k}_i) \gamma_\nu u_1}{\ell^2 (\ell + k_i)^2 (\ell - k_j)^2}, \quad (3.83)$$

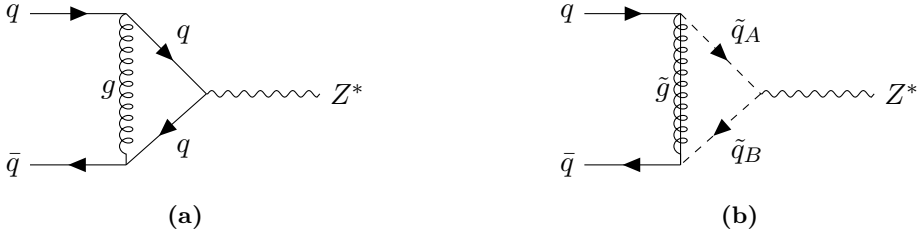


Figure 3.5: The two triangle diagrams contributing to NLO QCD corrections to the quark tensor.

where I have summed over the $SU(3)$ generators $T_{ac}^k T_{cb}^k = C_F \delta_{ab}$. Doing Passarino-Veltman reduction discussed in Section 1.4 using the **FeynCalc** [35, 36, 37, 38] package, we can rewrite this to

$$\mathcal{M}_g = \frac{C_F g_s^2}{16\pi^2} [(7-d)B_0(\hat{s}, 0, 0) - 4B_0(0, 0, 0) + 2\hat{s}C_0(0, \hat{s}, 0, 0, 0, 0)] \mathcal{M}_0, \quad (3.84)$$

and I have defined

$$\mathcal{M}_0 = \delta_{ab} g \epsilon_\mu^*(q) \left[C_{qqZ}^L b_L^\mu(v_2, u_1) + C_{qqZ}^R b_R^\mu(v_2, u_1) \right]. \quad (3.85)$$

This last bit Eq. (3.85) is recognisable as the tree-level amplitude for $q\bar{q} \rightarrow Z^*$. The phase space is simpler in this case without any real emission: In the centre-of-mass frame of the quarks Eq. (3.82) becomes

$$\int d\Pi_H = \int \frac{d^{d-1}q}{(2\pi)^{d-1}} \frac{1}{2\sqrt{Q^2 + |q|^2}} (2\pi)^d \delta(Q - \sqrt{\hat{s}}) \delta^{d-1}(q), \quad (3.86)$$

which with respect to the integration variable Q^2 in Eq. (3.63) yields

$$\int d\Pi_H = \frac{2\pi}{\hat{s}} \delta(1-z), \quad (3.87)$$

where $z = \frac{Q^2}{\hat{s}}$ as before. The contribution to the quark tensor will to NLO come from the interference between \mathcal{M}_g and \mathcal{M}_0 , and so it follows that the contribution to the total cross-section contribution from Eq. (3.80) becomes

$$\frac{d\hat{\sigma}_g}{dQ^2} = \frac{C_F \alpha_s}{\pi} P(\epsilon) \hat{\sigma}_B F''_Z \frac{\delta(1-z)}{\hat{s}} \times \text{Re} \left\{ 2B_0(0,0,0) - \left(\frac{3}{2} + \epsilon\right) B_0(\hat{s},0,0) - \hat{s} C_0(0,\hat{s},0,0,0,0) \right\}, \quad (3.88)$$

where $\alpha_s = \frac{g_s^2}{4\pi}$, and I have defined the prefactor

$$P(\epsilon) = \left(\frac{4\pi\mu^2}{Q^2} \right)^\epsilon \frac{\Gamma(1-\epsilon)}{\Gamma(1-2\epsilon)} (1-\epsilon). \quad (3.89)$$

This prefactor will come again many times, and we will make use of its series expansion

$$P(\epsilon) = 1 + \left(\ln \frac{\mu^2}{Q^2} - \gamma_E + \ln 4\pi - 1 \right) \epsilon + \mathcal{O}(\epsilon^2), \quad (3.90)$$

where γ_E is the Euler-Mascheroni constant.

Doing the same for the supersymmetric gluino exchange diagrams Fig. 3.5b is a bit more involved, as the loop particles are massive, and the couplings are complex. Working out the amplitude with **FeynCalc**, we get

$$\begin{aligned} \mathcal{M}_{\tilde{g}} = & i 2 \delta_{ab} C_F \epsilon_\mu^*(q) \mu^{4-d} g_s^2 g \sum_{AB} (C_{qqZ}^L (R_{A1}^{\tilde{q}})^* R_{B1}^{\tilde{q}} + C_{qqZ}^R (R_{A2}^{\tilde{q}})^* R_{B2}^{\tilde{q}}) \\ & \times \int \frac{d^d \ell}{(2\pi)^d} \frac{\bar{v}_2 N_{AB} (2\ell - k_i + k_j)^\mu u_1}{(\ell^2 - m_{\tilde{g}}^2)((\ell - k_i)^2 - m_A^2)((\ell + k_j)^2 - m_B^2)}, \end{aligned} \quad (3.91)$$

where

$$N_{AB} = \left[\left(R_{A1}^{\tilde{q}} (R_{B1}^{\tilde{q}})^* \ell - m_{\tilde{g}} R_{A1}^{\tilde{q}} (R_{B2}^{\tilde{q}})^* \right) P_L + \left(R_{A2}^{\tilde{q}} (R_{B2}^{\tilde{q}})^* \ell - m_{\tilde{g}} R_{A2}^{\tilde{q}} (R_{B1}^{\tilde{q}})^* \right) P_R \right]. \quad (3.92)$$

Computing the interference with the LO amplitude together, performing Passarino-Veltman reduction in **FeynCalc** again, and adding the phase space factor, we are left with

$$\begin{aligned} \int d\Pi_H 2 \operatorname{Re} \{ \mathcal{M}_0^* \mathcal{M}_{\tilde{g}} \} = & 8\pi(d-2) C_F \alpha_s \alpha_W \delta_{ab} \sum_{AB} \left| R_{A1}^{\tilde{q}} (R_{B1}^{\tilde{q}})^* C_{qqZ}^L + R_{A2}^{\tilde{q}} (R_{B2}^{\tilde{q}})^* C_{qqZ}^R \right|^2 \\ & \times \operatorname{Re} \{ C_{00}(0, \hat{s}, 0; m_A^2, m_{\tilde{g}}^2, m_B^2) \} \frac{\delta(1-z)}{\hat{s}}. \end{aligned} \quad (3.93)$$

The total contribution to the cross-section is then

$$\frac{d\hat{\sigma}_{\tilde{g}}}{dQ^2} = \frac{C_F \alpha_s}{\pi} P(\epsilon) \hat{\sigma}_B F_Z'' \tilde{V}_Z'' \frac{\delta(1-z)}{\hat{s}}, \quad (3.94)$$

where

$$\begin{aligned} \tilde{V}_Z'' = & \frac{2}{(C_{qqZ}^L)^2 + (C_{qqZ}^R)^2} \sum_{AB} \left(R_{A1}^{\tilde{q}} (R_{B1}^{\tilde{q}})^* C_{qqZ}^L + R_{A2}^{\tilde{q}} (R_{B2}^{\tilde{q}})^* C_{qqZ}^R \right)^2 \\ & \times \operatorname{Re} \{ C_{00}(0, 0, \hat{s}, m_A^2, m_{\tilde{g}}^2, m_B^2) \}. \end{aligned} \quad (3.95)$$

3.3.3 Counterterms

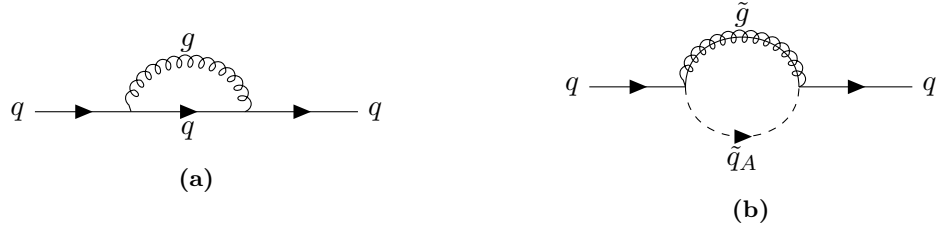


Figure 3.6: The QCD quark self-energy diagrams used for extracting quark renormalisations.

The UV divergences in the Passerino-Veltman functions in the virtual contributions Eqs. (3.88) and (3.94) can be cancelled through renormalisation of the quark field wave functions. Renormalisation of the Z -boson field wave function will not contribute at order α_s , so it will suffice to renormalise the quarks. I will follow the on-shell renormalisation procedure of the section Section 1.2.3, but I will not make use of any

mass counterterm. Reading off the amplitudes in Fig. 3.6 and inserting the Passarino-Veltman loop functions we have the self-energy

$$\begin{aligned} \Sigma_q(\not{p}) = & \frac{g_s^2 C_F \delta_{ab}}{16\pi^2} \left\{ \frac{d-2}{2} \not{p} B_0(0,0,0) \right. \\ & - 2 \sum_A [\not{p}(|R_{A1}^{\tilde{q}}|^2 P_L + |R_{A2}^{\tilde{q}}|^2 P_R) B_1(0, m_{\tilde{g}}^2, m_A^2) \\ & \left. + m_{\tilde{g}} (R_{A1}^{\tilde{q}} (R_{A2}^{\tilde{q}})^* P_L + R_{A2}^{\tilde{q}} (R_{A1}^{\tilde{q}})^* P_R) B_0(0, m_{\tilde{g}}, m_A^2)] \right\}. \end{aligned} \quad (3.96)$$

Renormalising the quark field wave function chirally, we have

$$\psi \rightarrow \sqrt{Z_L} P_L \psi + \sqrt{Z_R} P_R \psi, \quad (3.97)$$

which expanded into counterterms $Z_{L/R} = 1 + \delta_{L/R}$ yields through the on-shell conditions from Section 1.2.4⁸

$$\text{Re}\{\delta_L\} = \frac{g_s^2 C_F \delta_{ab}}{16\pi^2} \left\{ -\frac{d-2}{2} B_0(0,0,0) + 2 \sum_A |R_{A1}^{\tilde{q}}|^2 B_1(0, m_{\tilde{g}}^2, m_A^2) \right\}, \quad (3.98a)$$

$$\text{Re}\{\delta_R\} = \frac{g_s^2 C_F \delta_{ab}}{16\pi^2} \left\{ -\frac{d-2}{2} B_0(0,0,0) + 2 \sum_A |R_{A2}^{\tilde{q}}|^2 B_1(0, m_{\tilde{g}}^2, m_A^2) \right\}. \quad (3.98b)$$

The counterterm amplitude then becomes

$$\mathcal{M}_{c.t.} = g \delta_{ab} \epsilon_\mu^*(q) \left[\text{Re}\{\delta_L\} C_{qqZ}^L b_L^\mu(v_2, u_1) + \text{Re}\{\delta_R\} C_{qqZ}^R b_R^\mu(v_2, u_1) \right], \quad (3.99)$$

essentially turning $C_{qqZ}^X \rightarrow \text{Re}\{\delta_X\} C_{qqZ}^X$ in the LO amplitude Eq. (3.85) or, consequently, the effective coupling $Z^{XY} \rightarrow \text{Re}\{\delta_X\} Z^{XY}$. The contribution to the total cross-section comes again through interference with the tree-level amplitude Eq. (3.85), yielding

$$\frac{d\hat{\sigma}_{c.t.}}{dQ^2} = \frac{C_F \alpha_s}{2\pi} P(\epsilon) \hat{\sigma}_B F_Z'' \tilde{B}_Z'', \quad (3.100)$$

where the new mediator contribution is defined

$$\begin{aligned} \tilde{B}_Z'' = & -(1-\epsilon) \text{Re}\{B_0(0,0,0)\} \\ & + \frac{2}{(C_{qqZ}^L)^2 + (C_{qqZ}^R)^2} \sum_A \left((C_{qqZ}^L)^2 |R_{A1}^{\tilde{q}}|^2 + (C_{qqZ}^R)^2 |R_{A2}^{\tilde{q}}|^2 \right) \text{Re}\{B_1(0, m_{\tilde{g}}^2, m_A^2)\} \end{aligned} \quad (3.101)$$

Total Virtual Contribution

As mentioned before, the Passarino-Veltman functions in the virtual contributions above with their counterterms have analytic expressions. For the contributions including SUSY particles, there are more masses in the arguments of these functions, which complicates these expressions considerably. Packages such as `LoopTools` [39] already have efficient numeric implementations of these functions, so I will keep those as they are. Of note is that the mass of these SUSY particles naturally any IR divergences which could occur in these loop integrals, and so only UV cancellation needs to be ensured.

⁸The keen reader will notice that the counterterms do not cancel the divergences proportional to $m_{\tilde{g}}$ in Eq. (3.96). However, this is not necessary, as due to the unitarity of the quark mixing matrices, the divergences cancel after summing over squark eigenstates A .

For the Passarino-Veltman functions not containing SUSY particles, we can actually insert the analytic expressions and simplify the total contribution. In fact, the total non-SUSY contribution of the virtual diagrams with their counterterms is

$$\frac{d\hat{\sigma}_v^{\text{non-SUSY}}}{dQ^2} = \frac{\alpha_s C_F}{\pi} \frac{\hat{\sigma}_B}{\hat{s}} F''_Z \delta(1-z) P(\epsilon) \left\{ -\frac{1}{\epsilon_{\text{IR}}^2} - \frac{3}{2} \frac{1}{\epsilon_{\text{IR}}} + \frac{\pi^2}{3} - 4 \right\}, \quad (3.102)$$

where the UV divergences have cancelled completely.

The total virtual contribution with counterterms involving SUSY particles can then be encapsulated by

$$\frac{d\hat{\sigma}_v^{\text{SUSY}}}{dQ^2} = \frac{\alpha_s C_F}{\pi} \frac{\hat{\sigma}_B}{\hat{s}} F''_Z \delta(1-z) P(\epsilon) \tilde{C}_Z'', \quad (3.103)$$

where we have defined an effective scaling from the LO contribution

$$\tilde{C}_Z'' = \frac{2}{(C_{qqZ}^L)^2 + (C_{qqZ}^R)^2} \quad (3.104)$$

$$\begin{aligned} & \times \left\{ \sum_{AB} \left(R_{A1}^{\tilde{q}} (R_{B1}^{\tilde{q}})^* C_{qqZ}^L + R_{A2}^{\tilde{q}} (R_{B2}^{\tilde{q}})^* C_{qqZ}^R \right)^2 \text{Re} \left\{ C_{00}(0, 0, \hat{s}, m_A^2, m_{\tilde{g}}^2, m_B^2) \right\} \right. \\ & \left. + \sum_A \left((C_{qqZ}^L)^2 |R_{A1}^{\tilde{q}}|^2 + (C_{qqZ}^R)^2 |R_{A2}^{\tilde{q}}|^2 \right) \text{Re} \left\{ B_1(0, m_{\tilde{g}}, m_A^2) \right\} \right\}. \end{aligned} \quad (3.105)$$

The cancellation of UV divergences in these Passarino-Veltman functions have been done symbolically using `FeynCalc`, where unitarity relations for the squark mixing matrices have been utilised.

3.3.4 Real Emission

The massless gluon and quarks in the loop of Fig. 3.5a will result in IR divergences. These divergences are cancelled by soft emission of strongly coupling massless particles. For two incoming partons i, j we shall take into account the inclusive production of a neutralino pair with either a gluon or a quark. Again, the only QCD NLO contributions can come from adjusting the quark tensor $H^{\mu\nu}$ as no strong interaction vertex can be added to the neutralino tensor.

Gluon Emission



Figure 3.7: Gluon emission diagrams

The production of a gluon with four-momentum k^μ together with an off-shell Z-boson with q^μ through two partons goes through a quark-antiquark pair as seen in Fig. 3.7.

The matrix element for this is

$$\begin{aligned} \mathcal{M}_{r,g} = & g_s g T_{ab}^k \bar{v}_2 \left\{ \gamma^\mu (C_{qqZ}^L P_L + C_{qqZ}^R P_R) \frac{\not{q} - \not{k}_j}{(q - k_j)^2} \gamma^\nu \right. \\ & \left. + \gamma^\nu \frac{\not{k} - \not{k}_j}{(k - k_j)^2} \gamma^\mu (C_{qqZ}^L P_L + C_{qqZ}^R P_R) \right\} u_1 \epsilon_\mu^*(q) \epsilon_\nu^*(k), \end{aligned} \quad (3.106)$$

where a, b are the colour indices of the quark and antiquark respectively and k is the gluon index. Now, we define the Mandelstam variables

$$\hat{s} \equiv (k_i + k_j)^2 = (q + k)^2, \quad (3.107a)$$

$$\hat{t} \equiv (k_i - k)^2 = (k_j - q)^2, \quad (3.107b)$$

$$\hat{u} \equiv (k_i - q)^2 = (k_j - k)^2, \quad (3.107c)$$

where I note that \hat{t} and \hat{u} are *not* the same as the definitions Eq. (3.30). Squaring the matrix element and summing over spins, external polarisations and colours, we get

$$|\mathcal{M}_{r,g}|^2 = (d-2) N_C C_F g_s^2 g_W^2 ((C_{qqZ}^L)^2 + (C_{qqZ}^R)^2) \left(2(d-4) + (d-2) \left(\frac{\hat{t}}{\hat{u}} + \frac{\hat{u}}{\hat{t}} \right) + \frac{4Q^2 \hat{s}}{\hat{t}\hat{u}} \right). \quad (3.108)$$

The phase space is a $2 \rightarrow 2$ process as in the LO case, so we can use the differential phase space defined in Eq. (3.5). Using the change of variable from earlier of $y = \frac{1}{2}(1 + \cos \theta)$ and using z from before, we can express these Mandelstam variables as

$$\hat{s} = \frac{Q^2}{z}, \quad (3.109a)$$

$$\hat{t} = -\frac{Q^2}{z}(1-z)(1-y), \quad (3.109b)$$

$$\hat{u} = -\frac{Q^2}{z}(1-z)y. \quad (3.109c)$$

The phase space integral over the squared amplitude to be inserted into Eq. (3.80) then looks like

$$\begin{aligned} \int d\Pi_H \sum_{\substack{\text{spin} \\ \text{colour}}} |\mathcal{M}_{r,g}|^2 = & \frac{N_C C_F \mu^{4-d} g_s^2 g_W^2}{(4\pi)^{\frac{d-2}{2}}} \frac{1}{\Gamma(\frac{d-2}{2})} \frac{p^{d-3}}{8\hat{s}\sqrt{\hat{s}}} (d-2)((C_{qqZ}^L)^2 + (C_{qqZ}^R)^2) \\ & \times \int_0^1 dy (y(1-y))^{d-4} \left(2(d-4) + (d-2) \left(\frac{1-y}{y} + \frac{y}{1-y} \right) + \frac{4z}{(1-z)^2 y(1-y)} \right), \end{aligned} \quad (3.110)$$

which evaluated in $d = 4 - 2\epsilon$ space-time dimensions becomes

$$\begin{aligned} \int d\Pi_H \sum_{\substack{\text{spin} \\ \text{colour}}} |\mathcal{M}_{r,g}|^2 = & (1-\epsilon) \frac{2\pi^{3/2} N_C C_F \alpha_s \alpha_W}{\Gamma(1-\epsilon) \Gamma(\frac{3}{2}-\epsilon)} ((C_{qqZ}^L)^2 + (C_{qqZ}^R)^2) \left(\frac{4\pi\mu^2}{Q^2} \right)^\epsilon \left(\frac{4z}{(1-z)^2} \right)^\epsilon \\ & \times \Gamma(-\epsilon) \left((1+z)^2 \epsilon^2 - (5z^2 - 6z + 7)\epsilon - 4z(1-z) + 2 \right), \end{aligned} \quad (3.111)$$

where we have used the integral definition of the Euler-Beta function

$$B(a, b) \equiv \int_0^1 dy y^{a-1} (1-y)^{b-1} = \frac{\Gamma(a)\Gamma(b)}{\Gamma(a+b)}. \quad (3.112)$$

We can $z^\epsilon = 1 + \epsilon \ln z + O(\epsilon^2)$ and the *plus distribution* to write

$$(1-z)^{1-2\epsilon} = -\frac{1}{2\epsilon} \delta(1-z) + \left[\frac{1}{1-z} \right]_+ - 2\epsilon \left[\frac{\ln(1-z)}{1-z} \right]_+ + O(\epsilon^2). \quad (3.113)$$

Plus distributions are defined such that for an arbitrary function $g(z)$ and a plus distribution $f_+(z)$

$$\left[\frac{f(z)}{1-z} \right]_+ \equiv \frac{f(z)}{1-z} - \delta(1-z) \int_0^z dy \frac{f(y)}{1-y} \quad (3.114)$$

Using this, we can rewrite Eq. (3.111) as

$$\begin{aligned} \int d\Pi_H \sum_{\substack{\text{spin} \\ \text{colour}}} |\mathcal{M}_{r,g}|^2 &= 16\pi N_C C_F \alpha_s \alpha_W ((C_{qqZ}^L)^2 + (C_{qqZ}^R)^2) P(\epsilon) \\ &\times \left(\frac{1}{\epsilon^2} \delta(1-z) - \frac{1}{\epsilon} (1+z^2) \left[\frac{1}{1-z} \right]_+ - \frac{(1+z^2) \ln z}{1-z} + 2(1+z^2) \left[\frac{\ln(1-z)}{1-z} \right]_+ \right), \end{aligned} \quad (3.115)$$

where again, the ϵ -dependent prefactor $P(\epsilon)$ has been extracted, as with the virtual contributions above. This yields a total contribution to the cross-section

$$\begin{aligned} \frac{d\hat{\sigma}_{r,g}}{dQ^2} &= \frac{\hat{\sigma}_B}{\hat{s}} F_Z'' \frac{\alpha_s C_F}{\pi} P(\epsilon) \\ &\times \left(\frac{1}{\epsilon^2} \delta(1-z) - \frac{1}{\epsilon} (1+z^2) \left[\frac{1}{1-z} \right]_+ - \frac{(1+z^2) \ln z}{1-z} + 2(1+z^2) \left[\frac{\ln(1-z)}{1-z} \right]_+ \right). \end{aligned} \quad (3.116)$$

We can see here that the $\frac{1}{\epsilon^2}$ -pole cancels with that from the virtual contribution Eq. (3.102). However, the $\frac{1}{\epsilon}$ -term here is proportional to a plus-distribution and cannot cancel with anything from the $2 \rightarrow 2$ cross-sections. In fact, these divergences are fundamentally different in nature, and do not come from the radiation of soft gluons, where the real and virtual exchanges become indistinguishable. The remaining divergences are *collinear* divergences, arising from the limits where $y \rightarrow 0, 1$, or equivalently $\cos\theta \rightarrow \pm 1$, meaning the radiated gluons are collinear with the incoming partons. The means for removing these divergences is different, and involve redefining the parton distribution functions in a manner similar to the renormalisation of the fields and couplings of the bare Lagrangian in Section 1.2, and is performed explicitly in the next chapter.

Quark Emission



Figure 3.8: Quark emission diagrams

It is also possible for two partons to produce a quark or an antiquark together with an off-shell Z -boson. This process goes through a gluon and a(n) quark/antiquark, as

shown in Fig. 3.8. Assigning the momenta $q(k_i)g(k_j) \rightarrow q(k)g(q)$ and labelling the incoming quark colour a , the outgoing quark colour b and the incoming gluon index k , the amplitude reads

$$\mathcal{M}_{r,q} = gg_s T_{ab}^k(q) \epsilon_\nu(k_j) \bar{u}(k) \left\{ \frac{C_{qqZ}^L(\gamma^\mu \not{k}_j \gamma^\nu + 2k_i^\nu \gamma^\mu) P_L + C_{qqZ}^R(\gamma^\mu \not{k}_j \gamma^\nu + 2k_i^\nu \gamma^\mu) P_R}{\hat{s}} \right. \\ \left. - \frac{C_{qqZ}^L(\gamma^\nu \not{k}_j \gamma^\mu - 2k_i^\nu \gamma^\mu) P_L + C_{qqZ}^R(\gamma^\nu \not{k}_j \gamma^\mu - 2k_i^\nu \gamma^\mu) P_R}{\hat{u}} \right\} u(k_i). \quad (3.117)$$

Again evaluating in **Mathematica** using the **FeynCalc** package, the squared matrix element becomes, after averaging over the two initial quark spins and N_C colours, and two initial gluon polarisations and $N_C^2 - 1$ gluon states,

$$\frac{1}{4N_C(N_C^2 - 1)} \sum_{\substack{\text{spin/pol.} \\ \text{colour}}} |\mathcal{M}_{r,q}|^2 = \frac{g^2 \mu^{2\epsilon} g_s^2 T_F}{N_C} ((C_{qqZ}^L)^2 + (C_{qqZ}^R)^2)(1 - \epsilon) \\ \times \left\{ -\frac{2Q^2 \hat{t}}{\hat{s}\hat{u}} + 2\epsilon - (1 - \epsilon) \left(\frac{\hat{s}}{\hat{u}} + \frac{\hat{u}}{\hat{s}} \right) \right\}, \quad (3.118)$$

where

$$T_F = \frac{T_{ab}^k T_{ba}^k}{N_C^2 - 1} \quad (3.119)$$

is the index of the fundamental representation of $SU(N_C)$. Changing to the Mandelstam variables Eq. (3.107) like with the gluon emission, and doing the phase space integral Eq. (3.5) with the change of variable to y , we can insert into Eq. (3.80) with the averaging factor replacing the colour average $\frac{1}{N_C^2} \rightarrow \frac{1}{N_C(N_C^2 - 1)}$ and get

$$\frac{d\hat{\sigma}_{r,q}}{dQ^2} = \frac{\hat{\sigma}_B}{\hat{s}} F_Z'' \frac{T_F \alpha_s}{2\pi} P(\epsilon) \\ \times \left\{ -\frac{1 - 2z(1 - z)}{\epsilon} + \frac{1}{2}(1 + 6z - 7z^2) + (1 - 2z(1 - z)) \ln \frac{(1 - z)^2}{z} \right\}. \quad (3.120)$$

One IR divergence arises in this contribution, which cannot cancel with the contribution of any of the other contributions we have calculated thus far, owing to its differing prefactor including T_F instead of C_F . This divergence will be dealt with in the next chapter through renormalisation of the parton distribution functions, which will relate this process with different incoming partons to the processes with an initial quark-antiquark pair.

The cross-section contribution for real antiquark emission works out to the same as for real quark emission. This effectively adds another cross-section contribution $\frac{d\hat{\sigma}_{r,\bar{q}}}{dQ^2} = \frac{d\hat{\sigma}_{r,q}}{dQ^2}$

To summarise the parton cross-sections we have to NLO:

$$\frac{d\hat{\sigma}_{q\bar{q}}}{dQ^2} = \hat{\sigma}^0 \frac{\delta(1 - z)}{\hat{s}} + \frac{d\hat{\sigma}_v^{\text{non-SUSY}}}{dQ^2} + \frac{d\hat{\sigma}_v^{\text{SUSY}}}{dQ^2} + \frac{d\hat{\sigma}_{r,g}}{dQ^2}, \quad (3.121a)$$

$$\frac{d\hat{\sigma}_{qg}}{dQ^2} = \frac{d\hat{\sigma}_{r,q}}{dQ^2}, \quad (3.121b)$$

$$\frac{d\hat{\sigma}_{\bar{q}g}}{dQ^2} = \frac{d\hat{\sigma}_{r,\bar{q}}}{dQ^2}. \quad (3.121c)$$

3.4 Gaugino Corrections

The corrections at NLO in QCD to gaugino pair production come from corrections to the \hat{t} - and \hat{u} -channels in Fig. 3.2. These come in the form of a gluon or gluino between the initial quarks, creating the box diagrams in Fig. 3.9, the vertex corrections to the quark-squark-neutralino vertices in Fig. 3.10 or self-energy insertions corrections to the squark propagator in Fig. 3.12.

The IR-divergences from exchanging real gluons in these diagrams are cancelled by taking into account the real gluon emission diagrams in Fig. 3.13. Furthermore, quark emission should be included in the inclusive cross-section with the gaugino-like vertices enabling the diagrams in Fig. 3.14.

In the case of production of a neutralino-chargino pair or a pure chargino pair, the higgsino-like interactions go through an \hat{s} -channel whereas the gaugino-like interactions go through \hat{t} - or \hat{u} -channels as with the neutralino pair described above. Therefore, the discussion that follows in this chapter will be equally valid for all electroweakino pair production.⁹

Two subtleties must be addressed when computing these contributions. First, when using dimensional regularisation, the dimensionality of vector fields go from $4 \rightarrow d$, whereas Dirac spinors remain four-dimensional. This comes from the fact that the Dirac spinors are generated from the Dirac gamma-matrices defined by the Clifford algebra with the anticommutation relation

$$\{\gamma^\mu, \gamma^\nu\} = 2g^{\mu\nu}\mathbb{I}, \quad (3.122)$$

of which there is no true realisation in fractional dimensions.

The result is that the degrees of freedom between the SM gauge bosons and their fermion partners are no longer the same — breaking supersymmetry. Others have shown that this can be remedied by introducing a counterterm to the weak Yukawa coupling of the quark-squark-neutralino interaction [40]

$$g \rightarrow \hat{g} = g \left(1 - \frac{\alpha_s C F}{8\pi} \right). \quad (3.123)$$

The other subtlety comes from the real quark emission of the leftmost diagrams in Fig. 3.14, going through an intermediate squark state. This squark can go on-shell if $m_{\tilde{\chi}_{i,j}} < m_{\tilde{q}_A}$ and $\hat{s} > (m_{\tilde{\chi}_{i,j}} + m_{\tilde{q}_A})^2$, which overlaps with the production of a neutralino and a squark followed by the subsequent decay of the squark into a neutralino and a quark. To avoid this double-counting, we must subtract the cross-section for neutralino-squark production with the corresponding branching ratio:

$$\sum_A \left\{ \frac{d\hat{\sigma}}{dQ^2}(qg \rightarrow \tilde{\chi}_i^0 \tilde{q}_A) \text{BR}(\tilde{q}_A \rightarrow \tilde{\chi}_j^0 q) + (i \leftrightarrow j) \right\}. \quad (3.124)$$

⁹There is one exception in the case of chargino pair production, however, as the gaugino-like chargino part does couple to the photon in the \hat{s} -channel in Fig. 3.4. This contribution can be factorised and worked out in the same manner as what has been done above for the higgsino-like cross-sections.

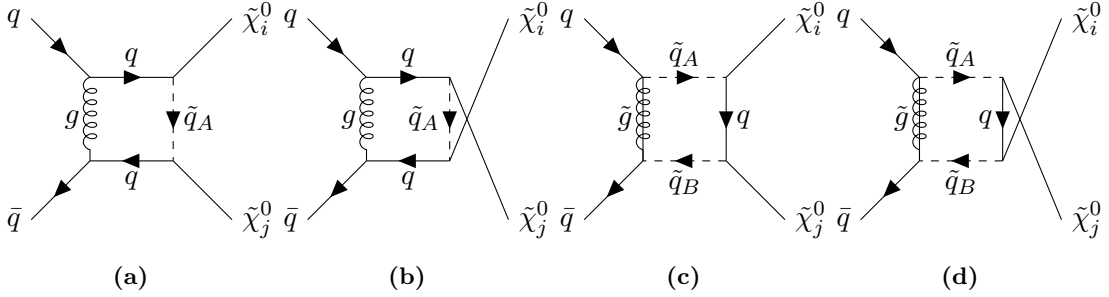


Figure 3.9: Box diagrams contributing to NLO QCD corrections to the gaugino part of neutralino pair production.

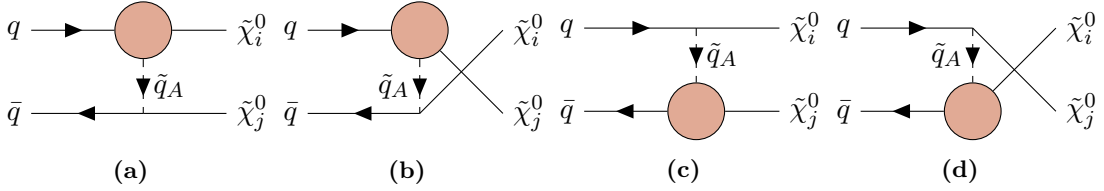


Figure 3.10: Vertex diagrams contributing to NLO QCD corrections to the gaugino part of neutralino pair production. The blobs are defined in Fig. 3.11.

3.4.1 Catani-Seymour Dipole Formalism

The loops in these virtual exchange diagrams will contain dependence on the Mandelstam variables in Eq. (3.30), which will complicate the phase space integral over \hat{t} considerably. Doing the phase space integral numerically instead will require some procedure for regularising and extracting the divergences such that they can cancel. For the IR-divergences to cancel, it will require matching between the phase space integrals of the $2 \rightarrow 2$ process of virtual gluon/quark exchange with the $2 \rightarrow 3$ of the real emission. The Catani-Seymour dipole formalism [41] rewrites these integrals such that the divergences cancel at the level of the integrand of the two phase space integrals separately. This allows for the reliable numerical implementation of the two phase space integrals.

More concretely, given a leading order differential, parton-level cross-section $d\hat{\sigma}_{ij}^{\text{LO}}(k_i, k_j)$ for two partons i, j , with a renormalised virtual NLO contribution $d\hat{\sigma}_{ij}^v(k_i, k_j)$ and real emission NLO contribution $d\hat{\sigma}_{ij}^r$, we can divide the phase space

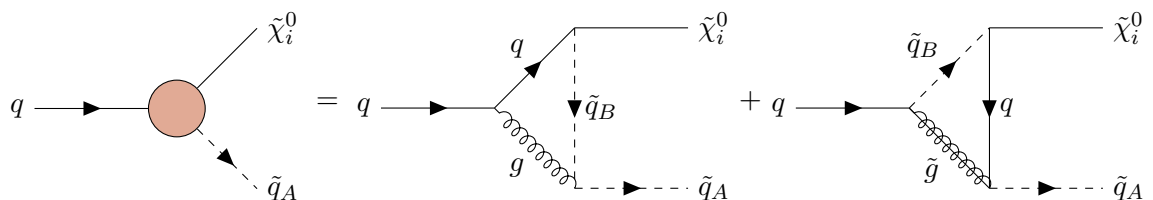


Figure 3.11: The vertex insertions used in Fig. 3.10.

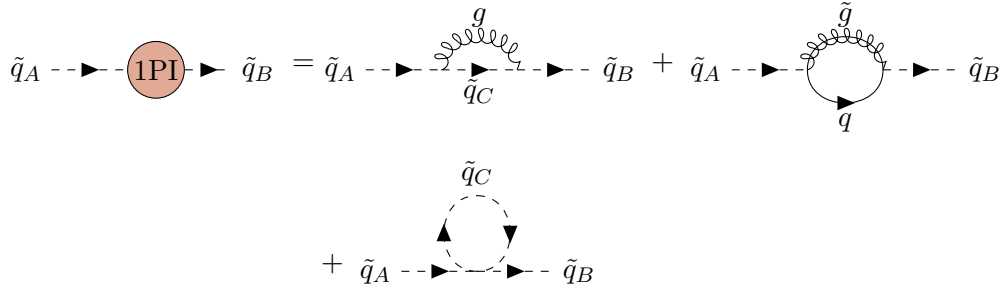


Figure 3.12: NLO QCD diagrams contributing to the self-energy of the squark.

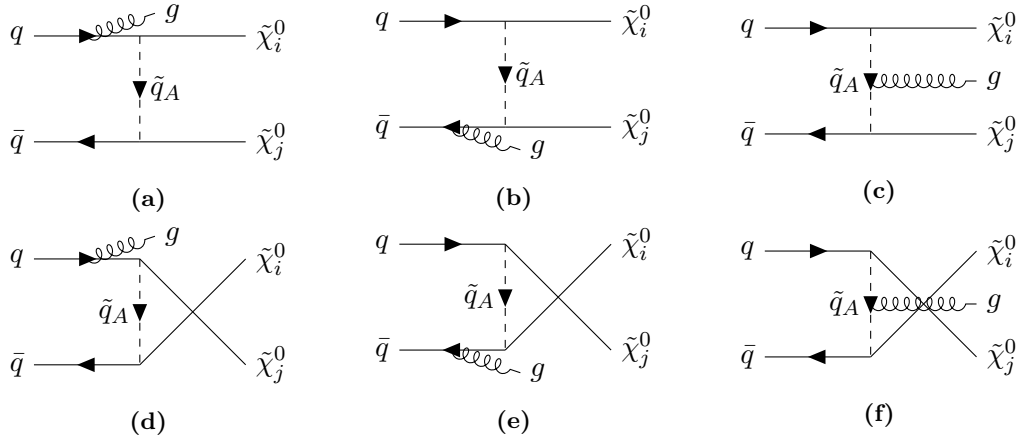


Figure 3.13: Gluon emission diagrams with gaugino-like vertices for neutralino pair production.

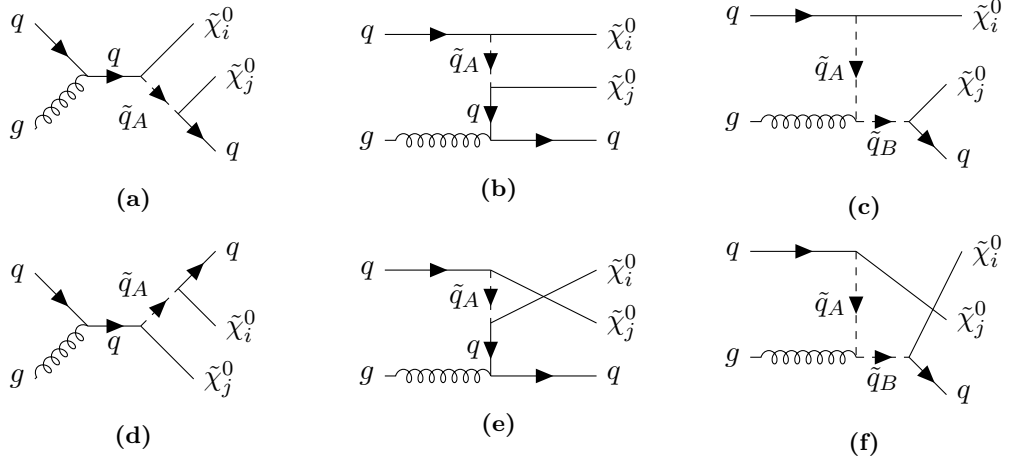


Figure 3.14: Quark emission diagrams with gaugino-like vertices for neutralino pair production.

integrals for the $2 \rightarrow 2$ and $2 \rightarrow 3$ processes as

$$\begin{aligned} \hat{\sigma}_{ij}^{\text{NLO}}(k_i, k_j) = & \int d\Pi_{2 \rightarrow 3} \left[d\hat{\sigma}_{ij}^r(k_i, k_j) \Big|_{\epsilon=0} - d\hat{\sigma}_{ij}^{r,c.t.}(k_i, k_j) \Big|_{\epsilon=0} \right] \\ & + \int d\Pi_{2 \rightarrow 2} \left[d\hat{\sigma}_{ij}^v(k_i, k_j) + d\hat{\sigma}_{ij}^{v,c.t.}(k_i, k_j) \right]_{\epsilon=0} + \int d\Pi_{2 \rightarrow 2} d\hat{\sigma}_{ij}^F(k_i, k_j). \end{aligned} \quad (3.125)$$

Effectively what is done is to introduce a counterterm to each of the real and virtual contributions separately, $\hat{\sigma}_{ij}^{r,c.t.}$ and $\hat{\sigma}_{ij}^{v,c.t.}$, each of which ensure the IR finiteness of the contributions. It can be shown that integrating over the extra degrees of freedom in the $2 \rightarrow 3$ phase space integral of real emission counterterm reproduces the virtual counterterm,

$$\int d\Pi_{2 \rightarrow 3} d\hat{\sigma}_{ij}^{r,c.t.} = \int d\Pi_{2 \rightarrow 2} \hat{\sigma}_{ij}^{v,c.t.}, \quad (3.126)$$

meaning it is just a rewrite of $\int d\Pi_{2 \rightarrow 3} d\hat{\sigma}_{ij}^r(k_i, k_j) + \int d\Pi_{2 \rightarrow 2} d\hat{\sigma}_{ij}^v(k_i, k_j)$. The final term is a compensation for the definition of the PDFs at a factorisation scale μ_F , and ensures that any cross-section dependence on this scale is cancelled to NLO. I will go into detail on the factorisation scale and dependence on this in the next chapter.

The extra terms can be shown to be given by

$$d\hat{\sigma}_{ij}^{r,c.t.}(k_i, k_j) = \sum_{\text{dipoles}} d\hat{\sigma}_{ij}^{\text{LO}} \otimes dV_{\text{dipole}}, \quad (3.127a)$$

$$d\hat{\sigma}_{ij}^{v,c.t.}(k_i, k_j) = d\hat{\sigma}_{ij}^{\text{LO}}(k_i, k_j) \otimes \mathbf{I}, \quad (3.127b)$$

$$\begin{aligned} d\hat{\sigma}_{ij}^F(k_i, k_j) = & \sum_k \int_0^1 dx \left[d\hat{\sigma}_{kj}^{\text{LO}}(xk_i, k_j) \otimes (\mathbf{P} + \mathbf{K})^{i,k}(x) \right. \\ & \left. + d\hat{\sigma}_{ik}^{\text{LO}}(k_i, xk_j) \otimes (\mathbf{P} + \mathbf{K})^{j,k}(x) \right]_{\epsilon=0}, \end{aligned} \quad (3.127c)$$

where $\mathbf{I} = \int d(\Pi_{2 \rightarrow 3-2}) \sum_{\text{dipoles}} dV_{\text{dipole}}$ ¹⁰ is a function extracting the soft/collinear limits ($k_{i,j} \cdot k \rightarrow 0$) of the real emission contributions, and \mathbf{P} and \mathbf{K} are insertion functions related to the Altarelli-Parisi splitting functions [42]. Explicit realisations of these functions are given in [41].

¹⁰The integration measure $\Pi_{2 \rightarrow 3-2}$ is meant to indicate an integral over the extra momentum of the $2 \rightarrow 3$ process as compared to the $2 \rightarrow 2$ one.

Chapter 4

Electroweakino Pair Production in Proton–Proton Collisions

In this chapter, I go through the computation of the hadronic cross-section. This entails renormalising infrared divergences the parton level cross-sections and the parton distribution functions (PDFs). I briefly go over the parton model, the hadron level kinematics and the renormalisation procedure, before presenting the concrete integral to be computed numerically in the next chapter.

4.1 The Parton Model and PDFs

So far, we have worked with the parton level cross-section, figuring out the contribution of the individual constituents of a proton to the cross-section for our final state. These do not individually result in any observable, as the partons are confined to the proton, and can therefore not be singled out in an experiment. To get an observable quantity comparable to experiment, we must sew the individual contributions together. This is done with the *parton model*, where scattering interactions with the proton is modelled with the interaction of free constituent particles inside. The parton model builds on the concept of *factorisation* which, owing to the weakening of the QCD coupling at high-energies, divides interactions with colour-neutral particles into a high-energy *hard* part between partons of the colliding protons, and a low-energy regime constituting interaction between the partons in a single proton. The hard part constitutes the partonic cross-sections calculated in the previous chapter, whereas the low-energy interactions are encapsulated in the PDFs which are fitted to experiment. The low-energy regime dictates that partons each carry a fraction of the total momentum of the proton, and the probability of encountering a given parton with said momentum fraction.

4.1.1 Hadronic kinematics

Consider the scattering of two protons with momenta P_1^μ and P_2^μ respectively into a set of final state particles χ, χ', X where X is some collection of unlabelled particles. Table 4.1 lists the definitions of kinematic variables at the hadronic level and their relation of the partonic kinematic variables defined in Section 3.3. I define the centre-of-mass energy of the protons $S \equiv (P_1 + P_2)^2$. The cross-section for a given process is then given in terms of the cross-section of two partons i, j with momenta $k_i = x_1 P_1$ and $k_j = x_2 P_2$ where $x_1, x_2 \in [0, 1]$ are the respective fractions of the proton momenta the partons carry. The

hadronic cross-section differential in the squared mass Q^2 of two final state particles χ and χ' is then given by

$$\begin{aligned}\frac{d\sigma}{dQ^2}(PP \rightarrow \chi\chi' + X) &= \sum_{ij} \int_0^1 dx_1 \int_0^1 dx_2 \theta(\hat{s} - Q^2) f_i(x_1) f_j(x_2) \frac{d\hat{\sigma}}{dQ^2}(ij \rightarrow \chi\chi' + X) \\ &= \sum_{ij} \int_\tau^1 dx_1 \int_{\tau/x_1}^1 dx_2 f_i(x_1) f_j(x_2) \frac{d\hat{\sigma}}{dQ^2}(ij \rightarrow \chi\chi' + X).\end{aligned}\quad (4.1)$$

The Heaviside function $\theta(\hat{s} - Q^2) = \theta(x_1 x_2 - \tau)$ ensures that there is enough energy between the scattering partons to produce the final state $\chi\chi'$ -pair with centre-of-mass energy $Q^2 = \tau S$.

Partonic variable	Definition in terms of hadronic variables
k_i^μ	$x_1 P_1^\mu$
k_j^μ	$x_2 P_2^\mu$
\hat{s}	$x_1 x_2 S$
z	$\frac{\tau}{x_1 x_2}$

Table 4.1: List of relations between hadronic and partonic kinematic variables.

4.1.2 Integration over PDFs

Practically, the two-dimensional integration over the parton momentum fractions x_1, x_2 can be alleviated by the fact that partonic cross-section contains terms proportional to either $\delta(1 - z)$ or plus distributions $f_+(z)$ as we have seen in Chapter 3. Let us consider these types of integrals in some generality. Let $g(x_1, x_2)$ be some function of x_1, x_2 , consider the integral

$$\int_{\tau/x_1}^1 \frac{dx_2}{x_2} g(x_1, x_2) \delta(1 - z). \quad (4.2)$$

Switching variables to $z = \frac{\tau}{x_1 x_2}$ while keeping x_1 constant yields

$$\int_{\tau/x_1}^1 \frac{dz}{z} g(x_1, \frac{\tau}{x_1 z}) \delta(1 - z) = g(x_1, \frac{\tau}{x_1}). \quad (4.3)$$

The plus-distributions are somewhat more complicated. Keeping in mind their definition

$$\int_0^1 dz g(z) f_+(z) = \int_0^1 dz (g(z) - g(1)) f(z), \quad (4.4)$$

we have that

$$\begin{aligned}
 \int_{\tau/x_1}^1 \frac{dx_2}{x_2} g(x_1, x_2) f_+(z) &= \int_{\tau/x_1}^1 \frac{dz}{z} g(x_1, \frac{\tau}{x_1 z}) f_+(z) \\
 &= \int_0^1 \frac{dz}{z} g(x_1, \frac{\tau}{x_1 z}) f_+(z) - \int_0^{\tau/x_1} \frac{dz}{z} g(x_1, \frac{\tau}{x_1 z}) f_+(z) \\
 &= \int_0^1 dz \left(\frac{1}{z} g(x_1, \frac{\tau}{x_1 z}) - g(x_1, \frac{\tau}{x_1}) \right) f(z) - \int_0^{\tau/x_1} \frac{dz}{z} g(x_1, \frac{\tau}{x_1 z}) f(z) \\
 &= \int_{\tau/x_1}^1 \frac{dz}{z} \left(g(x_1, \frac{\tau}{x_1 z}) - z g(x_1, \frac{\tau}{x_1}) \right) f(z) - g(x_1, \frac{\tau}{x_1}) \int_0^{\tau/x_1} dz f(z) \quad (4.5)
 \end{aligned}$$

$$= \int_0^1 dz \left(\frac{1}{z} g(x_1, \frac{\tau}{x_1 z}) - g(x_1, \frac{\tau}{x_1}) \right) f(z) - \int_0^{\tau/x_1} \frac{dz}{z} g(x_1, \frac{\tau}{x_1 z}) f(z) \quad (4.6)$$

$$= \int_{\tau/x_1}^1 \frac{dx_2}{x_2} \left(g(x_1, x_2) - \frac{\tau}{x_1 x_2} g(x_1, \frac{\tau}{x_1}) \right) f(z) - g(x_1, \frac{\tau}{x_1}) F(x_1), \quad (4.7)$$

where in the third line we have used that $f_+(z) = f(z)$ for $z < 1$ and in the last equality I switched integration variable back to x_2 . Now, the only plus distributions that have cropped up thus far have been $\left[\frac{1}{1-z} \right]_+$ and $\left[\frac{\ln(1-z)}{1-z} \right]_+$, so the last integral in Eq. (4.5) can be done analytically to get

$$F(x_1) \equiv \int_0^{\tau/x_1} dz f(z) = \begin{cases} -\ln(1 - \frac{\tau}{x_1}) & \text{if } f(z) = \frac{1}{1-z} \\ -\frac{1}{2} \ln^2(1 - \frac{\tau}{x_1}) & \text{if } f(z) = \frac{\ln(1-z)}{1-z} \end{cases}. \quad (4.8)$$

Together, this reduces the integration over the parton momentum fractions into a 1-dimensional and a 2-dimensional integral, easing the computational power necessary to compute it numerically. Writing the parton level differential cross-sections as

$$\frac{d\hat{\sigma}_{ij}}{dQ^2}(x_1, x_2) = \frac{\hat{\sigma}_c}{x_1 x_2} \left\{ w_{ij}^{\text{rad}}(z) + w_{ij}^{\text{soft}}(z) \delta(1-z) + \sum_f w_{ij}^{f+}(z) f_+(z) \right\}, \quad (4.9)$$

where $\hat{\sigma}_c$ is some common prefactor, we can factor the x_1, x_2 integrals into

$$\begin{aligned}
 \frac{d\sigma}{dQ^2}(Q^2) &= \hat{\sigma}_c \int_\tau^1 \frac{dx_1}{x_1} f_i(x_1) \left\{ f_j(\frac{\tau}{x_1}) \left[w_{ij}^{\text{soft}}(1) - \sum_f w_{ij}^{f+}(1) F(x_1) \right] \right. \\
 &\quad - \sum_f f_j(\frac{\tau}{x_1}) w_{ij}^{f+}(1) \int_{\tau/x_1}^1 \frac{dx_2}{x_2} \frac{\tau}{x_1 x_2} f(\frac{\tau}{x_1 x_2}) \\
 &\quad \left. + \int_{\tau/x_1}^1 \frac{dx_2}{x_2} f_j(x_2) \left[w_{ij}^{\text{rad}}(\frac{\tau}{x_1 x_2}) + \sum_f w_{ij}^{f+}(\frac{\tau}{x_1 x_2}) f(\frac{\tau}{x_1 x_2}) \right] \right\} \quad (4.10)
 \end{aligned}$$

I note that the sum over f used here means a sum over the different plus-distributions that show up in the cross-section.

4.1.3 Renormalised PDFs

As mentioned earlier in Section 3.3.4, there remain collinear divergences in the partonic cross-sections we have calculated thus far. These can be absorbed into the definition of the PDFs through a renormalisation procedure akin to that which is done when renormalising the fields and couplings. Renormalisation conditions can be imposed,

defining the parton distributions in such a way as to produce a finite observable cross-section at a reference energy μ_F called the factorisation scale. The trade-off is that the PDFs inherit scale-dependence as observables are computed at other energy levels. This scale dependence is encapsulated in the DGLAP equations, due to Dokshitzer, Gribov, Lipov, Altarelli and Parisi [43, 44, 42]. Abbreviating the factorisation scale $\mu_F \equiv \mu$, the DGLAP equations for the renormalised distribution PDFs of quarks/gluons $f_{q/g}(x, \mu)$ read¹

$$\mu \frac{d}{d\mu} \begin{pmatrix} f_q(x, \mu) \\ f_g(x, \mu) \end{pmatrix} = \frac{\alpha_s}{\pi} \int_x^1 \frac{d\xi}{\xi} \begin{bmatrix} P_{qq'}(\frac{x}{\xi}) & P_{qg}(\frac{x}{\xi}) \\ P_{gq'}(\frac{x}{\xi}) & P_{gg}(\frac{x}{\xi}) \end{bmatrix} \begin{pmatrix} f_{q'}(\xi, \mu) \\ f_g(\xi, \mu) \end{pmatrix}, \quad (4.11)$$

where $P_{ij}(z)$ are known as the DGLAP splitting functions, or sometimes just the splitting functions, and the sum goes over all quark flavours q' . A heuristic interpretation $P_{ij}(\frac{x}{\xi})$ is that they function in Eq. (4.11) to encapsulate the probability of an incoming parton j with momentum fraction ξ to radiate some energy, leaving parton i with momentum fraction x instead. To leading order, they are given by [14]

$$P_{qq}(z) = C_F \left[\frac{1+z^2}{[1-z]_+} + \frac{3}{2} \delta(1-z) \right], \quad (4.12a)$$

$$P_{qg}(z) = T_F [1 - 2z(1-z)], \quad (4.12b)$$

$$P_{gq}(z) = C_F \left[\frac{z^2 + 2(1-z)}{z} \right], \quad (4.12c)$$

$$P_{gg}(z) = 2C_A \left[\frac{z}{[1-z]_+} + \frac{1-z}{z} + z(1-z) \right] + \frac{\beta_0}{2} \delta(1-z), \quad (4.12d)$$

where $\beta_0 = \frac{11}{3}C_A + \frac{4}{3}T_F n_f$. Here, n_f is the number of light quark flavours, i.e. the quark flavours present in the hadron in question.

Now, let us investigate concretely how the divergences are absorbed, and the scale dependence arises in the PDFs. The idea is that when naively calculating the partonic cross-section, divergences can appear as a consequence of implicitly defining the factorisation between the soft and hard processes as we have. The divergences in the hard scattering cross-section should cancel with soft effects in the hadron. In some sense, the partonic cross-section we have is a *bare* cross-section, and so are the PDFs. Denoting the bare partonic cross-section for partons i, j as $\frac{d\hat{\sigma}_{ij}^{\text{bare}}}{dQ^2}$, we get the renormalised, finite cross-section $\frac{d\hat{\sigma}_{ij}^R}{dQ^2}$ by the rescaling

$$\frac{d\hat{\sigma}_{ij}^{\text{bare}}}{dQ^2}(\eta) = \sum_{kl} \int_0^1 dz_1 \int_0^1 dz_2 Z_{ik}(z_1) Z_{jl}(z_2) \frac{d\hat{\sigma}_{kl}^R}{dQ^2} \left(\frac{\eta}{z_1 z_2} \right), \quad (4.13)$$

where $Z_{ij}(z)$ are transition functions that hold the singular structure of $\frac{d\hat{\sigma}_{ij}^{\text{bare}}}{dQ^2}$ and work akin to the renormalisation constants Z used for the fields and couplings in Section 1.2.3. These transition functions also rescale the PDFs through a convolution, defining the renormalised PDFs as

$$f_i^R(x) = \sum_j \int_0^1 d\xi dz \delta(x - \xi z) f_j^{\text{bare}}(\xi) Z_{ji}(z) = \sum_j \int_x^1 \frac{dz}{z} f_j^{\text{bare}}\left(\frac{x}{z}\right) Z_{ji}(z). \quad (4.14)$$

¹A sum over the quark flavours q' is implied here.

4.1. The Parton Model and PDFs

The non-singular hadronic cross-section is then given by the finite renormalised PDFs and cross-section as

$$\frac{d\sigma}{dQ^2}(\tau) = \sum_{ij} \int_\tau^1 dx_1 \int_{\tau/x_1}^1 dx_2 f_i^R(x_1) f_j^R(x_2) \frac{d\hat{\sigma}_{ij}^R}{dQ^2} \left(\frac{\tau}{x_1 x_2} \right). \quad (4.15)$$

The relation to the bare quantities can be seen by inserting the renormalised PDF definition Eq. (4.14) into Eq. (4.15):

$$\begin{aligned} \frac{d\sigma}{dQ^2}(\tau) &= \sum_{ij} \int_\tau^1 dx_1 \int_{\tau/x_1}^1 dx_2 \sum_{kl} \int_0^1 d\xi_1 dz_1 \delta(x_1 - \xi_1 z_1) Z_{ki}(z_1) f_k^{\text{bare}}(\xi_1) \\ &\quad \times \int_0^1 d\xi_2 dz_2 \delta(x_2 - \xi_2 z_2) Z_{lj}(z_2) f_l^{\text{bare}}(\xi_2) \frac{d\hat{\sigma}_{ij}^R}{dQ^2} \left(\frac{\tau}{x_1 x_2} \right) \\ &= \sum_{ijkl} \int_0^1 d\xi_1 d\xi_2 dz_1 dz_2 Z_{ki}(z_1) Z_{lj}(z_2) f_k^{\text{bare}}(\xi_1) f_l^{\text{bare}}(\xi_2) \\ &\quad \times \frac{d\hat{\sigma}_{ij}^R}{dQ^2} \left(\frac{\tau}{z_1 z_2 \xi_1 \xi_2} \right) \theta(\xi_2 z_2 - \frac{\tau}{\xi_1 z_1}) \theta(\xi_1 z_1 - \tau) \\ &= \sum_{kl} \int_\tau^1 d\xi_1 \int_{\tau/\xi_1}^1 d\xi_2 f_k^{\text{bare}}(\xi_1) f_l^{\text{bare}}(\xi_2) \\ &\quad \times \int_{\tau/(z_1 \xi_2)}^1 dz_1 \int_{\tau/(z_1 \xi_1 \xi_2)}^1 dz_2 \sum_{ij} Z_{ki}(z_1) Z_{lj}(z_2) \frac{d\hat{\sigma}_{kl}^R}{dQ^2} (z_1 z_2 \xi_1 \xi_2 S) \\ &= \sum_{kl} \int_\tau^1 d\xi_1 \int_{\tau/\xi_1}^1 d\xi_2 f_k^{\text{bare}}(\xi_1) f_l^{\text{bare}}(\xi_2) \frac{d\hat{\sigma}_{kl}^{\text{bare}}}{dQ^2} \left(\frac{\tau}{\xi_1 \xi_2} \right), \end{aligned} \quad (4.16)$$

where in the second equality, I changed the order of integration and integrated over $x_{1,2}$. This shows that if we take the partonic cross-section we have worked with so far to be the bare cross-section integrated over bare PDFs in Eq. (4.1), then the restatement Eq. (4.15) with a finite cross-section and finite PDFs is equivalent. In other words, the divergences cancel between the partonic cross-section and the PDFs.

What remains is to find the insertion functions Z_{ij} to get the renormalised, finite quantities. Let us assume that we can expand the bare and renormalised cross-sections and the insertion functions as a power series in $\frac{\alpha_s}{2\pi}$. Furthermore, since the LO cross-section is already finite, we can choose the LO insertion function to be $\delta_{ij}\delta(1-z)$ leaving the LO contribution unchanged.

$$\frac{d\hat{\sigma}_{ij}^{\text{bare}}}{dQ^2}(z) = \sigma_{ij}^{\text{LO}}(z) + \frac{\alpha_s}{2\pi} \sigma_{ij}^{\text{NLO}}(z) + \dots, \quad (4.17a)$$

$$\frac{d\hat{\sigma}_{ij}^R}{dQ^2}(z) = \bar{\sigma}_{ij}^{\text{LO}}(z) + \frac{\alpha_s}{2\pi} \bar{\sigma}_{ij}^{\text{NLO}}(z) + \dots, \quad (4.17b)$$

$$Z_{ij}(z) = \delta_{ij}\delta(1-z) + \frac{\alpha_s}{2\pi} Z_{ij}^{\text{NLO}}(z) + \dots \quad (4.17c)$$

Expanding both sides of Eq. (4.13) we have to NLO

$$\begin{aligned} \sigma_{ij}^{\text{LO}}(\eta) + \frac{\alpha}{2\pi} \sigma_{ij}^{\text{NLO}}(\eta) &= \bar{\sigma}_{ij}^{\text{LO}}(\eta) + \frac{\alpha}{2\pi} \left\{ \bar{\sigma}_{ij}^{\text{NLO}}(\eta) + \sum_l \int_0^1 dz_2 Z_{jl}^{\text{NLO}}(z_2) \bar{\sigma}_{il}^{\text{LO}} \left(\frac{\eta}{z_2} \right) \right. \\ &\quad \left. + \sum_k \int_0^1 dz_1 Z_{ik}^{\text{NLO}}(z_1) \bar{\sigma}_{kj}^{\text{LO}} \left(\frac{\eta}{z_1} \right) \right\}. \end{aligned} \quad (4.18)$$

As anticipated, we see that the renormalised partonic LO cross-section is the same as the bare one. However, the renormalised NLO cross-section is given by

$$\bar{\sigma}_{ij}^{\text{NLO}}(\eta) = \sigma_{ij}^{\text{NLO}}(\eta) - \sum_k \int_0^1 dz \left\{ Z_{jk}^{\text{NLO}}(z) \bar{\sigma}_{ik}^{\text{LO}}\left(\frac{\eta}{z}\right) + Z_{ik}^{\text{NLO}}(z) \bar{\sigma}_{kj}^{\text{LO}}\left(\frac{\eta}{z}\right) \right\}. \quad (4.19)$$

The similarity between the insertion functions and the counterterms in field/coupling renormalisation is more evident here. There are many schemes for defining the insertion functions explicitly, but in this thesis, I will be using the $\overline{\text{MS}}$ scheme, in which they are defined such that they only remove terms proportional to $\frac{1}{\epsilon} = \frac{1}{\epsilon} - \gamma_E - \ln 4\pi$. Choice of scheme affects the PDFs through Eq. (4.14), and as such, care must be taken when using an explicit PDF set defined in a certain renormalisation scheme. In the next chapter, I will be using numerical values for the PDFs taken from LHAPDF [45], where they have been defined in the $\overline{\text{MS}}$ scheme, so it is most convenient to do so here too.

4.2 Total Hadronic Cross-Section Result

We can now put together the results from the previous section to get the full inclusive hadronic cross-section for neutralino pair production to NLO. To leading order, we have the partonic contributions

$$\frac{d\hat{\sigma}_{q\bar{q}}^{\text{LO}}}{dQ^2} = \hat{\sigma}^0 \frac{\delta(1-z)}{\hat{s}}. \quad (4.20)$$

In the language of Eq. (4.9), we can factor out $\hat{\sigma}_c = \hat{\sigma}^0$, leaving

$$w_{q\bar{q}}^{\text{soft}}(z) = \frac{1}{S}, \quad (4.21)$$

to LO. As a reminder, $\hat{\sigma}^0$ is the partonic LO cross-section defined in Eq. (3.46).

Recalling the NLO contribution Eq. (3.121) we have

$$\frac{d\hat{\sigma}_{q\bar{q}}^{\text{NLO}}}{dQ^2} = \frac{d\hat{\sigma}_v^{\text{non-SUSY}}}{dQ^2} + \frac{d\hat{\sigma}_v^{\text{SUSY}}}{dQ^2} + \frac{d\hat{\sigma}_{r,g}}{dQ^2}, \quad (4.22a)$$

$$\frac{d\hat{\sigma}_{qg}^{\text{NLO}}}{dQ^2} = \frac{d\hat{\sigma}_{r,g}}{dQ^2}, \quad (4.22b)$$

$$\frac{d\hat{\sigma}_{\bar{q}g}^{\text{NLO}}}{dQ^2} = \frac{d\hat{\sigma}_{r,\bar{g}}}{dQ^2}. \quad (4.22c)$$

From the explicit expressions for these contributions Eqs. (3.102), (3.104), (3.116)

and (3.120), we can extract the prefactor $\hat{\sigma}_c = \hat{\sigma}^0$ and get the partonic functions²

$$w_{q\bar{q}}^{\text{soft}}(z) = \frac{\alpha_s C_F}{\pi S} P(\epsilon) \left\{ -\frac{3}{2\epsilon} + \frac{\pi^2}{3} - 4 + \tilde{C}_Z'' \right\}, \quad (4.23a)$$

$$w_{q\bar{q}}^{\text{rad}}(z) = -\frac{\alpha_s C_F}{\pi S} P(\epsilon) \frac{(1+z^2) \ln z}{1-z}, \quad (4.23b)$$

$$w_{q\bar{q}}^{1/(1-z)_+} = -\frac{\alpha_s C_F}{\pi S} P(\epsilon) \frac{1}{\epsilon} (1+z^2), \quad (4.23c)$$

$$w_{q\bar{q}}^{(\ln(1-z)/(1-z))_+} = \frac{\alpha_s C_F}{\pi S} P(\epsilon) 2(1+z^2), \quad (4.23d)$$

$$\begin{aligned} w_{qg}^{\text{rad}}(z) &= \frac{\alpha_s T_F}{2\pi S} P(\epsilon) \left\{ -\frac{1}{\epsilon} (1-2z(1-z)) \right. \\ &\quad \left. + \frac{1}{2} (1+6z-7z^2) + (1-2z(1-z)) \ln \frac{(1-z)^2}{z} \right\}, \end{aligned} \quad (4.23e)$$

$$w_{\bar{q}g}^{\text{rad}}(z) = w_{qg}^{\text{rad}}(z). \quad (4.23f)$$

Renormalising the NLO contributions in the $\overline{\text{MS}}$ scheme, we choose the insertion functions such that the $\frac{1}{\epsilon}$ -poles in Eq. (4.23) are removed, together with the canonical $\overline{\text{MS}}$ factors $-\gamma_E + \ln 4\pi$. In practice, when taking the (now non-diverging) limit ϵ we replace $\frac{1}{\epsilon} P(\epsilon) \rightarrow \ln \frac{\mu_F^2}{Q^2}$ and $P(\epsilon) \rightarrow 1$. As a reminder, we had

$$P(\epsilon) = 1 + \left(\ln \frac{\mu_F^2}{Q^2} - \gamma_E + \ln 4\pi - 1 \right) \epsilon + \mathcal{O}(\epsilon^2), \quad (4.24)$$

so there is actually a factor of $-\epsilon$ in $P(\epsilon)$ that is not accounted for in the pole terms in the ordinary $\overline{\text{MS}}$ scheme. These can be removed by redefining the factorisation scale $\mu_F \rightarrow e^{1/2} \mu_F$, which can be seen by inserting into Eq. (4.24). In practice, this is what has been done, and the factorisation scale dependence of the PDFs has been defined accordingly.

Denoting the renormalised partonic cross-section functions with a bar, we get

$$\bar{w}_{q\bar{q}}^{\text{soft}}(z) = \frac{\alpha_s C_F}{\pi} \frac{\hat{\sigma}_B}{S} F_Z'' \left\{ -\frac{3}{2} \ln \frac{\mu_F^2}{Q^2} + \frac{\pi^2}{3} - 4 + \tilde{C}_Z'' \right\}, \quad (4.25a)$$

$$\bar{w}_{q\bar{q}}^{\text{rad}}(z) = -\frac{\alpha_s C_F}{\pi} \frac{\hat{\sigma}_B}{S} F_Z'' \frac{(1+z^2) \ln z}{1-z}, \quad (4.25b)$$

$$\bar{w}_{q\bar{q}}^{1/(1-z)_+} = -\frac{\alpha_s C_F}{\pi} \frac{\hat{\sigma}_B}{S} F_Z'' \ln \frac{\mu_F^2}{Q^2} (1+z^2), \quad (4.25c)$$

$$\bar{w}_{q\bar{q}}^{(\ln(1-z)/(1-z))_+} = \frac{\alpha_s C_F}{\pi} \frac{\hat{\sigma}_B}{S} F_Z'' 2(1+z^2), \quad (4.25d)$$

$$\begin{aligned} \bar{w}_{qg}^{\text{rad}}(z) &= \frac{\alpha_s T_F}{2\pi} \frac{\hat{\sigma}_B}{S} F_Z'' \left\{ -\ln \frac{\mu_F^2}{Q^2} (1-2z(1-z)) \right. \\ &\quad \left. + \frac{1}{2} (1+6z-7z^2) + (1-2z(1-z)) \ln \frac{(1-z)^2}{z} \right\}, \end{aligned} \quad (4.25e)$$

$$\bar{w}_{\bar{q}g}^{\text{rad}}(z) = \bar{w}_{qg}^{\text{rad}}(z). \quad (4.25f)$$

These functions are then inserted into Eq. (4.10) for numeric integration, which I will perform in the next chapter. To get the full, non-differential cross-section, we simply integrate over Q^2 with the integration limits given in Eq. (3.14).

²In the higgsino scenario we assume for these NLO contributions $\hat{\sigma}^0 = \hat{\sigma}_B F_Z''$.

Chapter 5

Numerical Results

In this chapter, I will go give an overview of the numerical implementation of the cross-sections from the earlier chapters. This is an entirely non-trivial process, and I use multiple external packages to do the calculations. Particularly, the numerical integration over the PDFs requires a good deal of finesse. The algorithm used for the integration is the `VEGAS` algorithm [46], implemented in `C++` in the GNU Scientific Library (`GSL`) [47]. The values for the PDFs at a given energy scale μ , along with values for α_s , are taken from the `LHAPDF` package [45]. MSSM and CMSSM particle spectra are generated in `SLHA` file format using `FlexibleSUSY` [48, 49]. To evaluate the Passarino-Veltman loop integrals, I use the package `LoopTools` [39].

The numerical results presented in this chapter are meant to showcase the possibility of parameter space exploration of the full MSSM Lagrangian for the cross-sections calculated in this thesis. To this end, only the expressions for neutralino pair production have been implemented, and will be the focus of this chapter. A proper analysis of the MSSM parameter space as it pertains to electroweakino production, and comparison to experiment at the LHC, is beyond the scope of this thesis.

The implementation of the cross-sections in this thesis have been done in `C++` in the currently unpublished codebase `smoking` [50].

5.1 Setup and Execution

There are a few things that go into setting up and performing the computation of a full cross-section given an MSSM parameter point – I will go briefly over some of these details here. All results are computed with a centre-of-mass energy for the proton collisions set to $\sqrt{S} = 13.6 \text{ GeV}$ to match the LHC run 3.

5.1.1 Renormalisation Scheme

Throughout the thesis, I have mentioned the renormalisation schemes that will be used, but I will take a moment to summarise them here. Masses of all particles are renormalised in the on-shell scheme, as has already been performed for the quarks in Section 3.3.3. Later in this section, I will go through our usage of the spectrum calculator `FlexibleSUSY`, which calculates on-shell renormalised masses for sparticles given an MSSM parameter point. The strong coupling α_s is renormalised in the $\overline{\text{MS}}$ scheme, and its value is calculated at the *renormalisation scale* μ_R . The numerical implementation of the running coupling values for α_s is done in `LHAPDF`, which we also use to evaluate the PDFs.

The scheme for the electromagnetic coupling $\alpha = \frac{e^2}{4\pi}$ is different, however. It is related to the parameters of electroweak symmetry breaking, and needs to be renormalised consistently together with these quantities. In this thesis, I will follow a renormalisation scheme for the electroweak parameters as utilised in [51], named the G_μ -scheme. From the weak coupling g , the hypercharge coupling g' and the Higgs vacuum expectation value v , we have the relations between the parameters of the electroweak sector after symmetry breaking

$$m_W = \frac{1}{2}vg, \quad (5.1a)$$

$$m_Z = \frac{1}{2}v\sqrt{g^2 + g'^2}, \quad (5.1b)$$

$$e = \frac{gg'}{\sqrt{g^2 + g'^2}}, \quad (5.1c)$$

$$\sin \theta_W = \frac{g'}{\sqrt{g^2 + g'^2}}. \quad (5.1d)$$

Keeping the same convention as `Resummino` [52], we will renormalise the W - and Z -boson masses in the on-shell scheme and the coupling strength and vacuum expectation value be fixed by the Fermi constant $G_F \approx 1.16638 \times 10^{-5} \text{ GeV}^{-2}$. This fixes the Weinberg angle and the fine-structure constant by

$$\sin^2 \theta_W = 1 - \frac{m_W^2}{m_Z^2}, \quad (5.2a)$$

$$\alpha = \sqrt{2} \frac{G_F m_W^2 \sin^2 \theta_W}{\pi}. \quad (5.2b)$$

For the α_W we have used in the calculations thus far, we then have

$$\alpha_W = \sqrt{2} \frac{G_F m_W^2}{\pi}. \quad (5.3)$$

This last equality shows the independence of the weak coupling we have used on $\sin \theta_W$, which is a free, running parameter in this scheme. Thereby, the running of this coupling is actually cancelled to two-loop order, according to [51], letting us treat α_W as a constant parameter for our purposes. There are factors of $\cos \theta_W$ and $\sin \theta_W$ that arise in our couplings in Table 2.3, which should receive higher order corrections, but these should be small in the G_μ -scheme. The running of α_s is significantly larger at these energy scales, and will be the primary source of scale uncertainty in the PDFs and NLO contributions.

5.1.2 Uncertainty and Errors

In the context of collider experiments, where collision data is compared to theoretical simulations using cross-sections such as the ones calculated here, uncertainties are important when statistically comparing predictions from different models. To make a proper search of the MSSM parameter space, the uncertainty in the theoretical predictions must be taken into account. These come from various sources; the numerical error from the integration algorithm used, errors in the values of the PDFs at given momentum fractions or factorisation scales, and theoretical uncertainties from truncating the perturbation series before convergence to a ‘true’ value. Most numerical integration methods have good error estimates, and for somewhat well-behaved functions, these will be adequate. As it turns out, the numerical precision is not the leading source

of error in the calculations we will do here. PDF errors are usually dealt with by computing the cross-sections for multiple independent PDF sets, and taking sample averages and variances from the cross-sections computed with the different PDFs. These errors are usually combined with the uncertainty in the strong coupling α_s , as experimentally, it is hard to differentiate the two and determine them accurately individually. Combined error from PDFs and α_s determination will be calculated this way using the PDF4LHC21_40 [53] PDF set, with 43 PDF members, indexed $i = 0, \dots, 42$. The first member gives the central value, and the cross-section computed using this member is regarded as the mean cross-section σ_{central} . Following the PDF error procedure outlined in [53], we compute the PDF error $\delta\sigma_{\text{PDF}}$ as

$$\delta\sigma_{\text{PDF}} = \sqrt{\sum_{i=1}^{42} (\sigma(\text{PDF member } i) - \sigma_{\text{central}})^2}. \quad (5.4)$$

Approximating the uncertainty from higher order corrections to the computation at a finite order is not entirely straight forward. The procedure we will use is to vary the factorisation and renormalisation scales μ_F and μ_R . These scales are artificially introduced into the theory, and should drop out of physical predictions of the full perturbation series. Therefore, we will assume that dependence on these scales should decrease as higher order corrections are taken into account – essentially meaning that the dependence on these scales is somehow proportional to the uncertainty from the truncation of the perturbation series. Concretely, we will use the *scale error* as an estimate for the theoretical uncertainty, which we will define by

$$\delta\sigma_\mu^+ = \max(|\sigma(2\mu) - \sigma(\mu)|, |\sigma(2\mu) - \sigma(\mu)|), \quad (5.5a)$$

$$\delta\sigma_\mu^- = \min(|\sigma(2\mu) - \sigma(\mu)|, |\sigma(2\mu) - \sigma(\mu)|), \quad (5.5b)$$

where μ can either be μ_F , μ_R or both at the same time. What scale we are varying will be noted where relevant.

5.1.3 Spectrum Generation and Scenarios

Going from the Lagrangian parameters of the MSSM to the mass eigenstates and mixing matrices is a non-trivial transition, as we have already seen when discussing the electroweakino mixing in Sections 2.4 and 2.5. Doing this procedure of spectrum generation makes sure that the renormalised parameters are physically cohesive, rather than what is often done when using simplified models where parameters like particle masses or mixing matrix elements are varied irrespective of their origin in the MSSM Lagrangian. In the following, I will present the scenarios that we will use for the numerical results in this chapter.

Benchmark Point

One of the parameter points that I will be using for many of the results is the common benchmark point SPS1a [54]. This is based on the mSUGRA [25] model, with the parameters set to

$$m_0 = 100 \text{ GeV}, \quad m_{1/2} = 250 \text{ GeV}, \quad A_0 = -100 \text{ GeV}, \quad \tan \beta = 10, \quad \text{sgn } \mu = +. \quad (5.6)$$

Here m_0 is a common soft mass for all the sfermions under the assumptions of no flavour violation, $m_{1/2}$ is a common gaugino mass parameter, A_0 is the common trilinear coupling

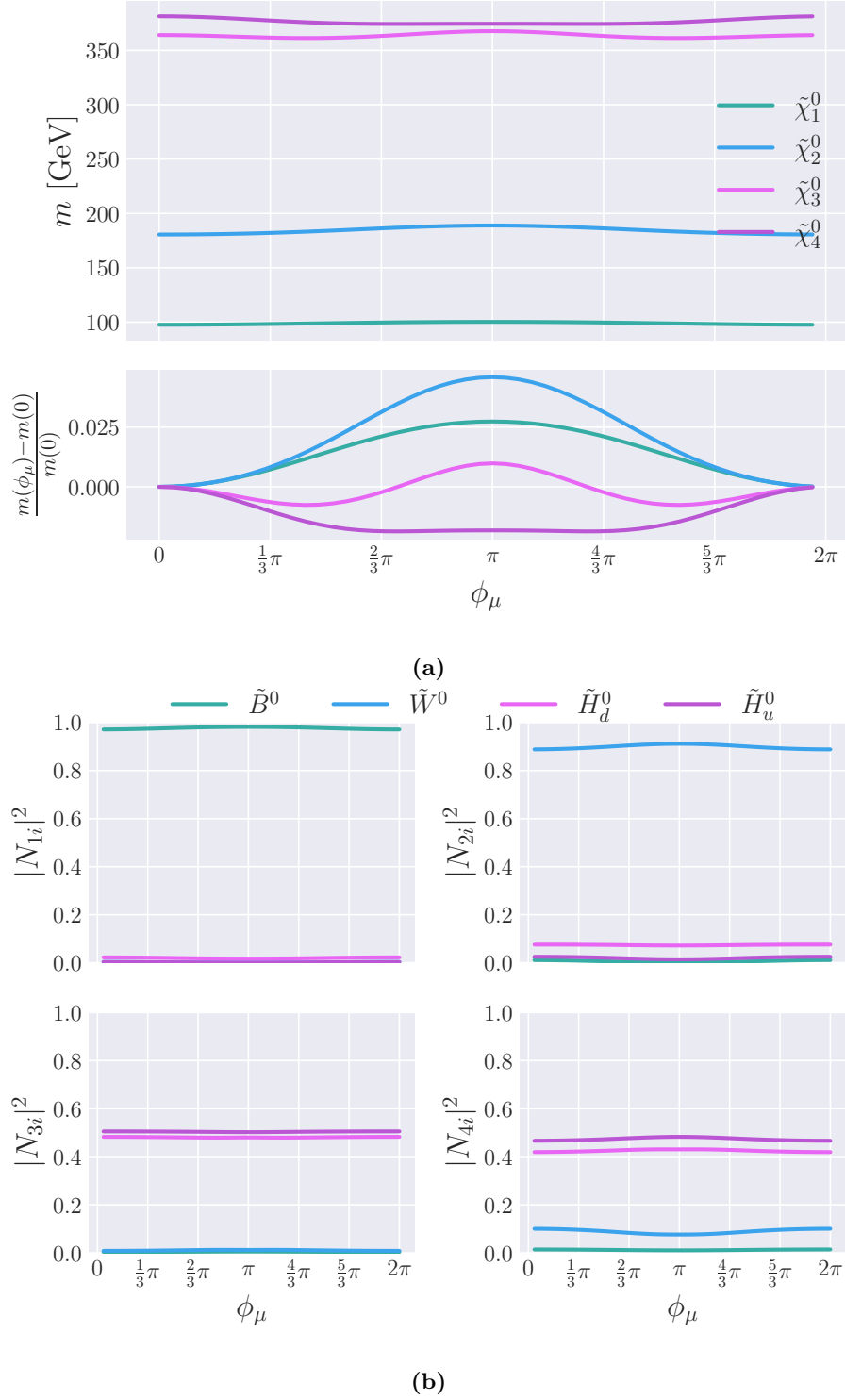


Figure 5.1: A plot showing the neutralino spectrum in the cSPS1a scenario. The first plot shows the neutralino masses as a function of the phase of μ , whereas the lower plot shows the amount of the interaction eigenstates in each neutralino mass eigenstate. The spectra were generated with `FlexibleSUSY`.

under the assumption of no flavour mixing and electroweak symmetry breaking is fixed by the SM parameters together with $\tan \beta = \frac{v_u}{v_d}$ and $\text{sgn } \mu$. The parameters are taken

to be defined at the scale of $m_{1/2} = 250$ GeV, and pole masses and mixing matrices are determined using **FlexibleSUSY** to run the various parameters from this scale.

Based on the SPS1a benchmark point, I will explore a variant where the above parameters are allowed to be complex, and the sign of μ is replaced by an arbitrary complex phase ϕ_μ . For future reference, I will refer to this scenario as complex SPS1a (cSPS1a). This will allow for CP violation in the resulting particle model, and showcases the generality of the calculations from the prior chapters, and implementation thereof. Particularly, I will explore scenarios where the phase of μ is rotated around the complex plane, introducing complex phases in the neutralino mixing matrices, but also slightly complex phases in the squark mixing matrices through the inclusion of loop effects to their mixing matrices. In fact, loop effects in this scenario also make flavour violating mass terms possible, so the general 6×6 squark mixing matrices discussed in Section 2.4.2 are used.

The mass spectrum and mixing of the neutralino sector in the cSPS1a scenario is shown in Fig. 5.1. It shows that the lightest neutralino is very bino-like at a mass of ~ 100 GeV, with the next-to-lightest neutralino being wino in nature at around 180 GeV. The higgsino states mix quite heavily to create two nearly degenerate mass eigenstates at around 375 GeV. Perhaps surprisingly, the gaugino-like lighter neutralino states are affected the most by the phase of the Higgs mass parameter μ , relative to the $\phi_\mu = 0$ case.

Higgsino Scenario

To explore the NLO results that have been calculated, we will need some scenario where two of the neutralino mass eigenstates correspond closely to the pure higgsino states. This is done by separating $|\mu|$ from $|M_1|, |M_2|$, which from a model building perspective is not unnatural, given that no mechanism implies that they should be of the same order of magnitude – μ comes from the supersymmetric part of the Lagrangian, whereas M_1, M_2 as soft masses derived from some supersymmetry breaking mechanism. Mixing between the higgsino and gaugino states will also be suppressed if $|M_1|, |M_2| \gg m_Z$, by looking at the non-diagonal terms in Eq. (2.53), so we will choose a scenario with $|\mu| \ll M_1, M_2$ and $|\mu| \sim m_Z$.

Such a scenario is significant for electroweakino pair production, as it is mediated by a Z -boson in the case of neutralino pairs, W -boson for a neutralino and a chargino, or a Z -boson and photon for chargino pairs, meaning the cross-sections can become relevant at the centre-of-mass energies at the LHC. This is opposed to the production of gaugino-like neutralinos and charginos, which is mediated through the squarks, which can be much heavier than the electroweak bosons, suppressing the cross-sections. The notable exception to this is the pair production of gaugino-like charginos, which is also mediated by the Z -boson and photon.

I will choose a scenario with three different scales: A low scale for the higgsino masses $|\mu| = 100$ GeV, a middle scale for the sfermion and gluino masses at 2000 GeV, and a high scale to decouple the wino and bino mass parameters from the Higgs mass parameter at $M_{1,2} = 100$ TeV. These values are all defined at the high scale, which I will call $M_{\text{SUSY}} = 100$ TeV, and then run down to get pole masses for the individual particles. All parameters except the higgsino mass parameter μ are taken to be real, whereas the phase of μ will be varied.

Scenario	$ \mu $	$\tan \beta$	$M_{1,2}$	M_3	m_0	M_A	A_0	M_{SUSY}
Higgsino	100	10	10^5	2000	2000	2000	1000	10^5

Table 5.1: Summary of MSSM parameters defining the Higgsino scenario used in this thesis. All parameters except $\tan \beta$ are given in GeV. m_0 denotes the common soft mass for all sfermions, taken to be diagonal in flavour space. A_0 is the common soft trilinear coupling, also taken to be diagonal in flavour space. A parametrisation of EWSB is chosen where M_A , the mass of the pseudoscalar Higgs boson, is kept as a free parameter.

Another scenario that will be used for comparison to the LCH SUSY Cross Section Working Group [55] (SXWG) is a simplified Higgsino scenario. This scenario is an unnatural scenario, meaning masses and mixing angles set ‘by hand’. In this scenario the lightest Higgs scalar is set to 125 GeV, whereas all other Higgs scalar and sfermion masses are set to 10^5 GeV. The gluino mass, the two largest neutralino masses and the largest chargino mass are all set to 10^5 GeV as well, effectively decoupling the supersymmetric particle spectrum except for the higgsinos. The two lightest neutralinos and lightest chargino are set to be mass degenerate, with a common mass $m_{\tilde{\chi}}$ which is varied from 100 GeV to 1500 GeV. The two higgsino states are set to be maximally mixed.

5.2 Comparison

To test the verity of our implementation, we first compare to established results. Particularly, we will compare to results obtained using `Resummino` [52]. Two scenarios will be used for comparison: To compare LO contributions, I will use the SPS1a [54] benchmark point, and to compare the NLO implementation of the higgsino channel, I will use the simplified model with two, mass degenerate, maximally mixed higgsinos, and the rest of the supersymmetric particle spectrum decoupled described in the previous subsection. This scenario is taken from [55].

5.2.1 Leading Order Comparison

To compare the LO implementations, I compare results from the `smoking` implementation to that of `Resummino` in the SPS1a benchmark point. All neutralino pair production processes are compared, as to make sure the implementation of Z -boson mediated contribution, squark mediated contribution, and interference between the two, is done correctly. The results, shown in Fig. 5.2, exhibit great agreement between the results. No relative error is above 0.2%, with most staying around 0.17%, which is reasonable up to numerical errors. However, our results seem to be systematically slightly above those of `Resummino`. Had the agreement not been as good, this could be investigated further.

5.2.2 Next-to-Leading Order Comparison

In Fig. 5.3 we see a comparison between results computed with `smoking` as compared to `Resummino` and SXWG to NLO. It shows that our results agree with `Resummino` up to a relative error of $\sim 0.2\%$, and at worst an error of $\sim 1.5\%$ relative to SXWG at high $m_{\tilde{\chi}}$ masses. Disagreement with `Resummino` is within what can be expected by numerical errors. Furthermore, there seems not to be systematic overestimation, as could perhaps be seen in Fig. 5.1. The discrepancies when comparing to SXWG can be accounted for by the fact that the SXWG results are computed using next-to-leading log (NLL)

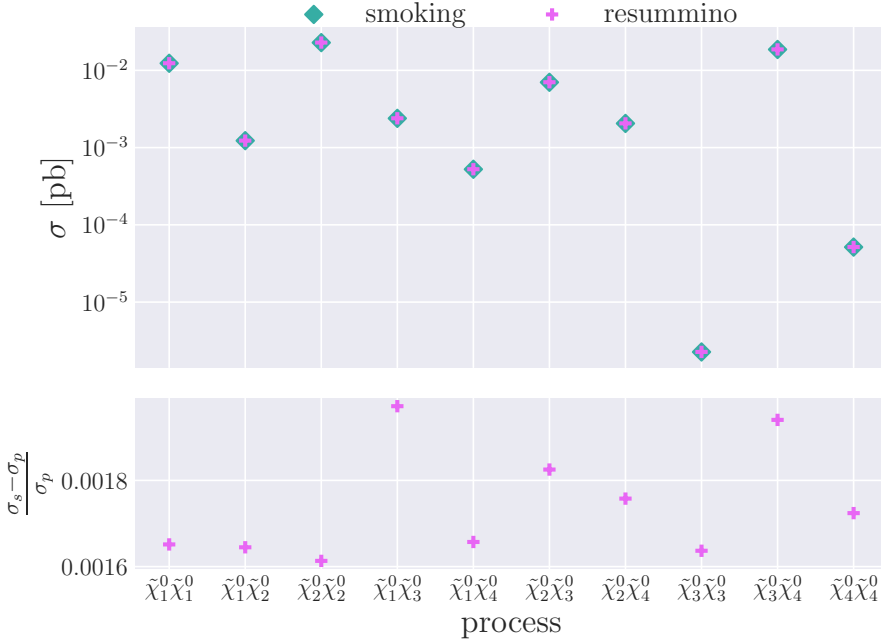


Figure 5.2: Comparison of LO results from this thesis to those from `Resummino` for all possible neutralino pair processes. All cross-sections computed in the SPS1a benchmark point. The cross-sections computed with the implementation from this thesis are denoted σ_s , whereas results computed with `Resummino` are denoted σ_p .

corrections from the resummation of large logarithms together with the NLO results. These corrections are indeed not that large, but do become more relevant at higher neutralino masses. This is because the resummed logarithms give corrections to the soft radiation limit where $Q^2 \rightarrow \hat{s}$. Since Q^2 is bounded from below by $(m_{\tilde{\chi}_i^0} + m_{\tilde{\chi}_j^0})^2$ kinematically, the soft radiation region becomes a larger part of the overall available phase space when the neutralino masses increase. This shows that the NLL effects in this Higgsino scenario is very small, particularly compared to even LO effects of complexification of the parameters, as we shall see promptly.

5.3 Scale Dependence and PDF Errors

In this section, I will explore the errors that go into the cross-section calculations. Particularly, I will focus on PDF errors and scale errors in the LO and NLO contributions in the Higgsino scenario. Nonetheless, much of the discussion applies more broadly.

5.3.1 Scale Dependence

To study the effects of the factorisation and renormalisation scales on the cross-sections, I chose to plot the LO and NLO calculations in the Higgsino scenario with $\phi_\mu = 0$. I varied μ_F and μ_R separately before varying them together, each on the interval $[\frac{1}{8}\mu_0, 8\mu_0]$ where $\mu_0 = (m_{\tilde{\chi}_i^0} + m_{\tilde{\chi}_j^0})/2$. The results are shown in Fig. 5.4.

In the top left plot of Fig. 5.4, we see that the NLO contributions mitigate the factorisation scale dependence on the cross-sections considerably, as we expected from

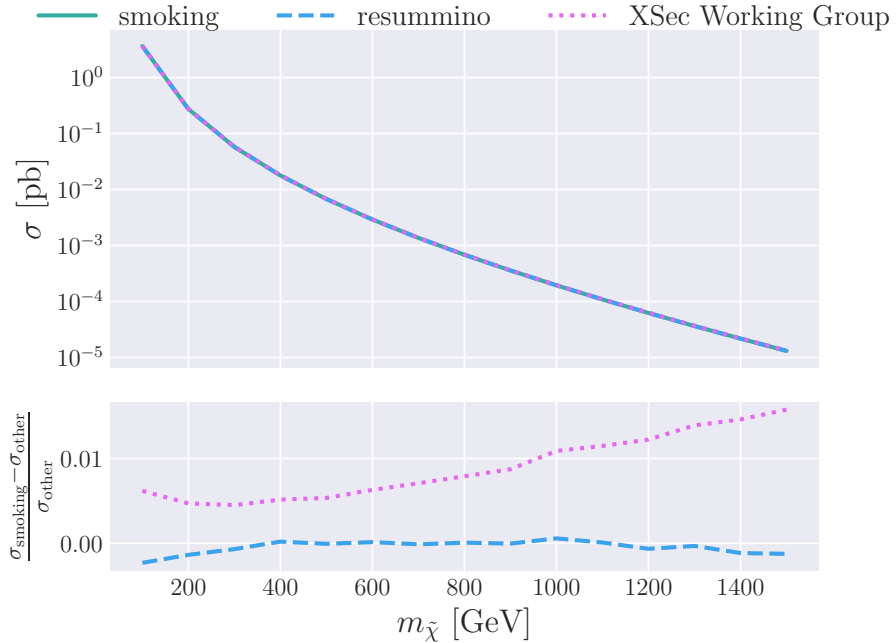


Figure 5.3: Comparison of results from this thesis to those from `Resummino` and the LHC SUSY Cross Section Working Group. Scale error is included in shaded regions around the lines in the upper plot, however, it is so inconsequential as to only be barely visible.

the discussion of renormalised PDFs from Section 4.1.3. The μ_F -dependence is slightly different between the same-type neutralino processes and the different-type neutralino processes, both to LO and NLO, with the overall shape being the same. There is no obvious explanation for why the different-type neutralino process should be more sensitive on the factorisation scale than same-type processes.

As expected, there is no renormalisation scale dependence in the LO cross-section, as the value of α_W is kept fixed in our renormalisation scheme discussed in Section 5.1.1, and there is no μ_R -dependence in the PDFs or kinematics of the LO contributions. However, at NLO the results varies up to $\sim 2.5\%$ up and $\sim 1.5\%$ down. This is mostly due to the change in the value of α_s , which is taken at the value of μ_R when doing the computations. It is worth taking note of the fact that the renormalisation scale dependence is inverse to the factorisation scale, in effect reducing the overall scale dependence when they are varied simultaneously in the bottom plot of Fig. 5.4. This should not necessarily be the case generally, but it is noteworthy that it can happen. The dependence on the renormalisation scale of the different-type neutralino process is different to the same-type processes.

When both scales are varied simultaneously, the overall dependence is somewhat dampened. Notably, the NLO scale dependence is such that the cross-section is heightened for sufficiently high and low values of $\mu = \mu_F = \mu_R$. In practice, this means the theoretical error estimation from the method we use will not have any lower bound below the cross-section value computed with the standard scale μ_0 . In these cases, I will set the lower bound to be that of the cross-section value $\sigma(\mu_0)$.

Finally, a note on estimating the theoretical error by using the scale dependence. At LO in Drell-Yan processes, like the ones we have studied in this thesis, α_s does not enter. This means scale dependence affecting α_s will not affect the cross-section to LO,

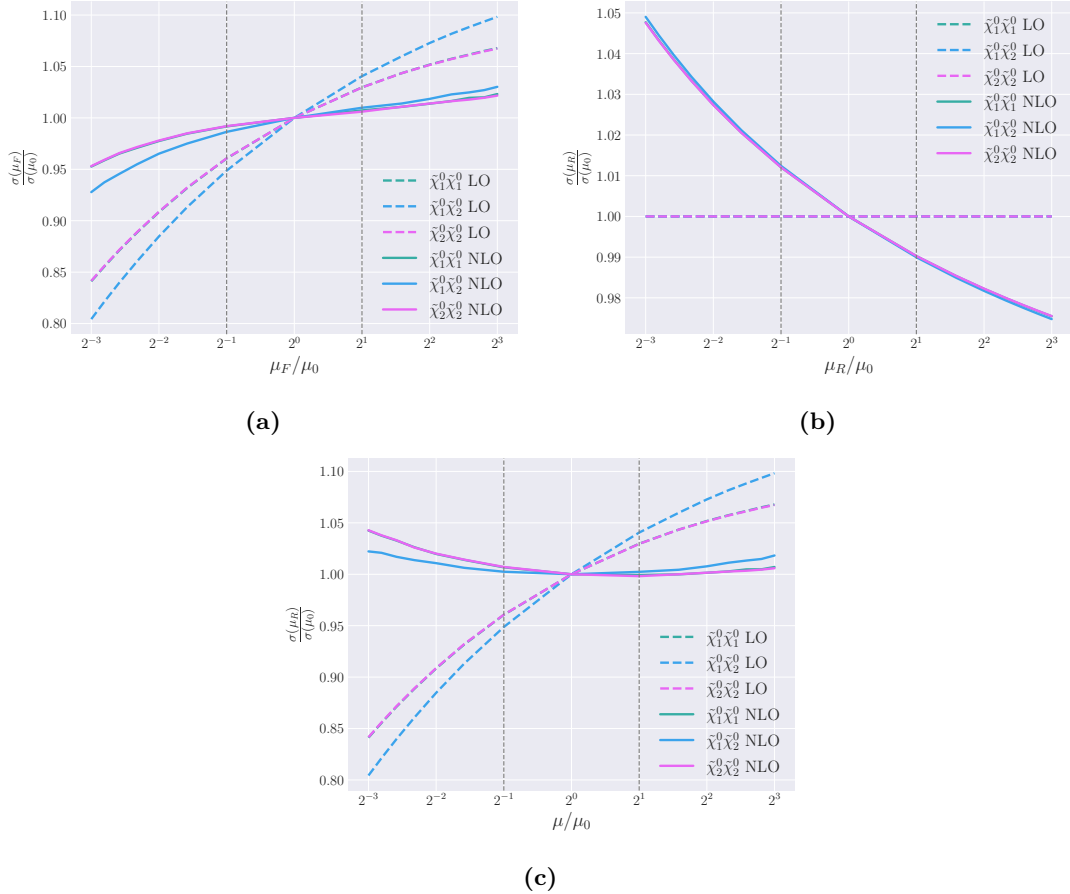


Figure 5.4: Scale dependence of the cross-section for the possible higgsino-like neutralino pairs. The vertical dashed lines indicate the lines for $\mu_0/2$ and $2\mu_0$ used to define the scale error.

and it will not provide any satisfactory estimation of error resulting from the truncation of the perturbation series in α_s . To LO, we are agnostic to the strong interaction, seeing only the perturbation series in α , whereas to NLO we ‘connect’ to another, *different* perturbation series in α_s .

5.3.2 PDF Errors

Fig. 5.5 showcases the PDF and α_s error for pair production of the two lightest neutralinos in the Higgsino scenario to NLO as a function of the Higgs mass parameter $|\mu|$. As μ is the parameter which governs the higgsino masses, this equates to varying the degenerate mass scale of the two lightest neutralinos in the Higgsino scenario. The NLO cross-section is again noticeably greater than the LO cross-section, but the overall mass dependence is similar. A couple of points to make on the PDF errors: First, it is clear that the errors increase relatively to the cross-section quite linearly with the mass of the produced neutralinos. This can be explained by the fact that the PDFs are determined to a much lower precision at high values of parton momentum fraction $x \rightarrow 1$ [53]. When the mass of the final state particles increase, more centre-of-mass energy between the colliding partons is necessary to produce the particles, and as such, higher x -regions of the integral over the PDFs dominate.

The second point to be made is that the PDF uncertainty does not decrease when NLO contributions are taken into account – to the contrary, the NLO uncertainties are

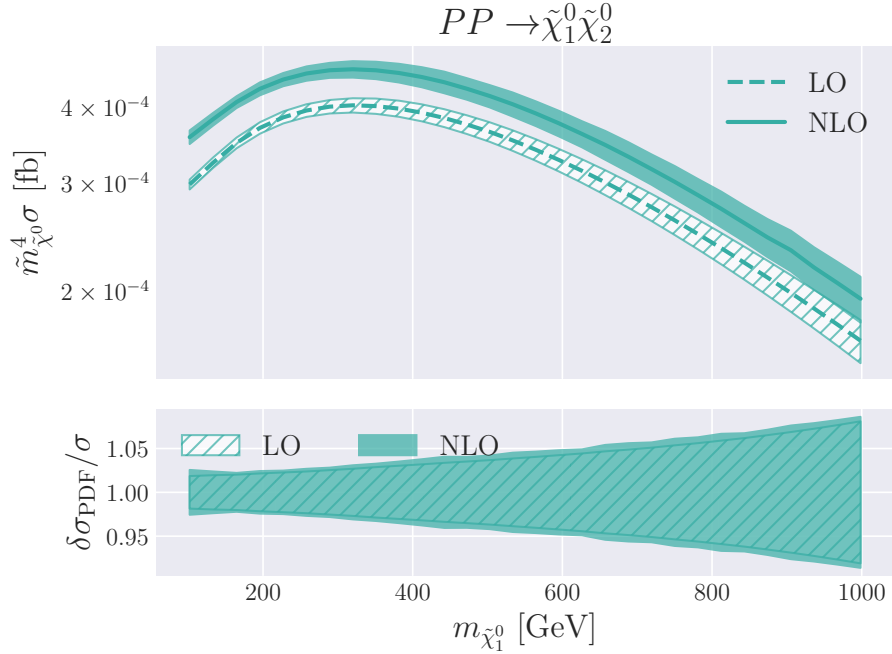


Figure 5.5: Plot of the cross-section for $\tilde{\chi}_1^0 \tilde{\chi}_2^0$ production in the Higgsino scenario with PDF errors added. Denoting the mean mass of the final state pair $m_{\tilde{\chi}^0} = (m_{\tilde{\chi}_1^0} + m_{\tilde{\chi}_2^0})/2$, the scaling of the cross-section is given by the dimensionless quantity $\tilde{m}_{\tilde{\chi}^0} = m_{\tilde{\chi}^0}/\max(m_{\tilde{\chi}^0})$. The mass gap between the two neutralinos $m_{\tilde{\chi}_2^0} - m_{\tilde{\chi}_1^0}$ is never greater than 1.113 GeV.

slightly greater than the LO ones. This could be explained by the fact that the NLO contributions not only depend on the PDFs for the quarks and antiquarks, but also on the PDF of the gluon, as in the quark emission contributions from Section 4.2. The PDF of the gluon is not as precisely determined, particularly in low x -regions, and can thereby add uncertainty to the cross-section.

5.4 Exploring CP-Violation

To explore the CP violating areas of the MSSM parameter space, I have chosen to focus on the phase of the Higgs mass parameter μ . From Fig. 5.1, we can see that all the neutralino masses are affected by the phase of μ , and so to mitigate the effect of the differing masses of the final states as ϕ_μ is varied, I will scale the cross-sections by the average mass of the final state. I chose to scale using $\tilde{m}_{\tilde{\chi}^0}^4$ with a dimensionless scale given by¹

$$\tilde{m}_{\tilde{\chi}^0}(\phi_\mu) = \frac{m_{\tilde{\chi}^0}(\phi_\mu)}{m_{\tilde{\chi}^0}(0)}, \quad (5.7)$$

where $m_{\tilde{\chi}^0}(\phi_\mu)$ is the average final state mass given by

$$m_{\tilde{\chi}^0}(\phi_\mu) = \frac{m_{\tilde{\chi}_i^0}(\phi_\mu) + m_{\tilde{\chi}_j^0}(\phi_\mu)}{2}. \quad (5.8)$$

¹Choosing a power of four here is done because the cross-sections roughly go as $\sigma \sim \frac{1}{m^4}$ where m is the average mass of the final state particles.

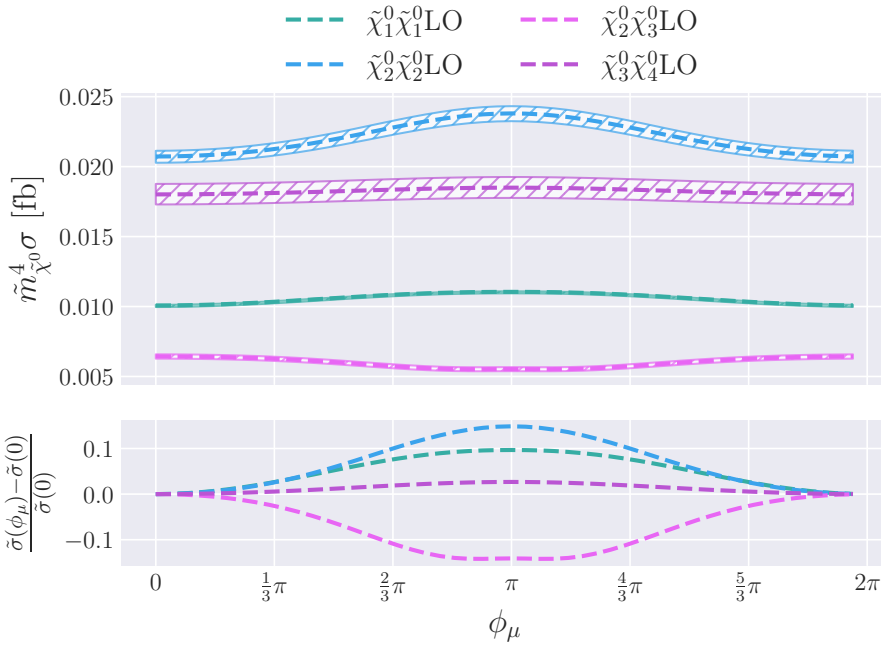


Figure 5.6: The scaled cross-section for various neutralino pair production processes as the phase of μ is varied in the cSPS1a scenario. Underneath, the relative deviance of the scaled cross-sections as the phase moves away from $\phi_\mu = 0$ is shown. Given the average mass of the final state particles $m_{\tilde{\chi}^0} = (m_{\tilde{\chi}_i^0} + m_{\tilde{\chi}_j^0})/2$, the scaling is given by $\tilde{m}_{\tilde{\chi}^0} = m_{\tilde{\chi}^0}(\phi_\mu)/m_{\tilde{\chi}^0}(0)$. This ensures the cross-section for $\phi_\mu = 0$ is unscaled. Scale error is shown with the hatched bands around the lines.

Scale error is included in the plots in this section, calculated by varying μ_F and μ_R together.

5.4.1 cSPS1a scenario

In the cSPS1a scenario, I chose to examine four different neutralino pairs: Same pair production of the bino-like $\tilde{\chi}_1^0$ and wino-like $\tilde{\chi}_2^0$, pair production mixing wino-like and higgsino-like states $\tilde{\chi}_2^0$ and $\tilde{\chi}_3^0$, and pair production of the two different higgsino-like states $\tilde{\chi}_3^0$ and $\tilde{\chi}_4^0$. The results are shown in Fig. 5.6.

Greatest relative effect is seen in the cross-sections for the $\tilde{\chi}_2^0$ pair and $\tilde{\chi}_2^0 \tilde{\chi}_3^0$ pair. This is not unnatural, as variation in the mass of $\tilde{\chi}_2^0$ is greatest from Fig. 5.1, relative to the original mass at $\phi_\mu = 0$. Perhaps more surprisingly, the cross-section for $\tilde{\chi}_2^0$ pair production is greater than that of the lightest neutralino $\tilde{\chi}_1^0$, by about a factor of two. It is worth noting that all cross-sections see the greatest difference in value when $\phi_\mu = \pi$, corresponding with flipping the sign of $|\mu|$. Scale dependence seems largely unaffected by ϕ_μ .

5.4.2 Higgsino Scenario

To explore the effect of the phase of μ on the NLO corrections to the cross-sections, I return to the Higgsino scenario, with $|\mu| = 100$ GeV. Computing just the process of pair production of the two different higgsino states in this scenario, the results are shown in Fig. 5.7.

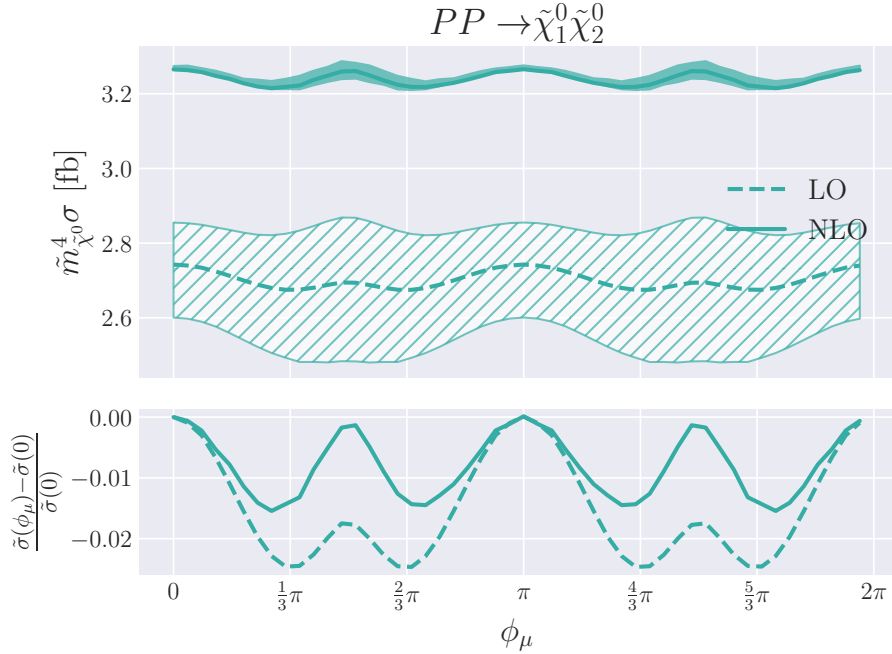


Figure 5.7: The scaled cross-section for neutralino pair production of $\tilde{\chi}_1^0 \tilde{\chi}_2^0$ as the phase of μ is varied in the Higgsino scenario. Underneath, the relative deviance of the scaled cross-sections as the phase moves away from $\phi_\mu = 0$ is shown. Given the average mass of the final state particles $m_{\tilde{\chi}^0} = (m_{\tilde{\chi}_1^0} + m_{\tilde{\chi}_2^0})/2$, the scaling is given by $\tilde{m}_{\tilde{\chi}^0} = m_{\tilde{\chi}^0}(\phi_\mu)/m_{\tilde{\chi}^0}(0)$. This ensures the cross-section for $\phi_\mu = 0$ is unscaled. Scale error is shown with the hatched bands around the lines for the leading order cross-section, and filled bands for the NLO cross-section.

As we have seen earlier, the NLO corrections boost the cross-section quite significantly from the LO result, far exceeding the scale error, as discussed in Section 5.3.1. I note that the scale error decreases by quite a bit in the NLO cross-section, which can be due to the cancellation between μ_F and μ_R errors, again discussed in Section 5.3.1. Furthermore, the ϕ_μ dependence is mitigated as the NLO contributions are taken into account, suggesting that the NLO contributions are not as sensitive to ϕ_μ as the LO contribution, at least in the scenario at hand. This seems reasonable, as the NLO contributions come from strongly interacting particles not directly tied to the Higgs mass parameter μ . The maximal relative deviance from the $\phi_\mu = 0$ cross-sections is near the regions of maximal complex phase of μ , contrary to what we see in Fig. 5.6. In fact, the cross-section seems invariant under a phase shift of $\phi_\mu \rightarrow \phi_\mu + \pi$, corresponding to multiplying μ by -1 .

5.5 Exploring Other Parameters

So far, we have mainly investigated the Higgs mass parameter μ and its phase ϕ_μ . In this section, I will explore variation of these two parameters simultaneously, and dependence on the squark and gluino masses. The squark mass is of particular interest, as it is the mediator of the interaction for producing gaugino-like neutralinos. I also note that all the plots are generated from a ten by ten grid of cross-section values with simple triangulation interpolation applied for visualisation. In general, this is not good practice, however in our case I am simply trying to present an idea of the parameter dependence,

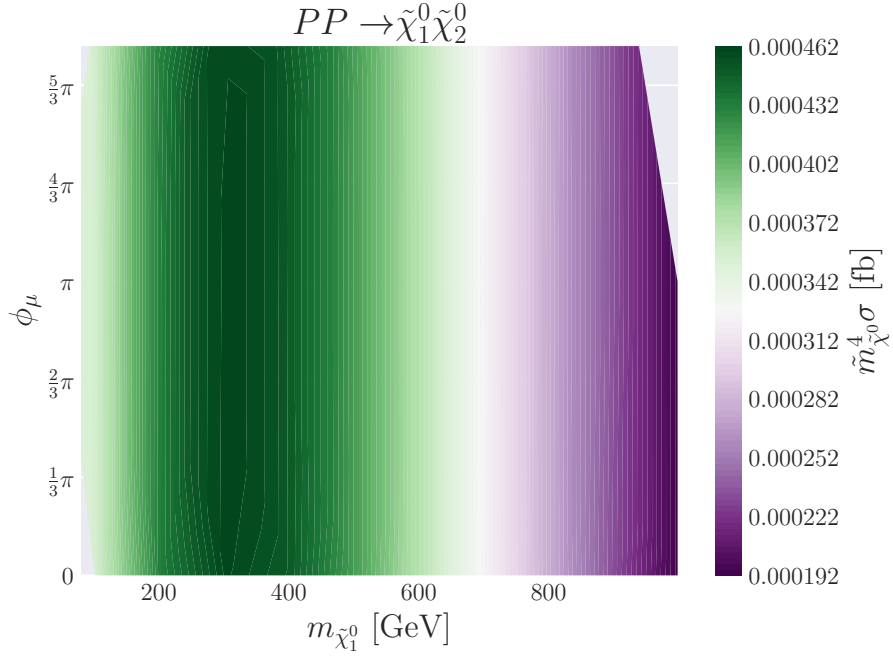


Figure 5.8: Scaled NLO cross-section results for pair production of the two lightest neutralinos in the Higgsino scenario as both $|\mu|$ and ϕ_μ are varied. Given the average mass of the final state particles $m_{\tilde{\chi}^0} = (m_{\tilde{\chi}_1^0} + m_{\tilde{\chi}_2^0})/2$, the scaling is given by $\tilde{m}_{\tilde{\chi}^0} = m_{\tilde{\chi}^0}(\phi_\mu)/m_{\tilde{\chi}^0}(0)$. This ensures the cross-section for $\phi_\mu = 0$ is unscaled.

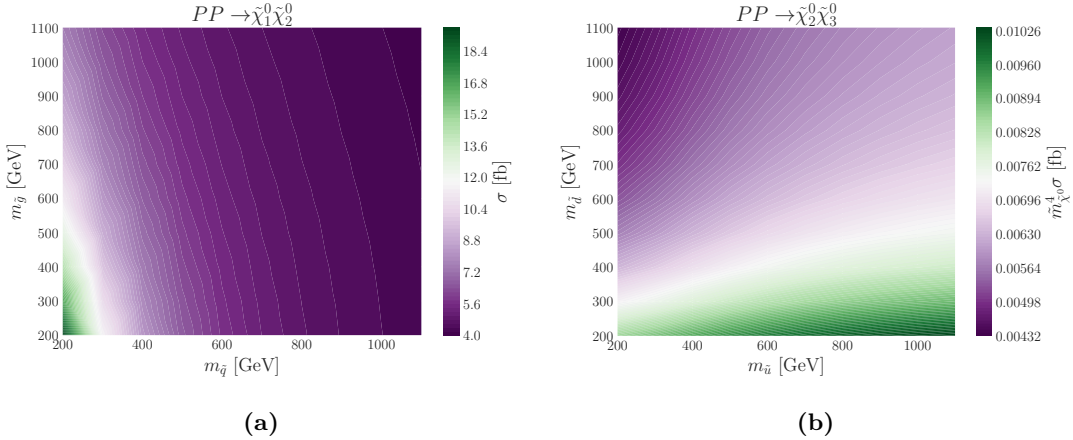


Figure 5.9: (a) Depicts the cross-section for pair production of the two lightest neutralinos to NLO in the simplified Higgsino scenario as the common squark mass and the gluino mass is varied separately.
(b) Depicts the cross-section for neutralino pair production in the cSPS1a scenario as the common up-type and down-type squark masses are varied separately.

rather than rigorous analysis in comparison to experiments.

5.5.1 Varying Higgsino Masses and CP-Violation

The magnitude and phase of the Higgs mass parameter μ were varied together in the Higgsino scenario in Fig. 5.8 to NLO. The cross-sections were scaled according to the

same prescription as in Section 5.4. Along the x -axis, the lightest neutralino mass is shown, but seeing as the two lightest neutralinos are quite mass degenerate in this scenario, the next-to-lightest neutralino mass is not much higher.

The dependence on the higgsino masses seem to have a shape overall similar to the results with $\phi_\mu = 0$ used in Fig. 5.5. In fact, this dependence seems to dominate over the effect of the complex phase of μ .

5.5.2 Varying Squark and Gluino Masses

To vary the squark and gluino masses, I will use slightly different scenarios to the ones I have used thus far, although they will be based on the cSPS1a and Higgsino scenarios. Particularly, I will not generate the particle spectra from MSSM Lagrangian parameters, but rather use the standard cSPS1a scenario with $\phi_\mu = 0$ (which reproduces the SPS1a scenario), and the simplified higgsino scenario from the comparison to SXWG from Section 5.2. When varying this cSPS1a scenario, I will keep all parameters fixed (including the squark mixing angles), while setting all up-type squark masses and down-type squark masses are set to be degenerate respectively. In the simplified higgsino scenario, no mixing between the chiral squark states is assumed, and all the squark masses are set to be the same.

The squark mass $m_{\tilde{q}}$ and gluino mass $m_{\tilde{g}}$ will then be varied separately in these simplified, unnatural scenarios.²

The results can be seen in Fig. 5.9. In the left plot, we can see the simplified Higgsino scenario to NLO, showing that even though no squark or gluino parameters affect the LO cross-section, there is still quite significant sensitivity to them at NLO. Particularly for low squark and gluino masses, the cross-section is enriched quite dramatically as compared to the higher values for these masses. The squark mass seems especially important when computing these effects.

In the right plot, we can see the LO production of the wino-like next-to-lightest neutralino together with the higgsino-like next-to-heaviest neutralino in the cSPS1a scenario. This cross-section is suppressed, as the two different neutralino types do not share a common channel. However, the cross-section is quite dependent on the squark masses, being enriched for low down-type squark masses and high up-type squark masses. This suggests that the up-type squark mediated contributions interfere negatively with the Z -boson mediated and down-type squark mediated contributions, as turning it off seems to increase the contribution.

In the right plot, we can see the production of bino- and wino-like lightest two neutralinos of the cSPS1a scenario to LO. Their production is mediated by the squark, so it is natural to see that the dependence on the squark masses governs the overall cross-section. In fact, the impact of the gluino

²These are unnatural in the sense that the parameters are not cohesive, being derived from a single, physical Lagrangian.

5.5. Exploring Other Parameters

Conclusion

Finally, some concluding remarks on the concepts and results of the previous chapter. In this thesis, I have performed the calculation of pair production of electroweakinos in proton–proton collisions in the context of Large Hadron Collider experiments. Furthermore, next-to-leading order contributions from quantum chromodynamics to higgsino-like neutralino production has been calculated, and implemented numerically, with complete generality in the Minimal Supersymmetric Standard Model (MSSM) parameters of the theory, including charge-parity invariance (CP) violating and quark flavour violating effects from complex and off-diagonal values. This generality extends the current results found in the literature.

A brief summary and outlook on the results are in order. To start, I went over some of the fundaments of quantum field theory as relevant to the calculations I performed. This was done largely by using simple examples, referencing the most important results along the way. Some time was spent developing the notion of the perturbation series and Feynman rules for deriving scattering interactions between particles. Particular detail was given to the interaction of fermions, including Majorana fermions. The foundation of the Standard Model interactions was introduced through Yang-Mills gauge theories, before reviewing the regularisation techniques and renormalisation procedures to be used in this thesis.

Next, I reviewed the building of supersymmetric Quantum Field Theories, specifically detailing the elements used to construct the MSSM. This included introduction of the super-Poincaré group, developing superspace as a vehicle for Lagrangian formulation of manifestly supersymmetric theories. I then developed the Yang-Mills gauge theory in this context, formulating the MSSM as a manifestly supersymmetric mirror to the Standard Model. From there, I derived the Feynman interaction rules for the neutralinos, and generalised them to the chargino interactions. Lastly, I outlined the procedure of deriving the electroweakino particle spectrum from the MSSM Lagrangian parameters, presenting an algorithm for the numerical diagonalisation of the neutralino mass matrix that works for complex Lagrangian parameters.

The parton-level calculation of the cross-sections were then performed symbolically, using self-written **Mathematica** scripts. I started by going through the leading order calculation for neutralino pair production, before generalising the result to any electroweakino pair production process. Next, I showed how the Z -boson mediated higgsino-like contribution to the neutralino pair production can be factorised into two separate processes, simplifying the computation of next-to-leading order contributions from quantum chromodynamics. The calculation of these contributions to the inclusive cross-section of neutral higgsino pairs was then performed, including the effects of real emission of gluons and quarks. These analytic expressions were symbolically compared and verified using **Mathematica** scripts with existing results in the literature. An

assessment was then made of the remaining next-to-leading order contributions to the general neutralino pair production process, outlining the procedure used in Catani-Seymour dipole formalism. The generalisation of the next-to-leading order contributions to the other electroweakino processes was commented on.

The hadron-level cross-section for proton–proton collisions was then calculated. I briefly outlined the parton model and factorisation of the cross-section into a soft part between the partons of a single hadron, and a hard part between the partons the colliding hadrons. The hadron level cross-section in the form of an integral over the parton distribution functions and parton-level cross-sections was then presented. Furthermore, I outlined the procedure of renormalising the parton distribution functions, handling the last remaining divergences in the parton-level cross-sections. The complete result for next-to-leading order neutralino pair production at hadron-level was then shown explicitly.

Finally, I implemented the general hadron-level cross-section for neutralino pair production to next-to-leading order numerically. Generating particle spectra from MSSM parameters using `FlexibleSUSY`, I presented two classes of scenarios, one as a complex, CP-violating extension of the SPS1a benchmark point, and another where we have a hierarchical split between light higgsino-like neutralinos and heavy gaugino-like neutralinos.

Correct calculation and numerical implementation was verified by comparing the results with results computed with `Resummino`. The results from this thesis improves upon `Resummino` by allowing for more general parameter values, specifically complex parameters and more general mixing in the squark sector. Theoretical errors from scale dependence, and PDF errors from uncertainty in parton distribution functions were also explored and presented, creating accurate uncertainties for a potential scan of the parameter space. This included investigating the dependence on both the renormalisation and factorisation scales, showing that the two dependencies can cancel when varied together. In detail, I presented parameter dependence on the complex phase of the Higgs mass parameter μ , neutralino masses, squark masses and gluon mass, showing the potential for the calculations of this thesis to be used in a broader context of parameter scans of the MSSM. This complex phase is not implemented anywhere else in the literature, and I show that it has greater relative effect on leading order cross-sections than higher order corrections such as those from resummation of large logarithms in a Higgsino scenario.

Outlook

Looking forward, there are many avenues are for future exploration possible. An obvious place to start would be to implement the calculations for other electroweakino pairs than the neutralinos numerically, generalising the code for neutralino pair production that is already implemented. Seeing as the next-to-leading order contributions were quite significant in the case of higgsino-like neutralino production, another point of interest would be to do the complete calculation of next-to-leading order contributions, for instance by using the Catani-Seymour formalism briefly presented in this thesis. This would allow for parameter scans where the higgsino-like states and gaugino-like states mix generally, and allow for the computation of the next-to-leading order cross-sections for light gaugino-like states, common in mSUGRA models for instance.

A proper scan of the parameter space is perhaps the most enticing possibility from

this thesis, making a statistical treatment of collision events simulated using the cross-sections from this thesis and comparing to event data from the ATLAS experiments. In doing so, cross-section values for many areas of the parameter space would be useful, and so using machine learning to perform regression on the parameter dependence of the cross-sections, as this can significantly improve the computational time necessary to get cross-section results for analysis.

Appendices

Appendix A

Weyl Spinors & Grassmann Calculus

Here, I present some general properties of Weyl spinors, and define what is meant by derivatives and integration on Grassmann-valued spaces. These definitions were in Chapter 2, particularly in defining superspace and working out Feynman rules from the superlagrangian.

A.1 Weyl Spinors

Weyl spinors are two-component vectors in a representation space of $SL(2, \mathbb{C})$. There are representations of $SL(2, \mathbb{C})$ that form Weyl spinor spaces – the self representation and its complex conjugate. Spinors in the self-representation space of $SL(2, \mathbb{C})$ are referred to as *left-handed* spinors, and spinors in the conjugate representation space as *right-handed*. Each of these vector spaces has a dual-space, which we keep track of by raising and lowering indices. Given a Weyl spinor ψ with components ψ_α in the self-representation space, we can raise its indices using the antisymmetric tensor

$$\epsilon^{\alpha\beta} = \begin{pmatrix} 0 & 1 \\ -1 & 0 \end{pmatrix}. \quad (\text{A.1})$$

To lower the indices, we can use

$$\epsilon_{\alpha\beta} = \begin{pmatrix} 0 & -1 \\ 1 & 0 \end{pmatrix}. \quad (\text{A.2})$$

We can define a vector ψ^\dagger in the conjugate representation by taking the complex conjugate of a vector in the self-representation:

$$\psi_{\dot{\alpha}}^\dagger = (\psi_\alpha)^\dagger, \quad (\text{A.3})$$

where I use dotted indices to indicate components of a vector in the conjugate representation. Contractions of two Weyl spinors ψ and ϕ is defined by

$$(\psi\phi) \equiv \psi^\alpha \phi_\alpha = \epsilon^{\alpha\beta} \psi_\beta \phi_\alpha = \psi_2 \phi_1 - \psi_1 \phi_2, \quad (\text{A.4a})$$

$$(\psi\phi)^\dagger \equiv \psi_{\dot{\alpha}}^\dagger \phi^{\dot{\alpha}\dagger} = \epsilon^{\dot{\alpha}\dot{\beta}} \psi_{\dot{\alpha}}^\dagger \phi^{\dot{\alpha}\dagger} = \psi_1^\dagger \phi_2^\dagger - \psi_2^\dagger \phi_1^\dagger. \quad (\text{A.4b})$$

For Grassmann-valued Weyl spinors, the components anti-commute. This implies

$$\psi^2 \equiv (\psi\psi) = -\psi_1 \psi_2. \quad (\text{A.5})$$

Some useful relations for Grassmann-valued Weyl spinors ψ, η, ϕ are

$$\eta\psi = \psi\eta, \quad (\text{A.6a})$$

$$\bar{\eta}\bar{\psi} = \bar{\psi}\bar{\eta}, \quad (\text{A.6b})$$

$$(\eta\psi)^\dagger = \bar{\psi}\bar{\eta}, \quad (\text{A.6c})$$

$$(\eta\psi)(\eta\phi) = -\frac{1}{2}(\eta\eta)(\psi\phi), \quad (\text{A.6d})$$

$$\eta\sigma^\mu\bar{\psi} = -\bar{\psi}\bar{\sigma}^\mu\eta, \quad (\text{A.6e})$$

$$(\sigma^\mu\bar{\eta})_\alpha(\eta\sigma^\nu\bar{\eta}) = \frac{1}{2}g^{\mu\nu}\eta_\alpha(\bar{\eta}\bar{\eta}), \quad (\text{A.6f})$$

$$(\eta\sigma^\mu\bar{\eta})(\eta\sigma^\nu\bar{\eta}) = \frac{1}{2}g^{\mu\nu}(\eta\eta)(\bar{\eta}\bar{\eta}), \quad (\text{A.6g})$$

$$(\eta\sigma^\mu\partial_\mu\bar{\psi})(\eta\psi) = -\frac{1}{2}(\psi\sigma^\mu\partial_\mu\bar{\psi})(\eta\eta), \quad (\text{A.6h})$$

$$(\partial_\mu\sigma^\mu\bar{\eta})(\bar{\eta}\bar{\psi}) = -\frac{1}{2}(\partial_\mu\psi\sigma^\mu\bar{\psi})(\bar{\eta}\bar{\eta}), \quad (\text{A.6i})$$

$$(\bar{\eta}\bar{\psi})(\eta\sigma^\mu\bar{\eta})(\eta\psi) = \frac{1}{4}(\eta\eta)(\bar{\eta}\bar{\eta})(\psi\sigma^\mu\bar{\psi}), \quad (\text{A.6j})$$

$$\eta\sigma^{\mu\nu}\psi = -\psi\sigma^{\mu\nu}\eta, \quad (\text{A.6k})$$

where $\sigma^\mu = (\mathbb{I}, \sigma^i)$, $\bar{\sigma}^\mu = (\mathbb{I}, -\sigma^i)$, $\sigma^{\mu\nu} = \frac{i}{4}(\sigma^\mu\bar{\sigma}^\nu - \sigma^\nu\bar{\sigma}^\mu)$, and σ^i are the Pauli matrices given by

$$\sigma^1 = \begin{pmatrix} 0 & 1 \\ 1 & 0 \end{pmatrix}, \quad (\text{A.7a})$$

$$\sigma^2 = \begin{pmatrix} 0 & -i \\ i & 0 \end{pmatrix}, \quad (\text{A.7b})$$

$$\sigma^3 = \begin{pmatrix} 1 & 0 \\ 0 & -1 \end{pmatrix}. \quad (\text{A.7c})$$

Dirac Spinors

We can construct Dirac spinors from the Weyl spinors by stacking a left- and a right-handed Weyl spinor into a four-component spinor. Given a two left-handed Weyl-spinors ψ_L and ψ_R , we can construct a Dirac spinor Ψ as

$$\Psi = \begin{pmatrix} \psi_L \\ \psi_R^\dagger \end{pmatrix}, \quad (\text{A.8})$$

with a conjugate spinor defined as

$$\bar{\Psi} = \Psi^\dagger\gamma^0 = \begin{pmatrix} \psi_R \\ \psi_L^\dagger \end{pmatrix}. \quad (\text{A.9})$$

Here I have used the zeroth gamma matrix. For reference, in the Weyl representation of Dirac spinors used here these are defined as

$$\gamma^\mu = \begin{pmatrix} 0 & \sigma^\mu \\ \bar{\sigma}^\mu & 0 \end{pmatrix}. \quad (\text{A.10})$$

A basis for operators on Dirac spinors space is

$$\Gamma^r = \left\{ \mathbb{I}, \gamma^5, \gamma^\mu, \gamma^\mu \gamma^5, \gamma^{\mu\nu} \right\}, \quad (\text{A.11})$$

where $\gamma^5 = i\gamma^0\gamma^1\gamma^2\gamma^3$ and

$$\gamma^{\mu\nu} = \frac{i}{2}(\gamma^\mu\gamma^\nu - \gamma^\nu\gamma^\mu). \quad (\text{A.12})$$

I also give the charge conjugation matrices, defined with the properties

$$C^{-1} = C^\dagger, \quad (\text{A.13a})$$

$$C^T = -C, \quad (\text{A.13b})$$

and work on an arbitrary operator on Dirac spinor space in the following way

$$C\Gamma_r^T C^{-1} = \eta_r \Gamma_r, \quad \eta_r = \begin{cases} 1 & \text{for } \mathbb{I}, \gamma^5, \gamma_\mu \gamma^5 \\ -1 & \text{for } \gamma_\mu, \gamma_{\mu\nu} \end{cases}. \quad (\text{A.14})$$

A.2 Grassmann Calculus

Here I present the calculus of two-component Grassmann valued Weyl spinors θ_α . Grassmann number are defined such that they anticommute. For two Grassmann number θ and η we have

$$\theta\eta = -\eta\theta, \quad (\text{A.15})$$

implying $\theta^2 = \eta^2 = 0$. This in turn means that a function $f(\theta)$ can be expanded in full as

$$f(\theta) = a_0 + a_1\theta, \quad (\text{A.16})$$

for some coefficient real-valued (or potential complex-valued) coefficients a_0, a_1 . This is seen by a Taylor expansion of f around $\theta = 0$.¹

Integration is defined a kind of projection operator, defining

$$\int d\theta \equiv 0, \quad \int d\theta \theta \equiv 1, \quad (\text{A.17})$$

we have

$$\int d\theta f(\theta) = a_1, \quad (\text{A.18a})$$

$$\int d\theta \theta f(\theta) = a_0. \quad (\text{A.18b})$$

If we define derivation with respect to a Grassmann variable θ as

$$\frac{d\eta}{d\theta} \equiv 0, \quad \frac{d\theta}{d\theta} \equiv 1, \quad (\text{A.19})$$

we get that it will work similarly to integration in that

$$\frac{d}{d\theta} f(\theta) = a_1 = \int d\theta f(\theta). \quad (\text{A.20})$$

¹0 is trivially a Grassmann number too.

Appendix A. Weyl Spinors & Grassmann Calculus

Expanding this to the four Grassmann variable in superspace, $\theta_\alpha, \theta_{\dot{\alpha}}$, we define the integration measures

$$d^2\theta \equiv -\frac{1}{4}d\theta^\alpha d\theta_\alpha, \quad (\text{A.21a})$$

$$d^2\theta^\dagger \equiv -\frac{1}{4}d\theta_{\dot{\alpha}}^\dagger d\theta^{\dagger\dot{\alpha}}, \quad (\text{A.21b})$$

$$d^4\theta \equiv d^2\theta d^2\theta^\dagger, \quad (\text{A.21c})$$

such that we have

$$\int d^2\theta (\theta\theta) = 1, \quad (\text{A.22a})$$

$$\int d^2\theta^\dagger (\theta\theta)^\dagger = 1, \quad (\text{A.22b})$$

$$\int d^4\theta (\theta\theta)(\theta\theta)^\dagger = 1. \quad (\text{A.22c})$$

Appendix B

Takagi Factorisation Algorithm

Here, I go through the proofs necessary for the procedure defined in Section 2.5 to find the Takagi diagonalising matrix U s.t. for a complex, symmetric matrix

$$A = U^T A U. \quad (\text{B.1})$$

B.1 Proofs

The Takagi vector. For any $A \in M_n(\mathbb{C})$ such that AA^* only has real, non-negative eigenvalues, there exists a non-zero vector $\mathbf{v} \in \mathbb{C}^n$ such that $A\mathbf{v}^* = \sigma\mathbf{v}$, where σ is a real, non-negative number.

Proof. Consider a vector $\mathbf{x} \neq \mathbf{0} \in \mathbb{C}^n$ that is an eigenvector of AA^* with corresponding eigenvalue λ . There are two cases:

- (a) $A\mathbf{x}^*$ and \mathbf{x} are linearly dependent.
- (b) $A\mathbf{x}^*$ and \mathbf{x} are linearly independent.

In case (a), we must have that $A\mathbf{x}^* = \mu\mathbf{x}$ for some $\mu \in \mathbb{C}$, since they are linearly dependent. Then $AA^*\mathbf{x} = A\mu^*\mathbf{x}^* = |\mu|^2\mathbf{x} \equiv \lambda\mathbf{x}$, which is non-negative by definition.

In case (b), the vector $\mathbf{y} = A\mathbf{x}^* + \mu\mathbf{x}$ is non-zero for any $\mu \in \mathbb{C}$, since $A\mathbf{x}^*$ and \mathbf{x} are linearly independent. Then we can choose μ such that $|\mu|^2 = \lambda$ to get that $A\mathbf{y}^* = A(A^*\mathbf{x} + \mu^*\mathbf{x}^*) = \lambda\mathbf{x} + \mu^*A\mathbf{x}^* = \mu\mu^*\mathbf{x} + \mu^*A\mathbf{x}^* = \mu^*(A\mathbf{x}^* + \mu\mathbf{x}) = \mu^*\mathbf{y}$.

As such, we can always find a vector $\tilde{\mathbf{v}} \in \mathbb{C}^n$ such that $A\tilde{\mathbf{v}}^* = \mu\tilde{\mathbf{v}}$ for some $\mu \in \mathbb{C}^n$. Furthermore, we can define a vector $\mathbf{v} = e^{i\theta}\tilde{\mathbf{v}}$ for a $\theta \in \mathbb{R}$ to get $A\mathbf{v}^* = A(e^{i\theta}\tilde{\mathbf{v}})^* = e^{-i\theta}A\tilde{\mathbf{v}}^* = e^{-i\theta}\mu\tilde{\mathbf{v}} = e^{-2i\theta}\mu e^{i\theta}\tilde{\mathbf{v}} = e^{-2i\theta}\mu\mathbf{v} \equiv \sigma\mathbf{v}$. This allows us to choose the phase of $\sigma = e^{-2i\theta}\mu$ to be such that σ is real and non-negative.

Eigenvalues of AA^* for symmetric A . Given an $N \times N$ complex matrix A , the eigenvalues of AA^* are always real and non-negative.

Proof. Consider $\mathbf{x} \neq \mathbf{0}$ an eigenvector of AA^* with corresponding eigenvalue λ . Then we must have that

$$\lambda\mathbf{x}^\dagger\mathbf{x} = \mathbf{x}^\dagger AA^*\mathbf{x} = (A^\dagger\mathbf{x})^\dagger (A^*\mathbf{x}) = (A^*\mathbf{x})^\dagger (A^*\mathbf{x}),$$

where we have used that $A^\dagger = (A^T)^* = A^*$. This means that $\lambda \geq 0$, since for any vector $\mathbf{v} \in \mathbb{C}^n$ we have that $\mathbf{v}^\dagger\mathbf{v} \geq 0$. As this holds for all eigenvectors \mathbf{x} of AA^* , all its eigenvalues must be non-negative.

Diagonalisation step of a symmetric matrix A . For any symmetric matrix $A \in M_n(\mathbb{C})$, there exist a unitary matrix $V \in M_n(\mathbb{C})$ such that

$$V^\dagger A V^* = \begin{pmatrix} \sigma & \mathbf{0} \\ \mathbf{0} & A_2 \end{pmatrix},$$

where σ is a real, non-negative number and $A_2 \in M_{n-1}(\mathbb{C})$ is also a symmetric matrix. *Proof.* Consider a normalised Takagi vector $\mathbf{v} \neq \mathbf{0}$ of A such that $A\mathbf{v}^* = \sigma\mathbf{v}$ for some real, non-negative σ and $\mathbf{v}^\dagger \mathbf{v} = 1$. We can then complete an orthonormal basis for \mathbb{C}^n with unit vectors \mathbf{v}_i where $i \in 1, \dots, n$, where we define $\mathbf{v}_1 \equiv \mathbf{v}$. Defining a unitary matrix $V = [\mathbf{v}_1, \dots, \mathbf{v}_n]$, the first column of the product

$$(V^\dagger A V^*)_{i1} = \mathbf{v}_i^\dagger A \mathbf{v}^* = \mathbf{v}_i^\dagger \sigma \mathbf{v} = \sigma \delta_{i1},$$

where δ_{ij} is the Kronecker delta symbol, and we have used the Takagi property of \mathbf{v} and the orthonormality of $\mathbf{v}_i^\dagger \mathbf{v}_j$. This means only the first component of the first column of $V^\dagger A V^*$ is non-zero, and has value σ . Now since A is symmetric, we have that $(V^\dagger A V^*)^T = V^\dagger A^T V^* = V^\dagger A V^*$ must also be symmetric, and thus must have the form

$$V^\dagger A V^* = \begin{pmatrix} \sigma & \mathbf{0} \\ \mathbf{0} & A_2 \end{pmatrix},$$

for a symmetric $A_2 \in M_{n-1}(\mathbb{C})$.

Bibliography

- [1] G. Gabrielse, D. Hanneke, T. Kinoshita, M. Nio, and B. C. Odom, *New Determination of the Fine Structure Constant from the Electron g Value and QED*, *Phys. Rev. Lett.* **97** (2006) 030802. [Erratum: Phys.Rev.Lett. 99, 039902 (2007)].
- [2] C.-N. Yang and R. L. Mills, *Conservation of Isotopic Spin and Isotopic Gauge Invariance*, *Phys. Rev.* **96** (1954) 191–195.
- [3] P. W. Higgs, *Broken Symmetries and the Masses of Gauge Bosons*, *Phys. Rev. Lett.* **13** (1964) 508–509.
- [4] S. Weinberg, *Implications of Dynamical Symmetry Breaking*, *Phys. Rev. D* **13** (1976) 974–996. [Addendum: Phys.Rev.D 19, 1277–1280 (1979)].
- [5] E. Gildener, *Gauge Symmetry Hierarchies*, *Phys. Rev. D* **14** (1976) 1667.
- [6] A. D. Sakharov, *Violation of CP Invariance, C asymmetry, and baryon asymmetry of the universe*, *Pisma Zh. Eksp. Teor. Fiz.* **5** (1967) 32–35.
- [7] N. Cabibbo, *Unitary Symmetry and Leptonic Decays*, *Phys. Rev. Lett.* **10** (1963) 531–533.
- [8] M. Kobayashi and T. Maskawa, *CP Violation in the Renormalizable Theory of Weak Interaction*, *Prog. Theor. Phys.* **49** (1973) 652–657.
- [9] M. B. Gavela, P. Hernandez, J. Orloff, and O. Pene, *Standard model baryogenesis*, in *29th Rencontres de Moriond: Electroweak Interactions and Unified Theories* (1994) 401–410, [[hep-ph/9407403](#)].
- [10] G. Jungman, M. Kamionkowski, and K. Griest, *Supersymmetric dark matter*, *Phys. Rept.* **267** (1996) 195–373, [[hep-ph/9506380](#)].
- [11] J. R. Ellis, *Supersymmetry and grand unification*, in *17th International Symposium on Lepton Photon Interactions* (1995) 0170–203, [[hep-ph/9512335](#)].
- [12] J. de Swart, G. Bertone, and J. van Dongen, *How Dark Matter Came to Matter*, *Nature Astron.* **1** (2017) 0059, [[arXiv:1703.00013](#)].
- [13] D. J. Gross and F. Wilczek, *Ultraviolet Behavior of Nonabelian Gauge Theories*, *Phys. Rev. Lett.* **30** (1973) 1343–1346.
- [14] M. D. Schwartz, *Quantum Field Theory and the Standard Model*. Cambridge University Press, 2014.
- [15] H. Lehmann, K. Symanzik, and W. Zimmermann, *Zur Formulierung quantisierter Feldtheorien*, *Nuovo Cimento* **1** (1955) 205–25.

Bibliography

- [16] M. E. Peskin and D. V. Schroeder, *An Introduction to quantum field theory*. Addison-Wesley, Reading, USA, 1995.
- [17] A. Denner, H. Eck, O. Hahn, and J. Kublbeck, *Feynman rules for fermion number violating interactions*, *Nucl. Phys. B* **387** (1992) 467–481.
- [18] J. Collins, *Foundations of Perturbative QCD*, vol. 32 of *Cambridge Monographs on Particle Physics, Nuclear Physics and Cosmology*. Cambridge University Press, 2023.
- [19] G. Passarino and M. J. G. Veltman, *One Loop Corrections for $e+ e-$ - Annihilation Into $\mu+$ $\mu-$ in the Weinberg Model*, *Nucl. Phys. B* **160** (1979) 151–207.
- [20] H. J. W. Müller-Kirsten and A. Wiedemann, *Introduction to Supersymmetry*. World Scientific, 2nd ed., 2010.
- [21] S. P. Martin, *A Supersymmetry primer*, *Adv. Ser. Direct. High Energy Phys.* **18** (1998) 1–98, [[hep-ph/9709356](#)].
- [22] ATLAS: G. Aad *et. al.*, *Search for direct production of electroweakinos in final states with one lepton, jets and missing transverse momentum in pp collisions at $\sqrt{s} = 13$ TeV with the ATLAS detector*, *JHEP* **12** (2023) 167, [[arXiv:2310.08171](#)].
- [23] ATLAS: G. Aad *et. al.*, *Search for pair production of higgsinos in events with two Higgs bosons and missing transverse momentum in $\sqrt{s} = 13$ TeV pp collisions at the ATLAS experiment*, [arXiv:2401.14922](#).
- [24] A. Djouadi, S. Rosier-Lees, *et. al.*, *The Minimal Supersymmetric Standard Model: Group Summary Report*, 1999.
- [25] A. H. Chamseddine, R. Arnowitt, and P. Nath, *Locally Supersymmetric Grand Unification*, *Phys. Rev. Lett.* **49** (1982) 970–974.
- [26] P. Z. Skands *et. al.*, *SUSY Les Houches accord: Interfacing SUSY spectrum calculators, decay packages, and event generators*, *JHEP* **07** (2004) 036, [[hep-ph/0311123](#)].
- [27] B. Allanach, C. Balázs, *et. al.*, *SUSY Les Houches Accord 2*, *Computer Physics Communications* **180** (2009) 825.
- [28] H. E. Haber and G. L. Kane, *The Search for Supersymmetry: Probing Physics Beyond the Standard Model*, *Phys. Rept.* **117** (1985) 75–263.
- [29] L. Autonne, *Sur les matrices hypohermitiennes et sur les matrices unitaires*. Annales de l’Université de Lyon. A. Rey, 1915.
- [30] T. Takagi, *On an Algebraic Problem Reluted to an Analytic Theorem of Carathéodory and Fejér and on an Allied Theorem of Landau*, *Japanese journal of mathematics :transactions and abstracts* **1** (1924) 83–93.
- [31] R. A. Horn and C. R. Johnson, *Matrix Analysis*. Cambridge University Press, 1990.
- [32] W. R. Inc., “Mathematica, Version 14.0.” Champaign, IL, 2024.

- [33] J. Debove, B. Fuks, and M. Klasen, *Threshold resummation for gaugino pair production at hadron colliders*, *Nucl. Phys. B* **842** (2011) 51–85, [[arXiv:1005.2909](#)].
- [34] M. Demirci and A. I. Ahmadov, *Search for neutralino pair production at the CERN LHC*, *Phys. Rev. D* **89** (2014) 075015, [[arXiv:1404.0550](#)].
- [35] R. Mertig, M. Bohm, and A. Denner, *FENY CALC: Computer algebraic calculation of Feynman amplitudes*, *Comput. Phys. Commun.* **64** (1991) 345–359.
- [36] V. Shtabovenko, R. Mertig, and F. Orellana, *New Developments in FeynCalc 9.0*, *Comput. Phys. Commun.* **207** (2016) 432–444, [[arXiv:1601.01167](#)].
- [37] V. Shtabovenko, R. Mertig, and F. Orellana, *FeynCalc 9.3: New features and improvements*, *Comput. Phys. Commun.* **256** (2020) 107478, [[arXiv:2001.04407](#)].
- [38] V. Shtabovenko, R. Mertig, and F. Orellana, *FeynCalc 10: Do multiloop integrals dream of computer codes?*, [arXiv:2312.14089](#).
- [39] T. Hahn and M. Perez-Victoria, *Automatized one loop calculations in four-dimensions and D-dimensions*, *Comput. Phys. Commun.* **118** (1999) 153–165, [[hep-ph/9807565](#)].
- [40] J. A. Aguilar-Saavedra *et. al.*, *Supersymmetry parameter analysis: SPA convention and project*, *Eur. Phys. J. C* **46** (2006) 43–60, [[hep-ph/0511344](#)].
- [41] S. Catani and M. H. Seymour, *A General algorithm for calculating jet cross-sections in NLO QCD*, *Nucl. Phys. B* **485** (1997) 291–419, [[hep-ph/9605323](#)]. [Erratum: Nucl.Phys.B 510, 503–504 (1998)].
- [42] G. Altarelli and G. Parisi, *Asymptotic Freedom in Parton Language*, *Nucl. Phys. B* **126** (1977) 298–318.
- [43] Y. L. Dokshitzer, *Calculation of the Structure Functions for Deep Inelastic Scattering and e+ e- Annihilation by Perturbation Theory in Quantum Chromodynamics.*, *Sov. Phys. JETP* **46** (1977) 641–653.
- [44] V. N. Gribov and L. N. Lipatov, *Deep inelastic e p scattering in perturbation theory*, *Sov. J. Nucl. Phys.* **15** (1972) 438–450.
- [45] A. Buckley, J. Ferrando, *et. al.*, *LHAPDF6: parton density access in the LHC precision era*, *Eur. Phys. J. C* **75** (2015) 132, [[arXiv:1412.7420](#)].
- [46] G. P. Lepage, *A New Algorithm for Adaptive Multidimensional Integration*, *J. Comput. Phys.* **27** (1978) 192.
- [47] M. Galassi, J. Davies, J. Theiler, B. Gough, and G. Jungman, *GNU Scientific Library - Reference Manual, Third Edition*, for GSL Version 1.12 (3. ed.). 2009.
- [48] P. Athron, J.-h. Park, D. Stöckinger, and A. Voigt, *FlexibleSUSY—A spectrum generator generator for supersymmetric models*, *Comput. Phys. Commun.* **190** (2015) 139–172, [[arXiv:1406.2319](#)].
- [49] P. Athron, M. Bach, *et. al.*, *FlexibleSUSY 2.0: Extensions to investigate the phenomenology of SUSY and non-SUSY models*, *Comput. Phys. Commun.* **230** (2018) 145–217, [[arXiv:1710.03760](#)].

Bibliography

- [50] C. Chang *et. al.*, “Smoking – The Universal Cross-Section Estimator.” In progress.
- [51] A. Denner and S. Dittmaier, *Electroweak Radiative Corrections for Collider Physics*, *Phys. Rept.* **864** (2020) 1–163, [[arXiv:1912.06823](https://arxiv.org/abs/1912.06823)].
- [52] J. Fiaschi, B. Fuks, M. Klasen, and A. Neuwirth, *Electroweak superpartner production at 13.6 Tev with Resummino*, *Eur. Phys. J. C* **83** (2023) 707, [[arXiv:2304.11915](https://arxiv.org/abs/2304.11915)].
- [53] PDF4LHC Working Group: R. D. Ball *et. al.*, *The PDF4LHC21 combination of global PDF fits for the LHC Run III*, *J. Phys. G* **49** (2022) 080501, [[arXiv:2203.05506](https://arxiv.org/abs/2203.05506)].
- [54] B. C. Allanach *et. al.*, *The Snowmass Points and Slopes: Benchmarks for SUSY Searches*, *Eur. Phys. J. C* **25** (2002) 113–123, [[hep-ph/0202233](https://arxiv.org/abs/hep-ph/0202233)].
- [55] CERN, *LHC SUSY Cross Section Working Group*, 2024.
https://twiki.cern.ch/twiki/bin/view/LHCPhysics/SUSYCrossSections#LHC_SUSY_Cross_Section_Working_G [Accessed: (June 4, 2024)].